# THE EFFECTS OF POWDER PROCESSING PARAMETERS ON THE MICROSTRUCTURE AND ENERGY ABSORPTION CHARACTERISTICS OF LOW VOLTAGE ZnO VARISTORS

By

**Damian Michael Mc Ardle BSc, Dis**

This Thesis is submitted as fulfillment
of the requirements for the award of Master of Engineering to

**Dublin City University**

Sponsoring Establishment: Harris Ireland Limited,
Dundalk, Ireland.

**Supervisor:** **Prof. M.S.J. Hashmi (DCU)**
**Dr. R. Puyane (Harris Ireland Ltd.)**

**Dedicated to:** **Cathy, Darina, Colleen.**

**"Everything I do I do it for you".**

**DECLARATION**

I hereby certify that this material, which I now submit for assessment on the programme of study leading to the award of Master of Science degree is entirely my own work and has not been taken from the work of others save and to the extent that such work has been cited and acknowledged within the text of my work.

Signed: Damian Mc Ardle Date: 15.2.95

**ACKNOWLEDGEMENT**

The author wishes to thank Professor M.S.J. Hashmi, head of school of Mechanical and Manufacturing Engineering for his supervision, guidance and help during this project.

The author would also like to express sincere appreciation to Dr. R. Puyane, at Harris Ireland, for his supervision, resourcefulness, advice and dedication to the project.

Special thanks to Marguerite Lambe, Brendan Daly, A.M. Duffner and Gearoid Cosgrove for advice and help in using the various equipments at Harris Ireland Limited.

Thanks also to Harris Ireland Limited for their financial support, in particular Mr Denis Hession, Operations Manager.

Thanks especially to Carol Beatty and everyone in Harris Ireland Limited and Dublin City University who contributed to this work.

# THE EFFECTS OF POWDER PROCESSING PARAMETERS ON THE MICROSTRUCTURE AND ENERGY ABSORPTION CHARACTERISTICS OF LOW VOLTAGE ZINC OXIDE VARISTORS.

**Damian McArdle, BSc, Dis.**

## ABSTRACT

The effect of comminution techniques used during the powder preparation stage of zinc oxide varistor powder was studied.

The continual requirement for downsizing in electronic components combined with improved performance, demand greater understanding of the parameters influencing the required characteristics. Improvements in energy absorption capability of low voltage zinc oxide varistors are highly desirable from both a commercial and end product performance perspective.

Enhanced energy absorption capability can be used to upgrade the rating of an existing varistor form factor capable of suppressing larger transients (Product capability enhancement) or alternatively reducing the part dimensions (Cost improvements). Current commercial applications for zinc oxide varistors demand energy performance improvements especially in automotive and telecommunications applications, where dimensions and costs as well as high reliability are imperative to compete in the world marketplace.

The physics of energy absorption indicates that in order to improve this, improvements must be made in thermal properties, material processing and testing. Materials parameters of interest include, uniform density, chemical homogeneity and grain size. A high degree of chemical homogeneity in the oxide powder mix prior to pressing and densification is required, in particular, particle size distributions of the oxide dopants and zinc oxide -oxide dopant mixture with maximum values $< 1\mu m$ are highly desirable. Varistors manufactured by the conventional ceramic process use comminution to achieve particle size reduction of oxide dopants, prior to their addition to the zinc oxide slip. This work compares the effects of using eight combinations of milling-mixing techniques on the particle size distribution of oxide dopants and the full formula slip, and examines the microstructural properties of the densified parts using scanning electron microscopy (SEM), and compares the energy absorption capabilities of the devices produced by each technique. The four comminution techniques studied were, Ball, Vibratory, Turbula, and Attrition milling. Shear mixing was used as in the conventional manufacturing process to mix the oxide dopants and zinc oxide.

The work has shown that attrition milling is the most efficient comminution technique, reducing particle size distribution averages to well below 1$\mu$m in less than two hours, compared to the other techniques which, regardless of milling time could not achieve the sub micron size distribution averages.

In all samples where comminution versus shear mixing was used to mix-mill the oxide dopants and zinc oxide together, the energy capability was always considerably improved over the samples where shear mixing alone was used. This work has also identified Vibratory milling of oxide dopants followed by attrition milling of the oxide dopants and zinc oxide together, gave 12% better average energy absorption capability performance over the conventional technique. (Ball milling followed by shear mixing)

**TABLE OF CONTENTS**

# 1. CHAPTER ONE

## 1.1 Introduction

Zinc oxide varistors are polycrystalline electronic devices in which the grain boundaries give rise to useful electrical properties. The objective of this work was to investigate the influence of powder processing parameters on the microstructure and subsequent energy absorption capabilities of low voltage zinc oxide varistors. Varistors with the same total composition were manufactured from raw materials, to fully assembled leaded devices. The comminution combinations used during the powder manufacturing process were varied, in doing so the effects on the particle size distributions of oxide dopants, and zinc oxide-oxide dopant mix were altered and measured in order to assess the homogeneity of the mix. Correlations were made regarding changes in particle size distributions produced by the comminution techniques employed, the microstructure of the devices and the electrical performance behaviour. This research is another step in determining the improvements during powder processing that are important in controlling the microstructural and electrical properties of zinc oxide varistors.

This thesis consists of five chapters.Chapter one contains the introduction to the work and the background for varistor device operation and processing. Chapter two reviews the literature on the significant stages in the powder manufacturing process and in particular how this relates to improvements in the performance of zinc oxide varistors. The experimental approach and methodology are discussed in chapter

three, this includes details of the wide variety of equipment used to carry out the work, sample preparation and powder and device testing.

In chapter four the test results for powder characteristics, microstructure and electrical capability are presented and discussed. Chapter five concludes with a summary of the thesis and examines suggestions for future work.

## 1.2 Introduction to varistors as transient suppressors

Zinc oxide varistors are electronic devices whose primary function is to repeatedly sense and limit transient voltage surges without being destroyed. They have highly non linear current voltage characteristics (Figure 1.1) similar to that of a zener diode. However varistors unlike a diode can limit the transient overvoltage equally in both polarities in ac or dc applications. Voltage ranges from a few tens of volts to tens of kilovolts and a wide range of operating currents from micro amperes to kilo amperes can be successfully suppressed,in addition high energy absorption capability, ranging from a few joules up to thousands of joules make varistors very versatile devices for use in the power and semiconductor industries.(Martzloff, F.D.).

The current voltage characteristics of varistors are split into three distinct regions of operation as described below and in Figure 1.1:-

1. The pre breakdown or low current linear region below the threshold voltage. Here the devices have a high ohmic value and act as a near insulator.
2. The breakdown or non linear region where the device exhibits a very

low ohmic value and acts as a conductor over a very wide range of currents and voltages.

3. The grain resistance or upturn region above the threshold voltage where the device is again highly ohmic.

A number of parameters measured from the current voltage curve are useful in characterising a varistor. The parameter for measuring the degree of non linearity $\alpha$, (Harris Semiconductor, 1993) is defined as

$$\alpha = \text{dln (I2-I1)/dln (V2-V1)} \qquad \text{.....Equation 1.1}$$

where I2 and I1 represent the currents at $V_2$ and $V_1$, respectively. For ohmic conduction $\alpha$ values equal unity. For non ohmic conduction seen in the breakdown region $\alpha$ values are typically of the order of 25. The value of $\alpha$ calculated for the breakdown region is not constant, but is highly dependant on the current range used in the calculation. The $\alpha$ values of samples produced in this work were calculated in the current density range of 1mA/cm$^2$ to 250A/cm$^2$. The breakdown voltages of the devices at the applied current density of 1mA/cm$^2$ is measured in the high $\alpha$ region of the voltage current curve. The maximum rated breakdown voltage where the device becomes ohmic is measured at 5A/cm$^2$.

The $\alpha$ values can be changed by varying the dopants added to the varistor composition. (Sato, K. ; 1989) (Gambino, J.P.; 1979).

The energy absorption capability of a varistor may calculated by the Equation 1.2:- (Harris Semiconductor, 1993)

$$\text{ENERGY} = \int Vc(t)I(t)dt = K.Vc.It. \qquad \text{.....Equation 1.2.}$$

where K is a constant determined by the shape of the waveform applied, Vc is the

clamping voltage recorded for the device at the rated current applied. (Harris Semiconductor, 1993).

Energy is applied in a 10/1000$\mu$s waveform. This means that the current rises to peak value in 10$\mu$s and decays to half this value in 1000$\mu$s. The energy density of a varistor is of critical importance especially in relation to device size, leakage current (Gupta, T.K.; 1990), and the rise in temperature resulting. During uninterrupted operation the varistor must quickly dissipate this energy to the environment and return to its normal steady operating temperature. The time scale of the disturbance, its frequency, the geometry of the device and the environment determine which thermal properties of the varistor are most important for heat dissipation. Both the specific heat capacity of the device and the thermal conductivity are of particular importance. In summary the physics of energy absorbtion indicates that to improve this characteristic, improvements must be made in thermal properties, materials processing and testing.

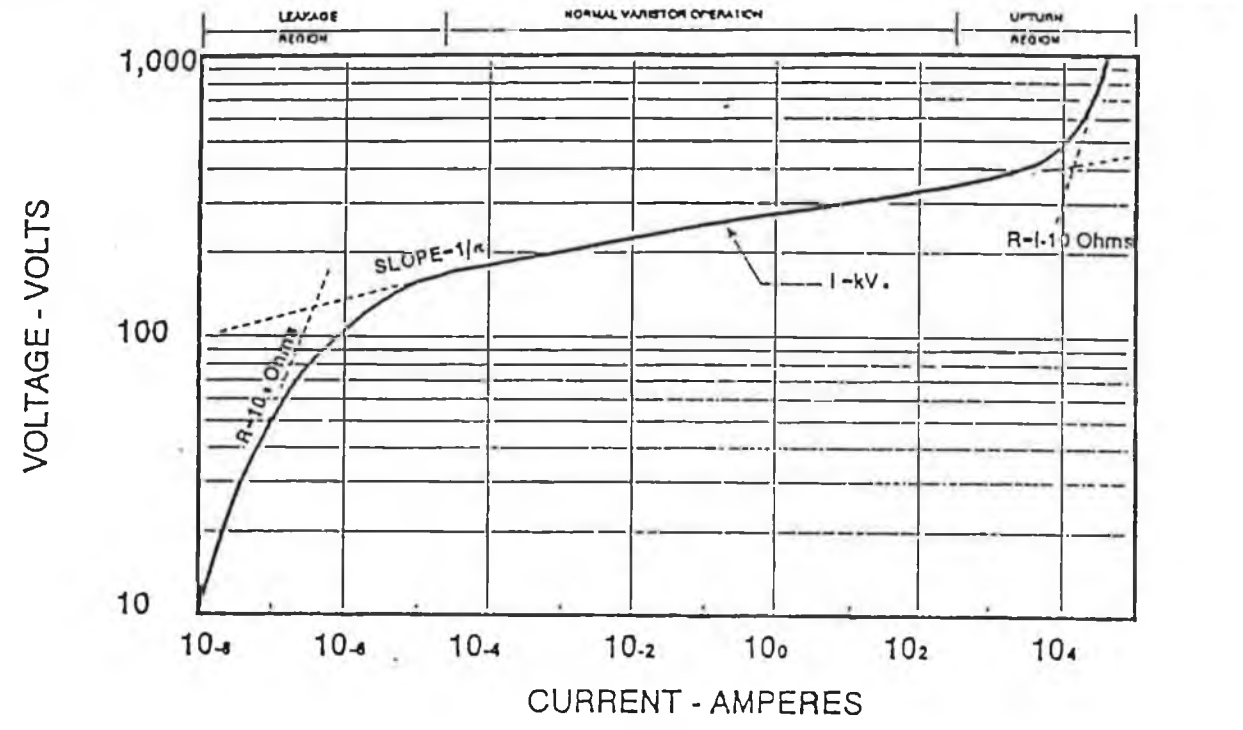


**(Harris Semiconductor, 1993)**

**Figure 1.1 Typical Varistor Current Voltage Curve.**

## 1.3 Varistor Microstructure

The device consists of conducting ZnO grains, surrounded by additions of $Sb_2O_3$, CoO, MnO, and $Cr_2O_3$ forming a thin insulating oxide layer of thickness t. (Olssen, E. et al; 1986) (Figure 1.2). The resulting microstructure consists of ZnO grains ($Zn_7Sb_2O_{12}$) and a number of bismuth rich intergranular phases. (Hoffmann, B.et al). Current flows between the electrodes of silver or aluminium. The varistor action is correlated with processes occurring at a ZnO - ZnO grain boundary. These grains are the predominant phase in varistors and consist of relatively small conducting ZnO crystals. Designing a varistor for a given nominal varistor voltage is basically a matter of selecting a device thickness such that the appropriate number of grains are in series between the electrodes. It is possible to control the grain size by altering the composition of oxide dopants in the varistor powder formulation and the sintering temperature. It is highly desirable to avoid generation of microstructural flaws such as microcracks in the varistor body as the excessive current concentration around the flaws may lead to device failure. (Bowen,L.J.; 1982) (Levinson, L.M.; 1985). A fundamental property of the ZnO varistor is the voltage drop across the single interface junction between grains, estimated at 2.5 volts per grain boundary. (Matsuoka, M.; 1971). Theories of the conduction mechanism are discussed in detail by Levinson, L.M.; 1985.

Two valid processes are discussed:

1. Thermionic emission over a field lowered barrier called Schottky emission.
2. Quantum mechanical tunnelling of the electron through the field

lowered barrier and is denoted Fowler - Nordheim tunnelling. Both are valid depending on the field applied and the temperature.

The microstructure of zinc oxide varistor devices is normally studied in order to understand more fully the mechanisms of varistor conduction. The equipments normally employed to do this include, X-ray power diffraction (XRPD), Scanning transmission electron microscopy (STEM), and electron probe microanalysis (EPMA). (Cerra, H. et al; 1988).

The presence of $Sb_2O_3$ in the varistor powder formulation leads to the spinel phase which is present in the form of small inclusions in grain boundaries and inhibits the grain growth, unlike the presence of $Bi_2O_3$ in ZnO varistors which results in enhanced grain growth. (Asoikan, T. et al; 1987).

Low voltage zinc oxide varistors are normally manufactured using the seed grain method. Here a predetermined grain size distribution is introduced into the spray dried varistor formulation and uniformly mixed prior to pressing into a green disc. (Kao, C.C. et al; 1990).

A uniform zinc oxide grain size distribution throughout the sintered body is vital if reductions in energy handling capability are to be avoided as a result of current concentration around flaws or large grains. (Eda, K.; 1984) (Mizukoshi, A. et al; 1983).

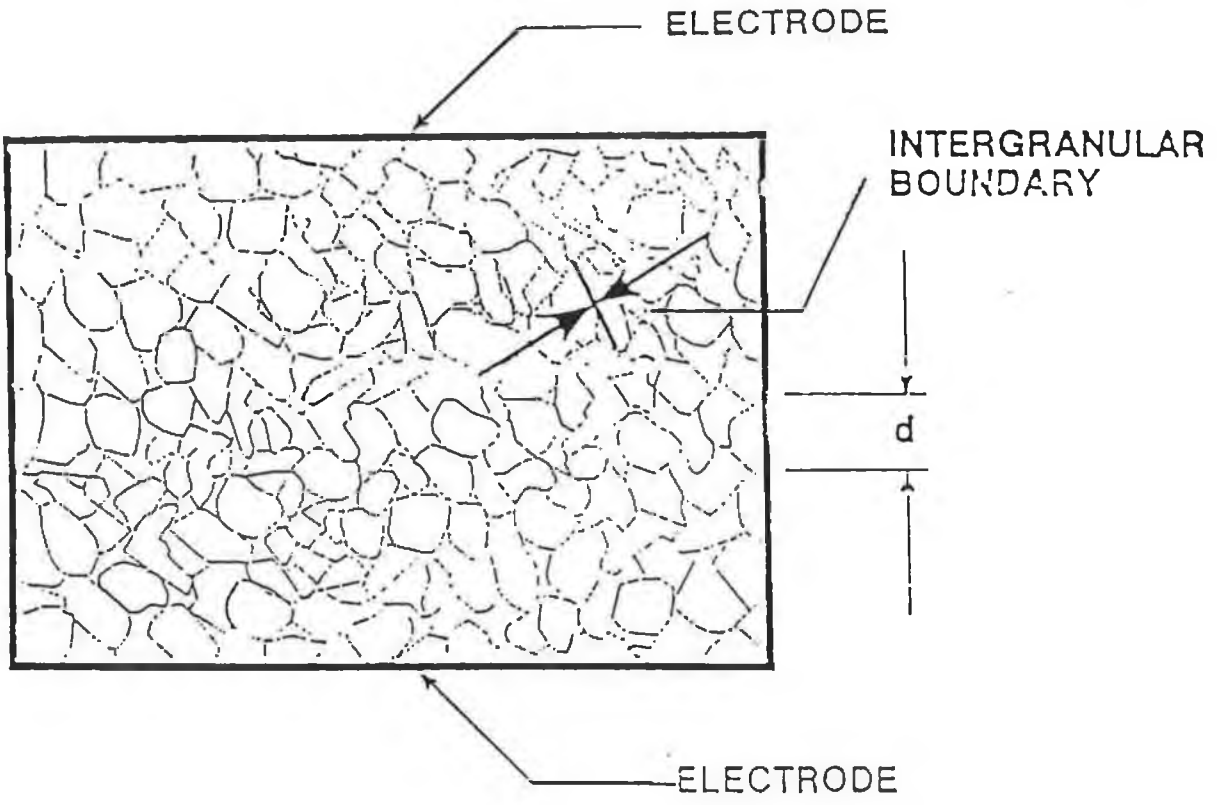


**Figure 1.2**

**Schematic Microstructure of Zinc Oxide Varistor**

**with grains of conducting ZnO average size d.**

**(Source Harris Semiconductor, 1993)**

## 1.4 - Varistor Manufacturing Process

Zinc Oxide Varistors contain up to 10% other oxides such as $MnO_2$, $SiO_2$, $CR_2O_3$, $Bi_2O_3$, $Sb_2O_3$, $Co_3O_4$. The typical ceramic processing route used in the manufacture of varistors and other electronic ceramics is shown in Figure 1.3 below. (Seitz, M. et al).

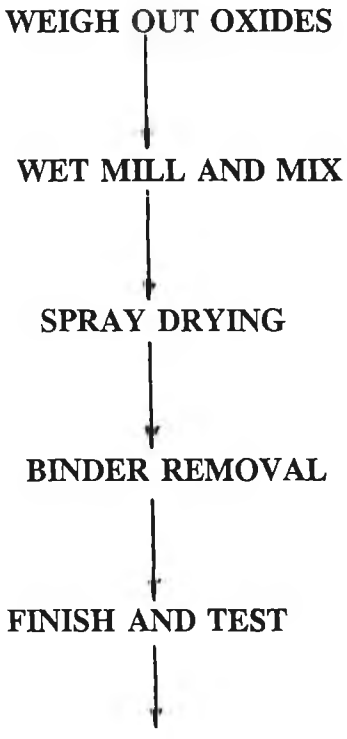


**Figure 1.3 - Mixed Oxide Ceramic Processing Route**

New processing routes such as Sol-Gel technology are being used in the manufacture of zinc oxide varistors, the advantage of particle sizes as low as 0.04 microns are attractive for the production of high homogeneity devices. (Thompson, M.S. et al; 1989).

Undesirable changes in current-voltage characteristics depend not only on the composition and the processing route, but also the variety of post processing events such as dc or ac current flow and the number and intensity of current surges,

mechanical stress, or heating. These events are termed degradation and devices can be restored by a process of annealing or sintering in air in the temperature range 500-700C. (Sonder, E. et al; 1983) (Loubiere, A. et al; 1990).

Process reproducibility is a key requirement to ensure consistent end product characteristics. The process should contain as few variables or process steps as possible and these steps should contain checks to monitor the process and ensure that the product properties are within acceptable limits.

To achieve the required particle characteristics of the oxides and varistor formulation (maximum particle size, minimum specific surface area, dispersion characteristics, etc) wet milling techniques have been extensively studied. (for a full discussion of comminution ref. CH. 2). Particle size distribution of the milled charge and homogeneity of the varistor powder composition are of paramount importance.

Spray drying the wet mix after particle size reduction and mixing is a single step process which converts particles held in suspension into a free flowing powder in a few seconds. (Tunno, J.; 1984). Basically the slurry is atomised into a heated chamber where the liquid is evaporated and the powder collected in a cyclone controlling the lower end of the particle size distribution. The resulting granules are doughnut shaped or hollow spheres (Frey, R.G. et al; 1984).

Four possible formation mechanisms of hollow spray dried granules are discussed by Lukasiewicz, S.L.; 1989. Three of these techniques can be applied in the production of zinc oxide powders, they are:

- A low permeability elastic film forms around the droplet. Reduced evaporation rates result in increased droplet temperature, interior moisture vaporises causing "ballooning".

- For slurries of insoluble oxides, liquid flows to the droplet surface under capillary action, particles are carried along as the liquid evaporates and internal voids result in the granules.
- The presence of occluded air in the slurry.

Problems that may occur during the spray drying produce non spherical particles and satellites or egg shells. These defects reduce the pressability of the powder, requiring high pressing tonnages to overcome higher friction and the presence of air trapped inside the granules.

### 1.4.1 Forming

A dry pressing operation is normally applied here. To aid pressing small amounts of organic additives incorporated in the powder act both as lubricants reducing pressing pressures and as binders to endow adequate strength to the pressed bodies (eg. polyethylene glycol and zinc stearate as a lubricant). The pressing aids must be able to be decomposed into gases well before the sintering temperature of the ceramic, escaping through the open porosity of the compacted powder. The spray drying process is intended to yield a free flowing granular powder to ensure uniform tool filling.

### 1.4.2 Organic Burn out

The key requirement here is that the organics must burn off at temperatures well below the sintering temperature of the ceramic. It is necessary to allow sufficient time during the firing process to ensure no residues exist that may cause undesirable effects to the electrical

properties.

The sintering process converts the green microstructure to the microstructure of a dense component. In electronic ceramics microstructural characteristics include density, grain size and pore size, as well as crystalline and amorphous phases.

## CHAPTER TWO - Literature Survey of Ceramic Processing.

### 2.1. Introduction to Comminution.

The physics of energy absorption indicates that improvements must be made in thermal properties, material processing and testing (Levinson, L.M. et al; 1974). Materials properties and processing will be looked at beginning with particle size reduction techniques of oxide additive dopants for varistors.

The material properties of interest are density, homogeneity, grain size distribution, porosity and defect chemistry. The objective is to strive for a high degree of homogeneity in the oxide powder mix, and in the disc characteristics, a high degree of uniform density combined with low porosity (porosity, besides acting as a low thermal conductor, can significantly weaken the ceramic strength of the press body.) uniform grain size and a desirable defect chemistry at the depletion layer so that the grain boundary junction remains stable to oncoming surges.

Non homogeneous milling of oxide dopants may cause hot spots within the discs on application of surges. This phenomenon can be identified by using a liquid crystal on the surface of the disc and observing the colour change that occurs as a consequence of thermal changes. Hence the distribution of the oxide dopants after particle size reduction is critical to the homogeneity of the oxide powder mix. It has been observed (Gupta, T.K.; 1975) that in the removal of the hot spot or "coning out" by diamond drilling, that the energy absorption capability rose significantly.

Particle size, shape and distribution affect the behaviour of raw materials when they are physically mixed together by ball milling or other techniques. They are also

related to other physical and chemical properties of the material. The particle size of a material determines its surface area which can have a significant effect on powder reactivity and sinterability, usually achieving higher densities for larger surface areas.

Some of the most commonly used types of particle size reduction and comminution techniques are:

1. Ball milling.
2. Vibratory milling.
3. Jet milling.
4. Ultrasonic milling
5. Attrition milling.
6. Energy milling
7. Hammer milling
8. Dispersion milling

Milling and mixing operations are frequently carried out in one operation using one piece of equipment. The principal aims of the milling operation are to:

1. To reduce primary particle size.
2. To reduce agglomerates or aggregates in size ideally to primary particle size.
3. Having achieved the desired particle size to retain it in a stable state.

The theory and practice of operation for each of these methods will now be discussed.

### 2.1.1 Ball Milling Technology

Ball milling is extensively used during the manufacture of ceramic powders for varistor applications. The ball mills generally constructed from a cyclindrical container of which the diameter and length vary in relation to each other and in relation to the capacity required. (Figure 2.1). The mills are normally lined with materials such as vulcanised rubber, polyurethane, high density alumina and stainless steel to mention but a few, however under certain conditions undesirable contamination can be introduced into the mix by wearing of the mill walls and media. Therefore, care must be taken during the selection of the mill lining and media material in order to avoid contamination of the milled powder. Another consideration includes the rate at which the lining wears away and the resultant efficiency of milling. The general approach in the selection of mill linings is to use one that will minimise any pick up of contamination and one that is resistant to an excessive or rapid wear rate. Depending on the application another approach is to select mill linings with the same composition as the material to be ground, which reduces the risk of contamination and subsequent failure of the milled powder to perform to specification. Another criteria for the selection of media is to use one that will introduce a predictable amount of material into the product in order to give it some desired characteristics after sintering (Takahashi, M.; 1971). The technique normally used during the milling of zinc oxide varistor dopants is to coat the interior of the ball mill with polyurethane and charge it with zirconia media. Choice of the shape and size of the media used are essential parameters to achieve the desired size distribution of the milled particles. (KIM, Y.S.; 1973).

### 2.1.2 Mill Charge

Efficiency of the ball milling operation in reaching the required particle size distribution is attributed to several characteristics of the mill itself and to the product for size reduction. Ball mills are generally filled to 50% by volume with media. The total charge of powder to be milled is dependant on the choice of either wet or dry milling. In the case of dry milling the typical powder charge is in the range of 20 - 25% of the total mill volume and in the case of wet ball milling powder charges of the order 30 - 40% of the mill volume can easily be accommodated (Pentecost, not dated). In varistor processing technology wet ball milling has been the preferred choice. Here a solid charge can be milled whilst suspended in a liquid medium. De-ionised water is usually the preferred solvent. Typical considerations when selecting the media are inertness to chemical reactivity with the mill lining, grinding media and powder charge. Enough liquid should be added to the powder charge to make a free flowing slurry or suspension having the optimum viscosity for milling. Slurries for milling with high viscosity gives rise to low milling rates whilst suspensions with high levels of fluidity give rise to high levels of contamination from wear of the mill lining and grinding media. A common practise in wet grinding is to add a dispersing agent in amounts up to 1% weight which inhibits particle flocculation in the suspension and enables further particle size reduction as well as significantly reducing the viscosity of the suspension. Some dispersing agents include sodium silicate and tetrasodium phosphate. However, these materials are, in most cases, not suitable for the preparation of electronic grade ceramic powders due to the alkaline contamination which they introduce in the case of n-type semiconductor ceramics, as is the case with zinc oxide, they will significantly increase their conductivity. Choice of wet or dry

milling will be an important consideration in the processing of fine powders for varistor applications. This choice is influenced by the downstream processing operations and their ability to handle a wet mix, how can it be dried, its cost effectiveness, and which of the two methods produces the desired particle size distribution. In practice, it is found that wet milling produces a much finer particle size distribution much more quickly than dry milling. The typical minimum particle size attainable with wet milling is as low as 0.5$\mu$m whilst with dry milling is 15$\mu$m.

### 2.1.3 Stages in Ball Milling

There are other reasons for the selection of ball mills as a means of particle size reduction during the manufacture of varistor powders. They include dispersion of the multiple components by thorough mixing in the ball mill. However, the primary purpose of the ball milling operation is to reduce the size of the individual particles and agglomerates to the desired particle size distribution. The physical process of ball milling can be considered to take place in three stages. The first stage showing significant reduction in agglomerate size by a process of light milling, secondly, after a longer time the fracture of individual particles combined with changes and defects caused within the particles, serves to produce particles reduced in size to a range as determined by the milling time. Finally, the particles may reagglomerate if the milling time is prolonged, as a result of the free surface area created.

This has been observed many times at the laboratory and pilot line facilities at Harris Ireland.

Taking the three stages as applied to varistor processing technology the incoming dopants vary in size from chemical to chemical and manufacturer to manufacturer. Taking as an example bismuth trioxide, a major constituent in any varistor powder, the supplier delivered particle size distribution average may be of the order 19$\mu$m and after a light milling for 1 hour the agglomerates will break up and the initial particle size reduction takes place. Milling for a further five hours gives an average particle size distribution of 2$\mu$m, suitable for use as a zinc oxide dopant. The smaller agglomerate and particle size distribution have a favourable response to the subsequent forming and sintering process. The distribution of particle size becomes narrower as the milling time increases because of the reduction of large particles into finer particles with a corresponding decrease in the maximum size.

### 2.1.4 Critical Parameters - Ball Milling

In order to obtain effective and efficient milling it is absolutely critical to observe the following parameters:

#### 2.1.4.1 Rotational Speed

The action of the grinding media inside the mill is determined by the speed at which the mill cylinder is turned. A speed which includes the cascading action of the media is most desirable. Cascading is the case where the grinding media break away from the wall of the mill at an angle of 45 to 60 degrees from the horizontal and fall in a coherent mobile mass as suggested

by a waterfall. The impact crushes the grains of the charge. Other secondary actions lead to intensive disintegration, better dispersion and more complete particle wetting due to the high rate of shear from the spinning of the media. If rotational speed is too fast centrifuging will occur, if too slow slipping occurs. The point at which centrifuging occurs is called the critical speed calculated as follows:

$$\text{critical speed } Nc = 76.6 / \sqrt{dm}$$

(Source Harris Internal)

Where the diameter of the mill, dm, is measured in metres. Normal operating speeds are in the region of 35 - 80% of the critical speed Nc.

### 2.1.4.2 **Grinding Media and Material charge.**

Apart from the importance of the materials from which the media is constructed there are other fundamental considerations in terms of the physical shape of the media and the forces being transmitted to the powder charge during the milling process. Grinding media can vary in shape from circular to cylindrical and in dimensions from a few millimetres in diameter to 50mm depending on the application. Zirconia cylinders with spherical ends, the radius of which is 12mm, are frequently used in the ball milling of varistor powders.

Grinding of a solid in a liquid to reduce particle size or to make a dispersion should be done at optimum viscosity commensurate with the grinding media being used. This is necessary to keep media wear down to

acceptable rates. When using zirconia grinding media the batch should be comparable to a free flowing slurry with a viscosity in the range 15-30 m Pa.

Good grinding practice calls for the mill to be filled to 45 - 55% of its total volume. To minimise excessive ball wear charges more than 45% are recommended. At values lower than 45% the media tends to slip on the wall of the mill. The rule of thumb for wet milling is to fill the mill to about an inch over media level with water. It is desirable to regulate the milling time required, to avoid excessive temperature rise causing excessive media wear. (Chemicals Engineers Handbook, 1985)

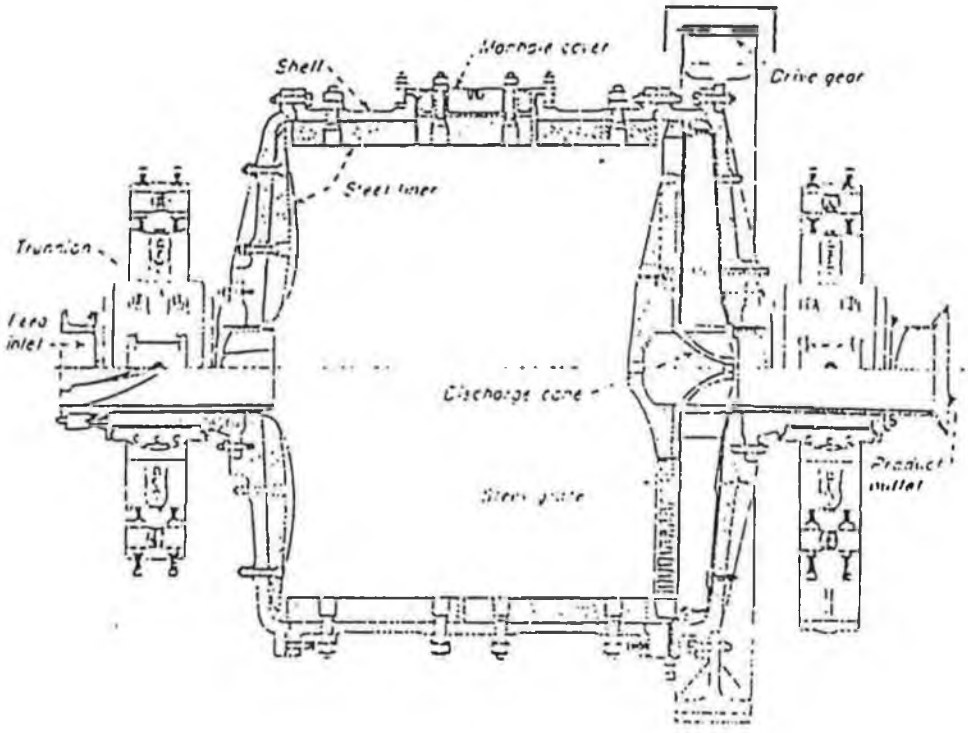


**(Source, Chemical Engineers Handbook, 1985)**

**Figure 2.1 Diagram showing construction of ball mill**

During the manufacture of varistors extreme care must be taken during the milling to avoid contamination of the milled powder by the lining or the media (Tukghashi, M.; 1971). The level of contamination increases proportionally with milling times and sintering of the products will be greatly influenced by the levels of contamination picked up during milling. During the milling of varistor powders using zirconia media it is absolutely vital to control the level of wear and subsequent contamination of lots by the periodic checking of the weight of media remaining. Generally it is vital to select the most optimum media and lining to attain the smallest possible wear rates.

### 2.1.5 Vibratory Milling

Vibratory milling equipment differs significantly in construction from ball milling action. Basic construction of the mill consists of a non rotary grinding chamber and a vibrating mechanism secured to the floor by bolting (figure 2.2). The grinding chamber is in the form of a vertical cylinder or annulus which is filled with milling media. In the case of varistor processing the media chosen is normally zirconia pellets, loaded from the top. The material to be ground is introduced between the voids of the grinding media suspended in deionised water. The grinding chamber and vibration mechanism are attached to the pedestal on high tensile springs thus all the

energy from the vibratory mechanism is imported directly into the grinding media without the necessity for intermediate gears, drives or clutches.

The vibrating mechanism consists of a specially designed electric motor having a heavy shaft mounted in heavy duty roller bearings. At each end of the shaft there are mounted, heavy duty out of balance weights. The top weight which is in the same horizontal plane as the top of the compression springs is connected to the motor in a fixed shaft position. (Sheppard, L.M.; 1984).

The top eccentric weight causes a horizontal gyration of the grinding chamber while the bottom eccentric weight provides a gyrating tilt. This unique motion causes a three dimensional high frequency vibration which constitutes the transfer agents converting motive energy into grinding impacts.

In general any material that can be broken by impact can be ground in a vibratory mill. Most materials processed in a ball mill could be processed to a finer particle size in much lesser time in a vibratory mill as when compared with a traditional ball mill.

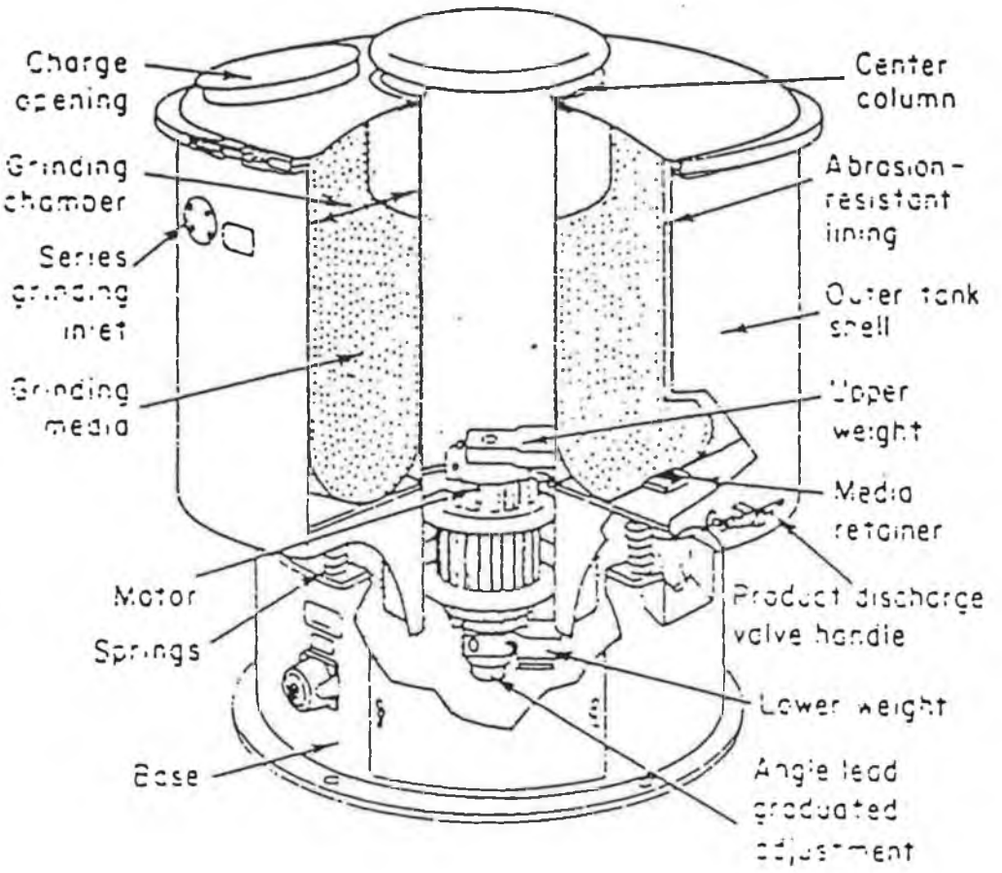


(Source, Chemical Engineers Handbook, 1985)

**Figure 2.2 - Basic layout of a Vibratory mill**

The basic limitations of conventional grinding systems are their inability to perform ultrafine grinding economically and their failure to produce an exact particle size distribution. However the vibration milling technique applies a high frequency three dimensional vibration to a cylinder containing small cylindrical grinding media and overcomes the limitations of economical ultrafine grinding and poor control of particle size distribution associated with other more traditional techniques.

It requires less total energy to reduce or break a small particle than a large one. In the case of ultrafine grinding only very small impact forces are necessary. Forces applied in excess of that needed to break the material will result in energy dissipated as heat or may increase media wear. Additionally the greater number of impacts per unit of time the faster a given particle size distribution will be attained. Therefore, the vibration energy mill using small amounts of energy with high frequency vibration is more efficient than the high impact, low frequently principle applied in conventional grinding systems such as ball milling (Chemical Engineers handbook, 1985).

In the ceramic industry which processes finely ground materials uniform particle size is of the utmost importance. However this close particle size distribution has been extremely difficult to achieve with ball and pebble mills. In the lowest micron range the point contact offers decreasing probability of further particle size reduction and increasing probability of wide particle size distribution.

The media chosen offers a combination of point line and force contact. When the two pieces of cylindrical grinding media are vibrating against each other the large particles will be worked on first and reduced in size whilst the smaller particles remain protected. When the larger particles are reduced by the combination of point, line and face contact to the same size as the smaller ones, close particle size reduction will have been achieved. Further size reduction maintains this same close range.

#### 2.1.5.1 Advantages of Vibratory Milling

Vibratory mills have high grinding efficiency compared to other technologies because of their ability to maximise all available mechanical energy. Ball, pebble, hammer and dispersion mills waste large amounts of input energy through non productive drag and friction of the media charge. This excess energy will be dissipated as heat, thus requiring a water cooling jacket or heat exchanger. The high frequency low amplitude motion as employed by the vibromill is the most effective method of converting energy to accomplish particle size reduction from approximately 100$\mu$m to the submicron ranges.

The ability to control particle size distribution is important when processing materials to very fine particle sizes. This gives the vibratory mill significant advantages over conventional milling techniques. The amount of contaminating materials introduced into the powder using the vibratory mill is small because of the small impact forces created during the comminution

process.

### 2.1.5.2 Vibratory Milling Criteria

Variables or characteristics of the vibratory milling process will include information on the hardness of the feed material and its specific gravity and the pre milling particle size analysis. Suitability of the material to be ground in wet or dry form and type of media preferred in addition to the ratio of solids to liquid, the viscosity of the formulation and its reactivity with deflocculants and wetting agents. These criteria are considered inputs to the milling system. Outputs of the system include the desired end particle size range and required average value. In the selection of the equipment for particle size reduction, consideration must be given to the desired production rate and whether batch or continuous grinding is desirable. Milling duration will be important especially in the determination of particle size but also in terms of contamination.

## 2.1.6 Fluid Energy or Jet Milling

This type of mill has attracted considerable interest and investigation in both process industry and laboratory research, because this device has the advantage of being able to produce fine powders, with control of particle size, whilst maintaining purity. The jet mill principles revolve around the production of high velocity particles through jets. This action fractures the particles through self attrition upon impact, and then they pass through a size classifier. Compressed air is used to pulverise both hard and soft materials

down from micron to sub micron particle sizes. Other fluid media can be used, eg. superheated steam, nitrogen, carbon dioxide, water and slurries. The capacity of jet mills can range from grams to thousands of pounds per hour with effective particle size reduction. The relatively simple operation of a jet mill is now discussed. The essential features of this mill are shown in (figure 2.3). A vibratory hopper feeds the solid material to be ground into a stream of compressed air that is expanded through two diametrically opposing jets. The solid particles are accelerated in the air to very high velocities where particle fracture takes place on impact or collision between the particles in the grinding chamber coming from the opposite jet. The particles undergo impact and surface grinding.

### 2.1.6.1. THE RATE OF GRINDING

The rate of grinding is proportional to jet pressure and cross sectional area of the jet opening kinetic energy density. The maximum stress created by the assumed elastic collision of the particles is proportional to the particle velocity and independent of particle size (Rumpf, P.; 1970). After self attrition of the feed particles, the product particles travel in rectilinear paths through an up stack channel at reduced velocities and are carried tangentially into a flat, shallow, circular classifying chamber. Particles with a high surface to mass ratio spiral through a central exhaust opening, leading to a collector system for regrinding, whereas those with a low ratio (the larger particles) continue to travel along the periphery of the classifying chamber and

are accelerated by the second of the two jets, colliding with new material on a continuous basis. The synthesis of particles with controlled size and distribution is accomplished by the nature and size of the feed material, feed rate, design and alignment of the jets, design of the classifying chamber and the fluid pressure temperature and volume.

The jet milling method of fine grinding produces a finished powder with essentially no contamination. There are two primary reasons for this achievement. The first is that the jet milling operates with no moving parts. the second that appropriate liner components such as polyurethane methane or hard ceramic materials can be selected for use. If small particles of polyurethane are picked up during milling, these particles can be burned out of the milled powder by a subsequent oxidising treatment at elevated temperatures before the sintering of the compacted powder. Jet milling can influence the particle size distribution of a powder and consequently the structural development of the sintered material made from the powder.

Sintered material, after jet mill processing can exhibit a uniform single phase microstructure if virtually single phase powder is fed into the mill. However if the fed material is not single phase then the microstructure developed from the jet milled powder can exhibit a non uniform distribution of isolated second phase, compared to ball milling where the select second phase will not exist because in ball milling the complete powder charges remain in the closed mill, and are homogeneously mixed, whereas in the jet mill the different particle sizes and densities lead to different rates of particle classification leading to differences in the composition of the final powder

(Compositional stratification). In all fluid energy mills, particle recovery is a problem since very fine particles are difficult to collect. Large volumes of gasses must be handled, that are inefficient for micron size particles and filters clog rapidly.

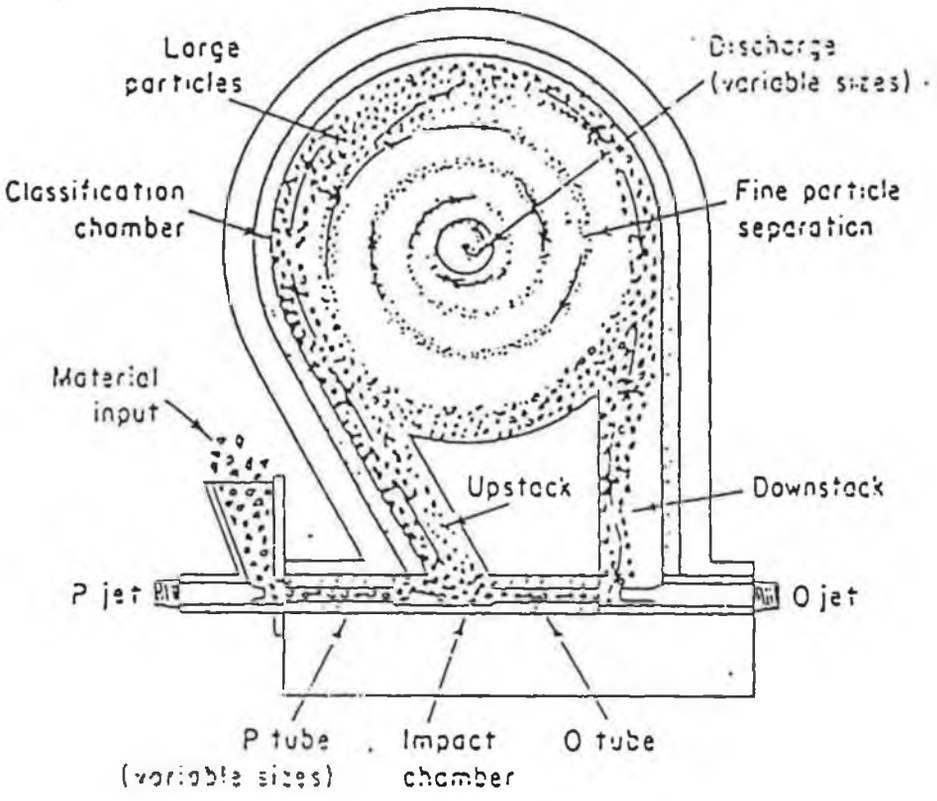


**(Source, Chemical Engineers Handbook, 1985)**

**Figure 2.3 - Typical Fluid Energy Mill Layout**

### 2.1.7 Ultrasonic Milling

The ultrasonic mill is constructed from three major components, namely, the generator, the converter and the disruptor (Heat Systems - Ultrasonics, Commercial Brochure). They function together in that the generator provides high voltage pulses of energy at 20kHz from a 50 Hz source and adjusts for varying load conditions such as viscosity and temperature by sensing impedance changes, the power to the probe (Figure 2.4) can be increased or decreased from zero to a maximum value. Generator voltage is converted to mechanical energy at frequencies of the order of 20 kHz and transmitted by a disruptor - comprising piezoelectric crystals that radiate energy into the suspension being treated. A phenomenon known as cavitation occurs, resulting in the formation and collapse of microscopic vapour bubbles generated by the strong sound waves producing a grinding action in front of the probe tip. Variables to control when using this technique include milling time, temperature and output energy.

The ultrasonic process can also be used for particle size reduction and homogenising, deagglomeration and disintegration of slurries. Ultrasonics are generally used when the required degree of mixing cannot be achieved by high speed mixing equipment.

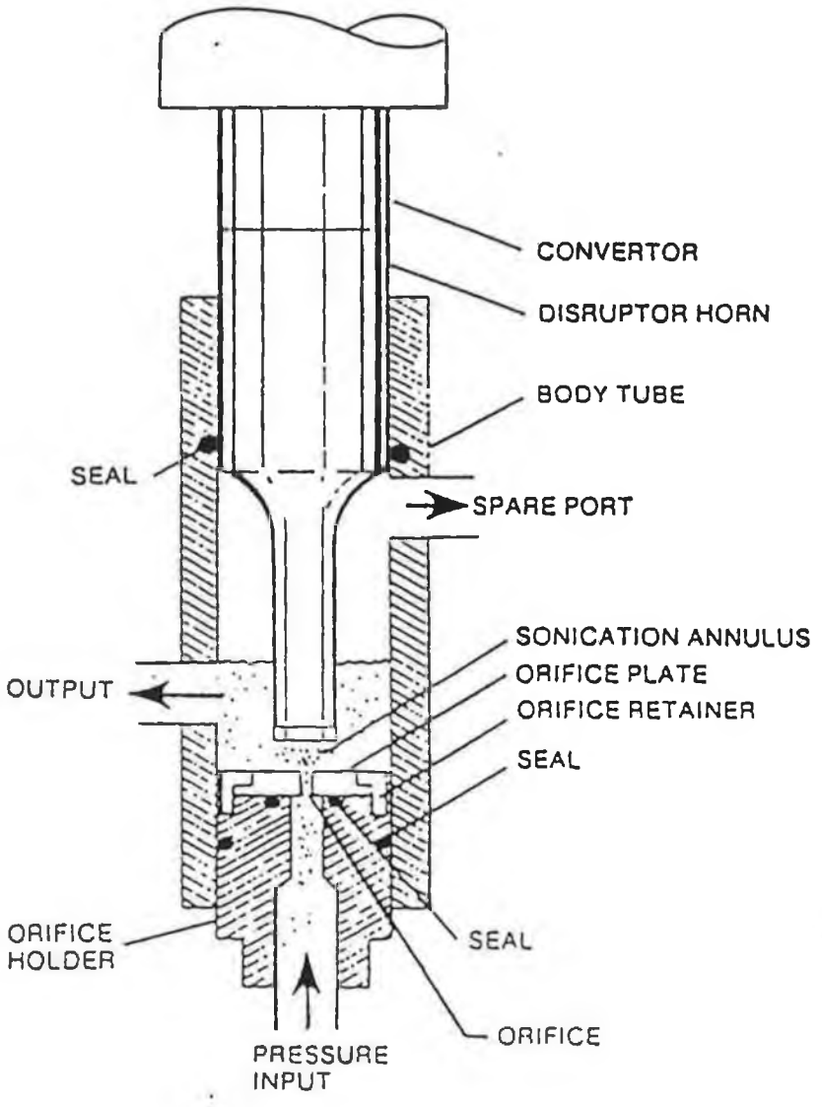


**(Source, Commercial brochure)**

**Figure 2.4 - Layout of Ultrasonic Disruptor Horn Mill**

### 2.1.8 Attrition Milling

This type of milling equipment is used when particle sizes of the order of 1$\mu$m are desirable. (Nishida, M. et al). One outstanding characteristic of the attrition mill action is its ability to reach sub micron particle sizes up to ten times more quickly than conventional ball mill technology. Construction of attrition mills comprises a stationary outer grinding tank contrasted with the revolving tank of the ball mill. Filled with grinding media and fitted with an internal rotating shaft, recirculation pump, whereby the whole charge is continuously agitated resulting in an intensive grinding action. The media used can vary in size from 5mm to 10mm in diameter and the materials used include ceramic balls, stainless steel and carbon steel. Temperature of the grinding process can be controlled as these mills are normally designed with a heating or cooling jacket and temperature gauge. Loading the mill is simple and it is easy to make additions to the charge during the milling cycle or at any time during processing. In addition the material processed can be inspected continuously and corrections can be made at any time.

One of the most interesting features of attrition mill technology is it's power consumption compared to other particle size reduction techniques. Manufacturers are keen to quote the efficiency of this mill compared to ball and vibro milling. "Union Process Company" makers of the 'ATTRITOR' (Figure 2.5) see reductions in particle size after 200 kw energy input, compared to ball and vibro mills where size reduction has stopped (Figure 2.6 (Union Process Company, Commercial Brochure). The time required for

grinding in an attrition mill is shorter than that required in a ball mill for a fixed specific energy input or to a desired particle size distribution ( Pentecost, J.L; 1976).

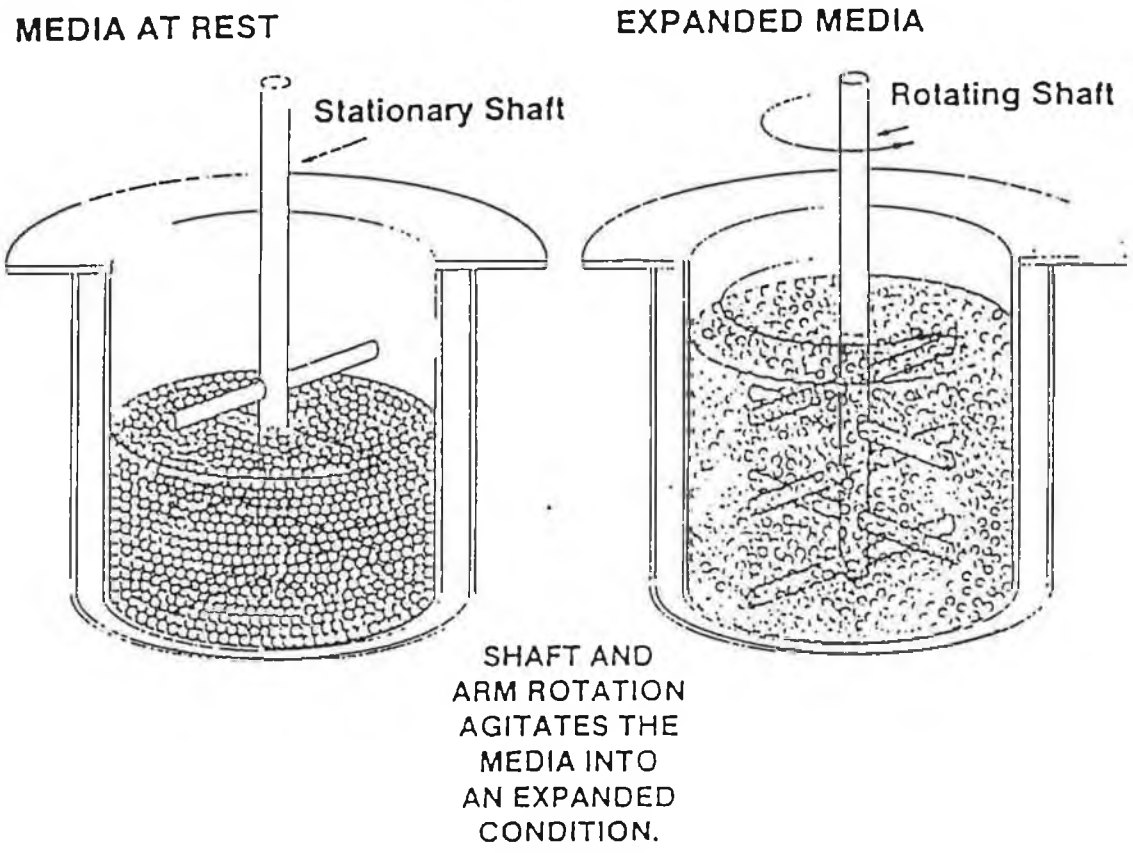


**(Source, Union Process Company, Commercial Brochure)**

**Figure 2.5 Attrition Mill Layout**

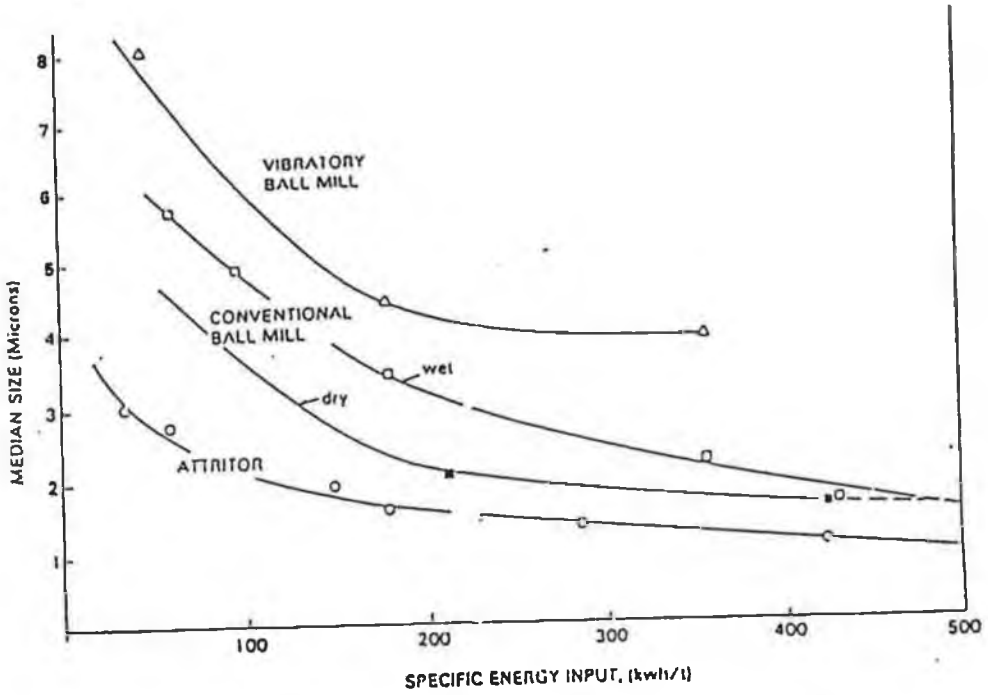


**(Source, Union Process Company, Commercial Brochure)**

**Figure 2.6 - Comparison of the effectiveness of three grinding devices for use in ultrafine grinding operations**

Attrition mills come in three types:

- Batch
- Circulation
- Continuous

In the batch types the material to be ground is charged into the mill, processed and discharged. No pre mixing is necessary and ingredients can be added anytime during processing. Inspections and formula corrections can be made during grinding without stopping the machine.

The circulation type rapidly pumps the material to be ground (slurry) through a confined bed of small agitated media. The media acts as a dynamic sieve, the small particles pass through easily and the larger particles are ground more finely, resulting in a narrow particle size distribution. The slurry makes several passes through the milling chamber until the desired particle size is attained.

In the continuous attrition mill a constant flow of finely ground processed material from a pre mixed slurry passes through the chamber. The particle size achieved is dependant on the "dwell time" within the chamber.

Attrition milling offers an efficient means of size reduction to the sub micron range, where grinding media contamination can be tolerated or removed the technique offers substantial advantages in both laboratory and production sizes compared to ball or vibratory milling.

### 2.1.9 Hammer Milling

These mills, used for pulverising and disintegration of materials by the high speed action of horizontally or vertically mounted shaft carrying hammers or beaters, either fixed or pivoted to the shaft (Figure 2.7). Rotational speeds in the range 1500 to 3000 RPM are common. The rotor is placed in a housing containing grinding plates or liners. The particle size can be changed by regulation of rotor speed, feed rate, or clearances between hammers and grinding plates, as well as by changing the number of and type of hammers used, and the sizes of the discharge openings. As the material to be ground enters the grinding chamber it is shattered by the hammer action, reducing it to fine particles.

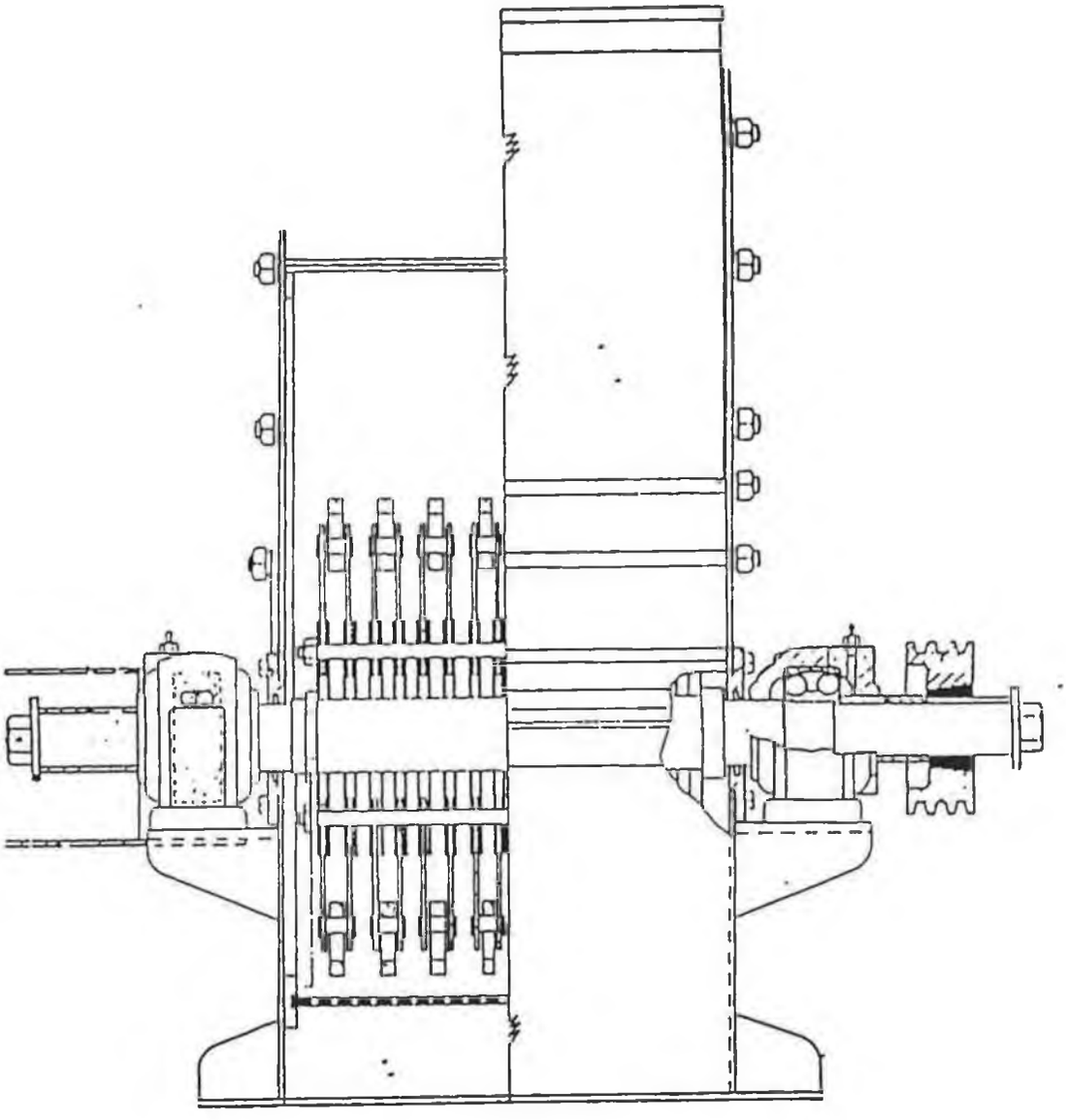

(Source, Miracle Mills, Commercial Brochure)

**Figure 2.7 - Hammer Mill Layout**

### 2.1.10 Roller Milling

Roller mills are normally used in the manufacture of ceramic inks, basically comprise a minimum of two rollers rotating in opposite directions at the same speed, forced together by the action of a hydraulic unit (Figure 2.8). The material to be milled is drawn through the rollers, where the stress generated on the materials by the action of the rollers reduces the particle size by crushing. The roller design used varies depending on the application, but three types of roller used include: smooth finish, which is mainly used for highly abrasive coarse products, secondly, thread rollers used for fine powder as they can improve chip behaviour and increase the output. Finally, protective rollers are always smooth rollers. The rollers themselves are protected against wear by hard materials which are welded onto the roller. Typical construction shown in Figure 2.8 where one of the rollers is fixed and the pressure applied during milling is applied by the pressure ram. At the nip angle the material is transported by force through the narrowest point of the gap. During the compression process air is pressed out which has to escape to the edges. Care must be taken at this stage as unstressed material may by pass the rollers. The gap width is not fixed, it results from the hardness, particle shape and fracture behaviour of the material being processed. Other influencing factors include humidity, the original particle size distribution, especially the maximum feed particle size, the friction between the product roller's and the grinding force applied. Speed of size reduction is dependant on speed of feed and the grinding force and pressure (Source Harris Internal).

Other influential measures include the diameter and length of the rollers and the roller grinding force and speed. It is difficult to achieve particle size less than 5$\mu$m using this technique. Its use is mainly mixing very high viscosity paste. (Harris Internal).

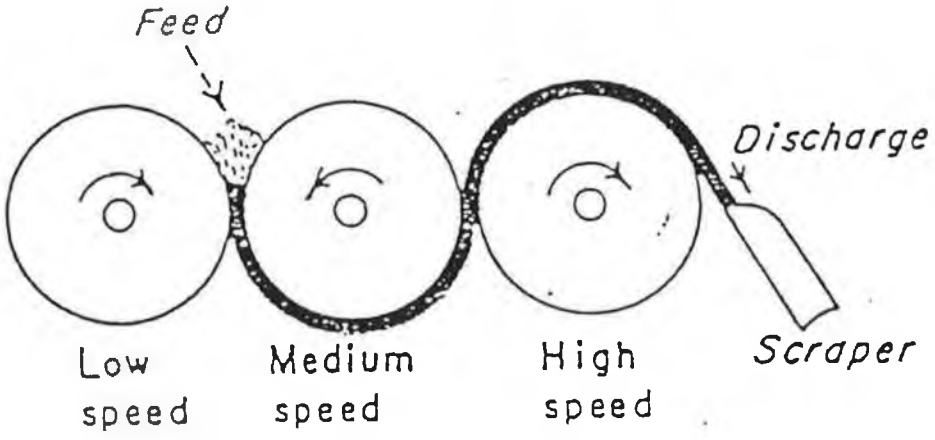


**(Source, Chemical Engineers Handbook, 1985)**

**Figure 2.8 - Typical Roller Mill Layout**

## 2.2.0 LITERATURE SURVEY OF SPRAY DRYING

### 2.2.1 Introduction

Spray drying is the process by which a fluid feed material is transformed into a dry powder in one operation, by spraying the feed into the hot drying medium. (Master, K; 1985). The feed material (Commonly termed Slip or Slurry ) is usually a water based suspension (in this work zinc oxide and oxide dopants suspended in deionised water), containing up to 80% solids which require the use of dispersants known as deflocculants. The slurry is pumped under pressure to an atomizer located within the drying chamber, converted into a spray of droplets and water is evaporated off these droplets forming dry powder. The rapid evaporation keeps the temperature of the sprayed droplets fairly low so that high drying air temperatures can be applied without affecting the product. The drying process takes anywhere from 5 to 30 minutes in most commercial installations. (Belcher, D. W, et al; 1963). Figure 2.9 is a schematic representation of a typical spray dry operation.

Spray drying has been successfully applied in the dairy industry from the late 19th century but has been practised in the chemical industry for the last fifty years. Today it is an important operation in the chemical, food, pharmaceutical and ceramic industries.

Spray drying systems have been developed to meet the needs for processing ceramic powders. In the case of zinc oxide for varistor applications the spray dried powder must be free flowing and of uniform agglomerate size distribution to ensure uniform filling of the dies during the pressing operation.

Uniformity at this stage may also affect the electrical properties of the finished varistor.

The effect of spray drying outlet temperature and slip feed rate on the bulk and tap density and the average particle size distribution of zinc oxide powders produced by this technique was studied (O'Sullivan, F; 1990). It was found that powders dried with outlet temperatures in the range 100-140C that the average particle size did not change, however the bulk density decreases as the outlet temperature increases. It was found that a less severe flash drying produced defective shaped agglomerates in the form of egg shells or doughnuts as opposed to the spherical particle shape desired for pressing. Further work carried out on zinc oxide powders for varistor applications shows that the average agglomerate size produced by spray drying, increases with increased slip feed rate. This occurs as a result of the higher volume of slip being pumped through the nozzle causing larger droplets in turn producing larger spray dried particles.

The spray drying of ceramics is a relatively recent phenomenon, their original intention did not include drying of heat sensitive products, yet by the mid 1960's more spray driers were being sold for heat sensitive inorganics than for foods and other organics. Included were many for clays, aluminas, ferrites, steatites, porcelain, etc. It is estimated that in Europe today over 50% of the total volume of wall and floor tiles, and of electronic ceramics are made on the basis of spray dried powders.

By using spray drying, several of the traditional ceramic processing steps are eliminated, (Figure 2.10), generating considerable savings in labour,

energy consumption and investment capital. Improved control of powder properties is another extremely important feature of this technique.

The conditions required to make spray drying a viable process include:

1. A pumpable feed slurry.
2. Resulting dry powders should not be of a tacky nature so as to avoid sticking to the interior of the spray drier or between the powder particles themselves.

Spray dried powders should be characterised before use, especially those requiring further processing such as dry pressing. Typical characteristics include:

1. Granule size analysis.
2. Powder flow rate and bulk density (ASTM, standards).
3. Percent residual moisture.
4. Percent organics.
5. Compaction behaviour.

### 2.2.2 Feed (Slip or Slurry) Preparation

The first step in slurry preparation is to disperse the ceramic powder in water, normally carried out during milling or dispersion by a mixer to eliminate the aggregates usually present in the starting material. Lack of uniformity in the mixing / milling procedures preceding the spray drying operation can cause inconsistent slurry characteristics necessitating the use of suitable dispersants to ensure the homogeneous non-agglomerated slip with an

economically high solids content. (Lukasiewicz, S.L.; 1989).

Milling is used when agglomerates are too large and need to be broken down into primary particles. This is typical for oxide dopants in a varistor formula, where several different oxides each with their own particle size distribution are added to the mix. Mixing is sufficient to ensure uniform distribution of the ceramic throughout the suspension. As solids approach 70%, or higher, dispersants or deflocculants are used to maintain adequate rheological properties. The objective of slurry preparation is to obtain as high a solids to liquid ratio as possible, with a low viscosity (Tunno, J.L.; 1984). In this way, the amount of energy needed to evaporate the water is minimised and the low viscosity ensures that the suspension can be pumped without serious difficulty.

Binders to aid pressing are added during the slurry preparation stage. The purpose of binders is to hold the discrete particles together during the spray drying step and also hold the agglomerates together after pressing.

### 2.2.3 Droplet Drying

The latent heat of evaporation is supplied to the atomised droplets of slurry by the hot air causing the water to evaporate. Rapid drying rates are possible because an enormous liquid surface area is exposed to the drying air when the liquid stream is atomised into fine droplets.

The droplet is a film of slurry being broken up first into ligaments, then into droplets by the atomization technique. In the case of centrifugal atomization liquid leaves the edge of the discs at speeds of up to 100m/sec,

most of the evaporation takes place in milliseconds, otherwise the wet or pasty drops strike the wall and stick to it (Bowen, Commercial Brochure).

Moisture to be removed can be classified as free, internal and chemically bound or combined. Free moisture is that which is on the surface or can diffuse to the surface quickly enough to maintain a constant drying rate. Removal of chemically bound moisture may require further rise in particle temperature, necessitating further drying of the powder in a secondary drying step, by introducing the powder into a heated gas stream, for as long as the time temperature relationship requires, and powder is then separated from the gas.

Maintaining a low viscosity, high solids slurry, dictates use of a low - viscosity grade binder. Control of slurry viscosity is a measure of the size of droplets formed during atomization. Binders such as polyvinyl alcohol (PVA) are typically added to slurries to provide green strength to the compacted article. The method of binder addition is of extreme importance if defects in the sintered ceramic are to be avoided, especially in the case of undissolved or undispersed organics, which show up as holes or voids in the sintered press body (Hoffman, D.; 1972).

Immediately after entering the drying chamber, the droplet achieves its maximum drying or evaporation rate. The constant rate drying period follows where moisture migrates to the surface of the droplet maintaining surface saturation (Technical Engineers Handbook, 1973). Droplet temperature remains low and constant. The duration of constant rate drying is dependent on the water content of the droplet, the viscosity of the liquid, and the

temperature and humidity of the drying air.

When the entire droplet surface can no longer be maintained saturated by moisture migration and the falling rate drying period begins, here the droplet temperature begins to increase as the evaporation rate decreases. When the surface is unsaturated and the drying rate continues to decrease as the plane of the evaporation moves inside the droplet. The droplet is now surrounded by a solid crust which can later on show as "doughnuts" or "eggshells".

### 2.2.4 Slurry Atomization Techniques

Slurry atomization is most important for ceramic spray drying operations, in terms of producing the correct particle size and size range desired, and also considering the abrasion which will result on the atomisation head whilst pumping the slip under pressure. There are three types of atomization devices, each chosen for specific end product requirements especially the particle size distribution. Atomization involves the generation of a large number of small droplets from a bulk fluid. Rapid moisture removal is a significant feature of this equipment as a result of the high area to volume of the droplets (Master, K.; 1985).

#### 2.2.4.1 Centrifugal Atomization

Centrifugal atomizers are used in conical drying chambers for high

throughput capacities (Figure 2.11). The atomizer wheels rotate at high speeds (8,000 - 14,000 rpm). Atomization is accomplished by pumping the feed to the rotating head, from which it is ejected at high speeds and broken up into droplets leaving the periphery of the wheel.

Rotary atomizers do not contain small metering passages and are not prone to blockage. Control of droplet size is determined by the design of the wheel or disc. Large diameter drying chambers are required because the droplets exit the atomizer with high horizontal velocity. Both the feed rate and wheel rotational speed of rotary atomizers can be individually controlled offering flexibility to the finished particle size range.

The droplet size is proportional to the slurry feed rate, viscosity and surface tension and inversely proportional to the wheel rotational speed and diameter. Rotary atomizers placed in the upper portion of the drying region of large diameter spray driers offer high flexibility in feed rate and wheel rotational speed and hence control of droplet and agglomerate size, but they are not suited to handle high viscosity slurries (Marshall, K.; 1954).

#### 2.2.4.1.1 Atomizer Wheels

Usual wheel designs include: impact pin, varied and slotted wheels, radial hole, flat disc and inverted saucer types. Each produces particles with unique characteristics. The slotted wheel design is used where fine particles are desired or for a high viscosity feed. The impact pin atomizer is particularly suited to abrasive feeds. Radial hole discs provide a high degree

of particle size uniformity. Factors to consider in the design of atomizer wheels include:

1. Atomization speeds.
2. Power requirements at design speed and feed.
3. No vibration and little noise
4. Reliability
5. Resistance to abrasion.
6. Capacity requirements.

Design of atomizer wheels with ceramic coatings and inserts to increase abrasion resistance is possible (Figure 2.12). Wheel design controls parameters such as film thickness, acceleration rates, degree of aeration of droplets, particle size distribution and powder bulk density.

#### 2.2.4.1.2 Atomizer Drives

A centrifugal atomizer can be driven on an extended shaft by a standard motor through a gear on V-belt arrangement on top of the drying chamber. One drive for this application is a high speed electric motor in a water proof housing. The atomizer is mounted on a very short shaft, and the operating speed never reaches the critical shaft speed. A standard motor driven frequency converter, which can be located out of the process area, produces high frequency current for the motor. Atomization speeds can be varied by changing the frequency.

### 2.2.4.2 Single Fluid Atomization

Slurry is accelerated through a nozzle orifice assembly at high pressure to produce atomised droplets. The capacity or flow rate of this system is controlled by the diameter of the atomiser nozzle. These orifice nozzles are sensitive to highly abrasive slurries causing excessive wear and also to blockage from large particles. Pump maintenance is expensive and difficult to maintain because of the high pressure involved.

Strict control of nozzle wear is required to ensure a uniform spray drying pattern and minimize wall sticking. In single fluid atomization the droplet size is proportional to the size of the nozzle metering passages and to the slurry viscosity and surface tension. It is inversely proportional to the atomizing pressure.

### 2.2.4.3 Dual Fluid Nozzle Atomization

Atomization is effected using this technique when the feed slurry is impacted by a stream of high velocity air (Figure 2.13). It is a useful low capacity method suitable for use in laboratory and pilot plant driers.

Two common types of nozzles are characterised by the location at which the air impinges the liquid. Commonly termed "internal" mixing, when the air and the liquid contact inside the nozzle. "External" mixing when the air contacts the liquid outside the nozzle.

The external mix system is the more versatile because the feed rate and air flow are adjustable over a wide range. Pneumatic nozzles can handle both low and high viscosity fluids. Atomization pressure of the order 1 - 7 bar are required.

The powder characteristics such as size and distribution are determined by feed rate, air pressure and orifice sizes. A wide range of powder size distributions is possible using this method by varying these controls.

### 2.2.5 Drying Chamber Design and Air Flow

The important factors influencing chamber design include direction and degree of atomization, air flow pattern, product discharge, inherent and desired powder characteristics, retention time and air flow rate.

The direction in which atomized particles are thrown determines the basic design, whether it is to be a tall tower to give adequate vertical distance for droplets ejected in a narrow core from a nozzle, or a chamber of relatively large diameter but low height to accomodate droplets spun horizontally from a centrifugal atomizer.

Drying chambers are designed with either a conical or flat bottom, depending on the product to be dried. A flat bottom chamber with pneumatic powder discharge is often preferred for its low and compact construction and for the quick and continuous powder removal associated with this design. Conical bottoms are used when mechanical handling of the powder should be avoided.

Three types of air flow pattern exist, the choice of which is determined by the direction of travel of the atomized spray. They are termed co-current, countercurrent and mixed flow.

### 2.2.5.1 Co-current

Here the air inlet is located near the atomising device (Figure 2.14). Droplets exposed to the hottest air immediately after formation maintain low product temperatures as a result of high evaporation rates, also as the moisture content decreases, the droplet comes into contact with cooler air. Cocurrent air flow is common in driers utilizing rotary atomization.

### 2.2.5.2 Countercurrent

Here the air inlet is located at the opposite end of the drying chamber with respect to the atomizer (Figure 2.15). The droplet immediately contacts cooler air and comes into contact with increasingly hotter air just prior to leaving the dryer. This type should not be used for heat sensitive products.

### 2.2.5.3 Mixed Flow

This type is a mixture of both co and counter current conditions (Figure 2.16). The atomizer is placed at the base of the drying chamber

producing a fountain like spray, contacting with inlet air at the top of the chamber.

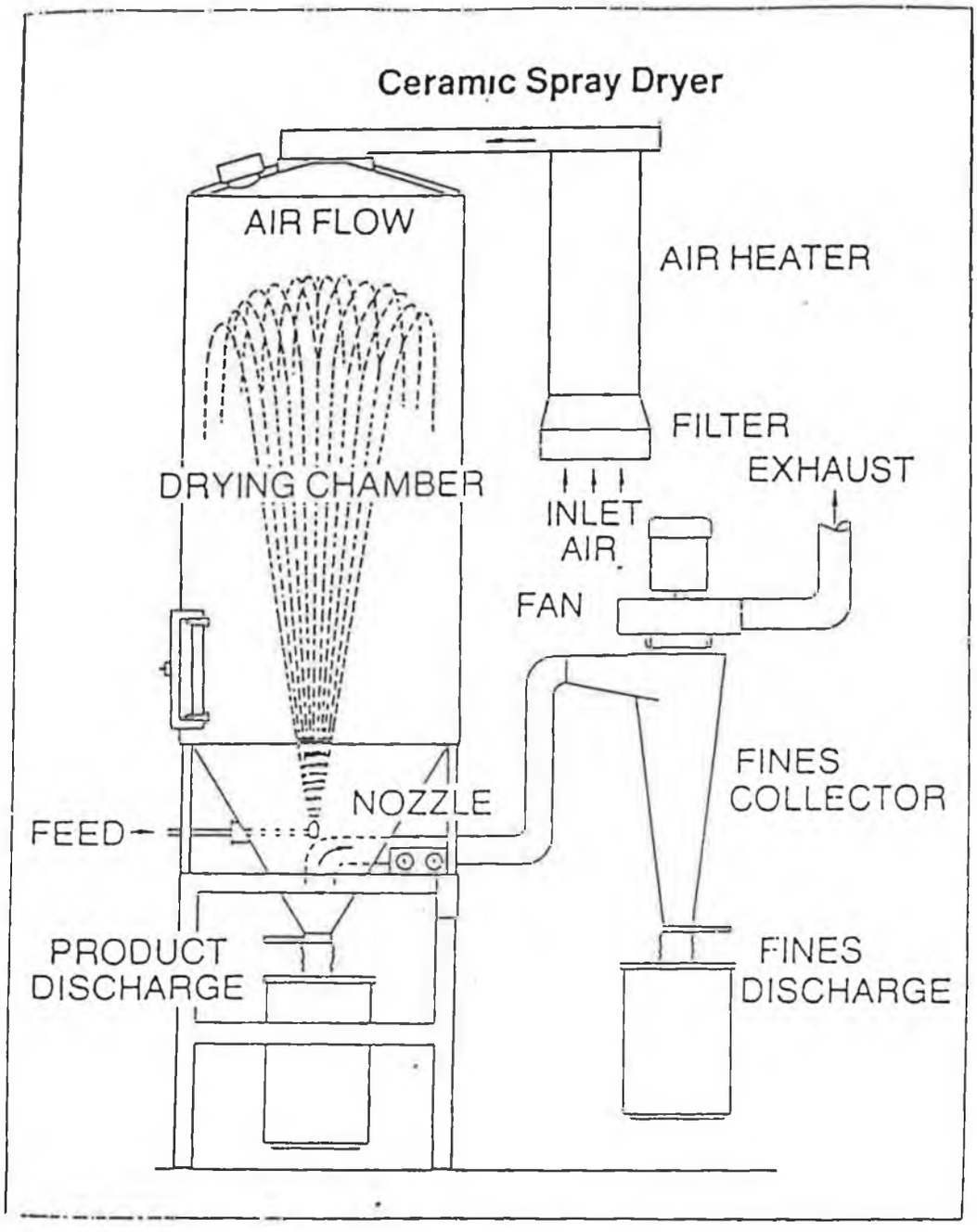


(Source, Master, M.J., 1977)

**Figure 2.9 - Typical Spray Drier Schematic**

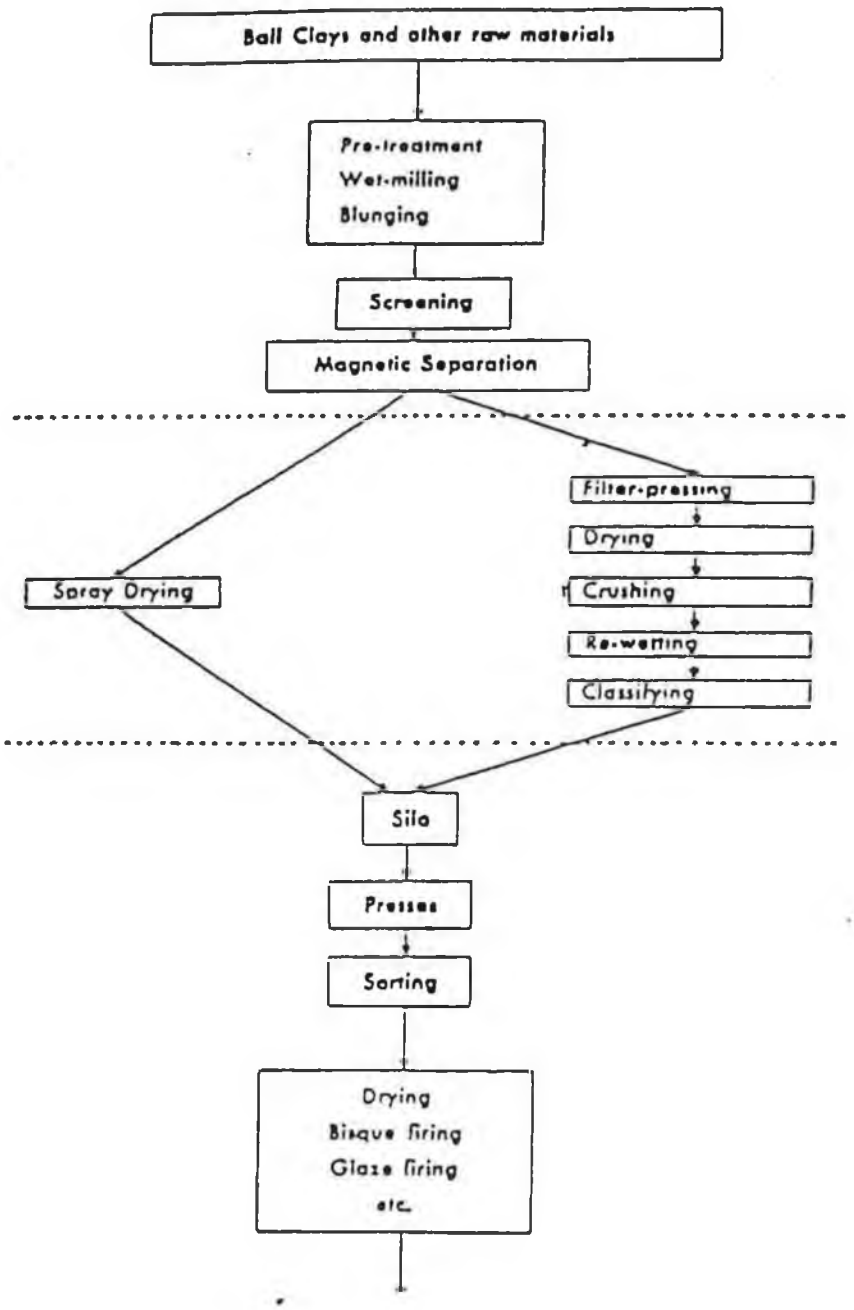


(Source, Master, M.J., 1977)

**Figure 2.10 - Comparison of Traditional Drying versus Spray Drying**

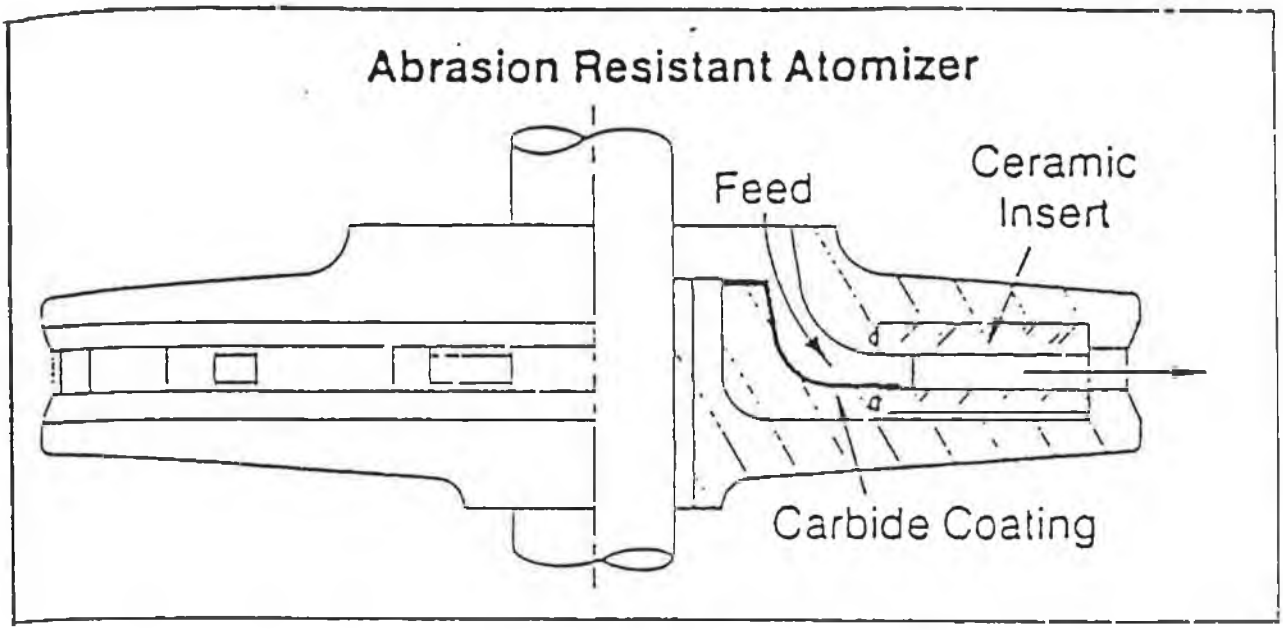


**(Source, Niro, Commercial Brochure)**

**Figure 2.11 - Atomizer Wheel with Ceramic Inserts**

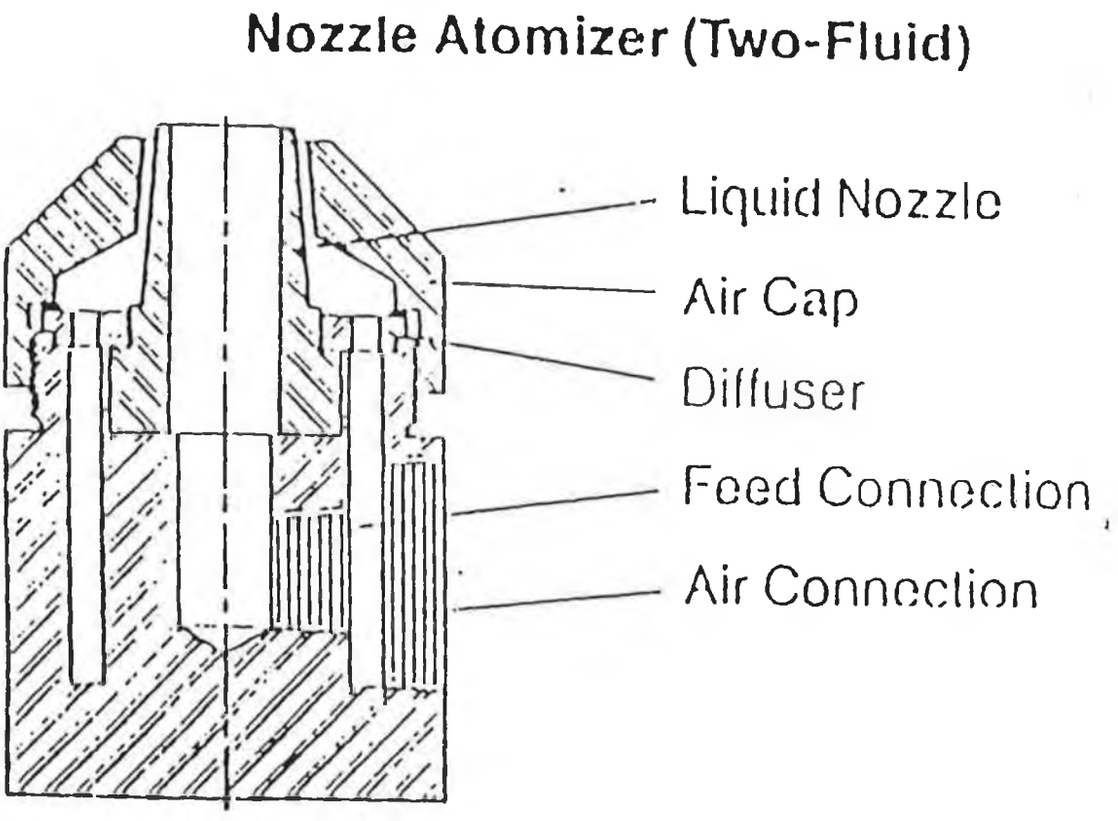


**(Source, Anhydro, Commercial Brochure)**

**Figure 2.12 - Dual fluid Atomization**

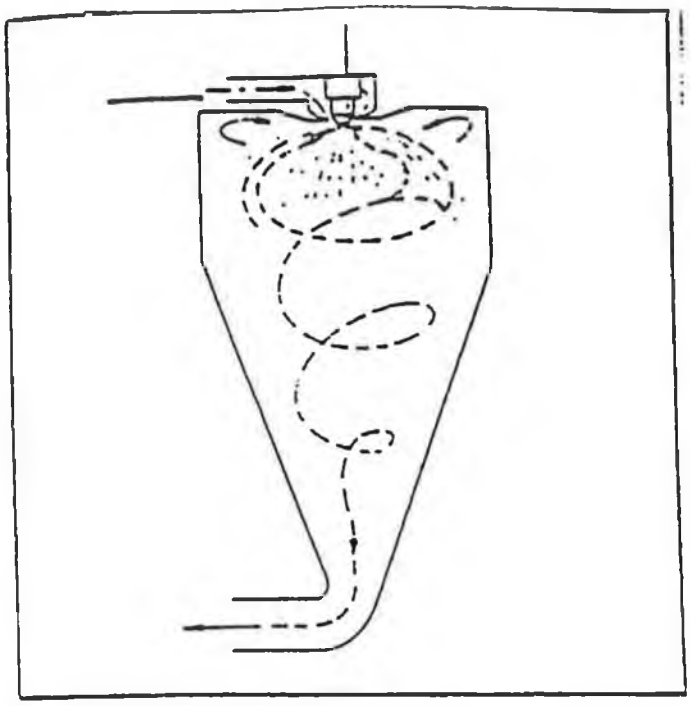

*General purpose applications: conical chamber with co-current air flow; centrifugal atomization; all product air-conveyed to collector, alternately coarse fraction separated at chamber.*

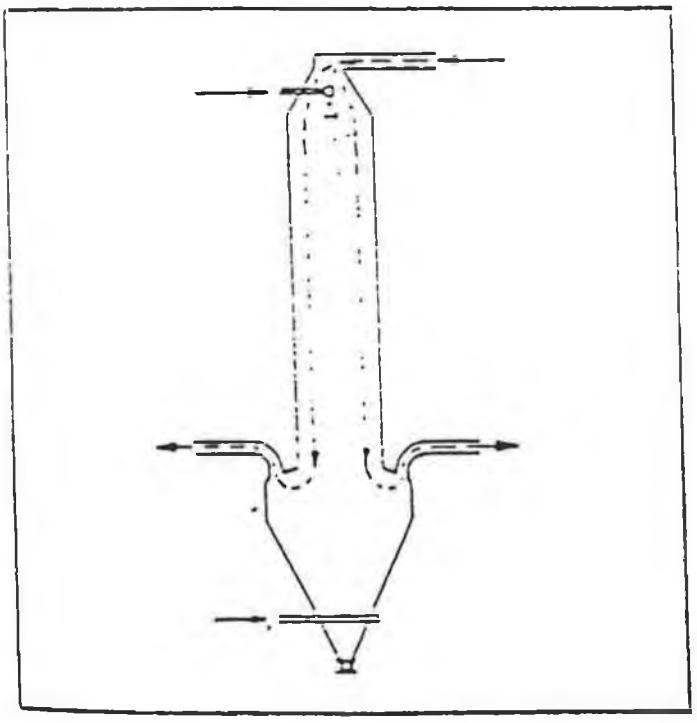

*For large fragile particles (e.g coffee): tower with co-current, linear air flow; settling zone with air inlet separates and cools product; pressure nozzle atomizer.*

**(Source, Master, M.J., 1977)**

**Figure 2.13 - Cocurrent Air Flow Chamber Design**

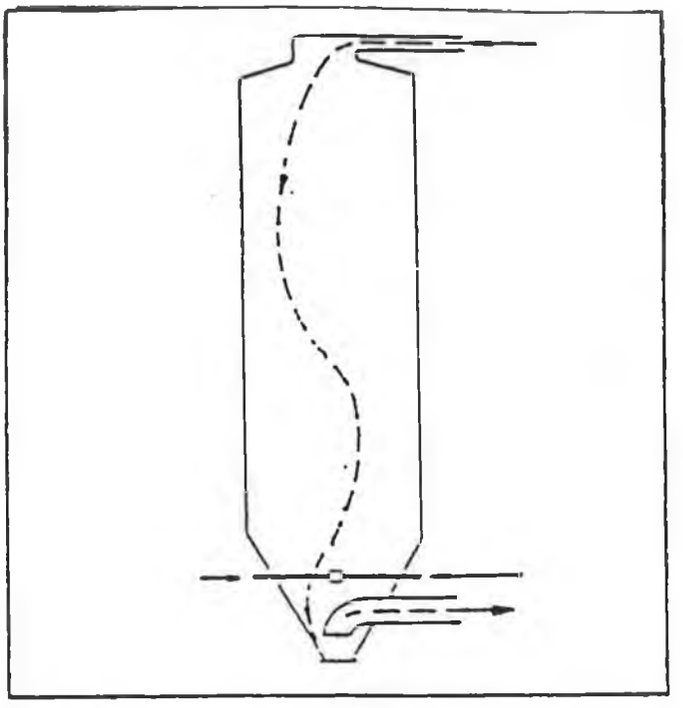

*For large particle size at low to medium evaporation rates, for non-heat-sensitive products (e.g. ceramics); tower with mixed air flow, 2 fluid or pressure nozzle atomizer in fountain spray*

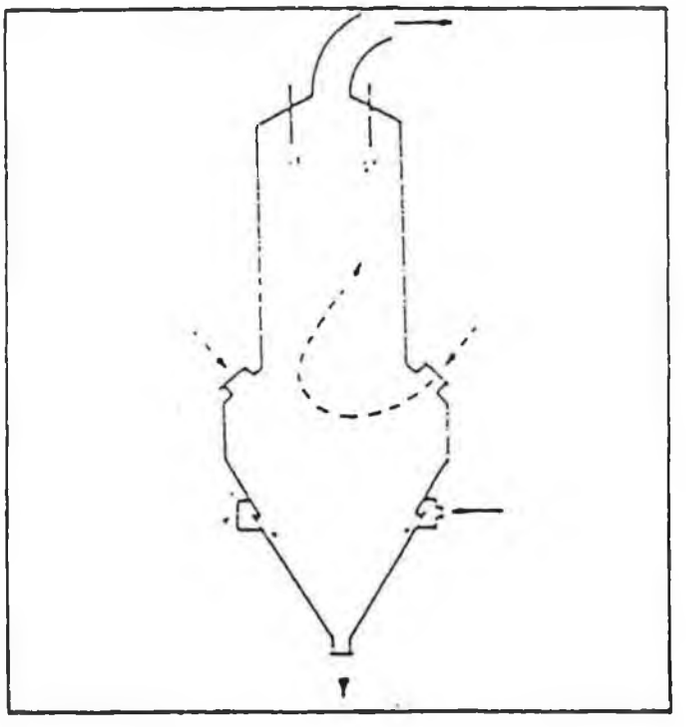

*For large particles, non-heat-sensitive products (e.g. detergents); tower with countercurrent air flow; settling zone with cold air inlet; multiple pressure nozzle atomizers.*

**(Source, Master, M.J., 1977)**

**Figure 2.14 - Countercurrent Air Flow Chamber Design**

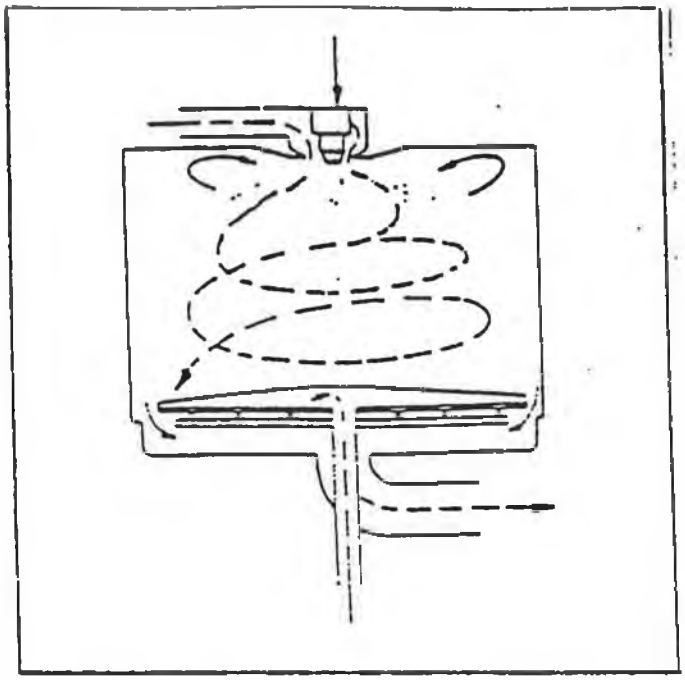

*For very heat-sensitive products: flat bottom with side air ports and air sweeper to cool particles before collection; centrifugal atomization; low headroom.*

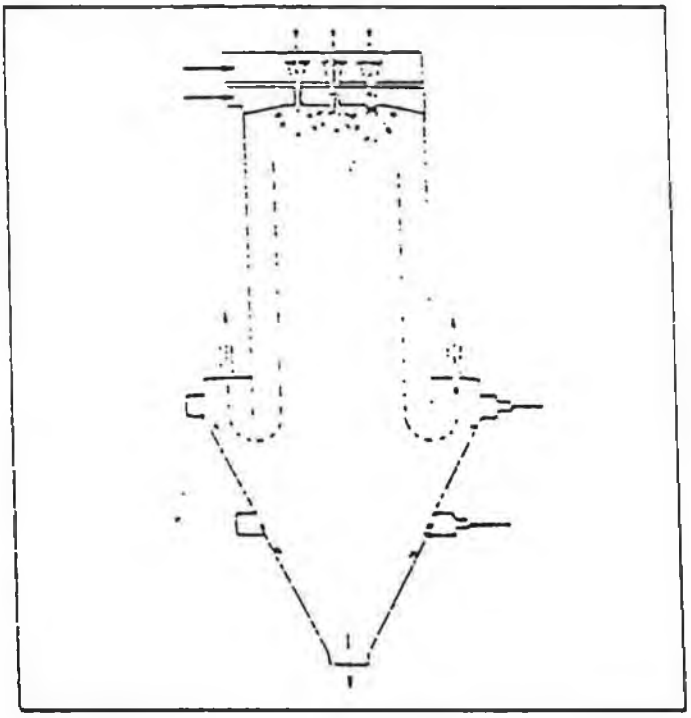

*For food and dairy applications: tower with multiple pressure nozzle atomizers, each with venturi hot air inlets for intensive air:spray mixing; settling zone with cold air inlet.*

**(Source, Master, M.J., 1977)**

**Figure 2.15 - Mixed Fast Flow Chamber Design**

## 2.3.0 LITERATURE SURVEY OF POWDER CHARACTERISATION AND COMPACTION

### 2.3.1 Introduction to Ceramic Powder Pressing

The manufacturing of ceramic bodies by dry pressing involves the simultaneous, compaction and shaping of a powder or granular feed material followed by sintering at high temperature. Some commonly used forming methods include mechanical and hydraulic pressing also both cold and hot isostatic pressing. Selection of the forming technique largely depends on the final part application.

Significant features of any formation technique include powder characteristics, choice of binders, pressure applied and the rate of application, pressing cycle and economic considerations such as cycle time/machine speed, number of punches. Highly fluid slurries may be cast at atmospheric pressure (0.1mPa), whereas viscous pastes used during extrusion processes require pressures up to 10 mPa. Dry powders need pressures up to 100 mPa in order to produce coherent compacts suitable for handling and further processing. The importance of this method lies in its speed, capacity and potential for automation, (Stuijts, A.L. et al; 1965).

This review will examine organic binder systems in pressing grade powders, and how they translate to powder characteristics such as compactability and green strength, and subsequently the stages during compaction of powders in a circular die by uniaxial pressing.

## 2.3.2 Review Organic Binder Systems

Organic additives used in the processing of zinc oxide varistors are essential to achieving powder properties suitable for further processing, however they are also a prime source of defects in both the finished sintered microstructure and the cause of manufacturing problems. They act as a processing aid to spray drying and pressing, after these stages, it is necessary to remove them from the ceramic body without generating defects such as pinholes or cracks during the organic removal stage of the sintering profile. A typical organic system used during the processing of zinc oxide powders for varistor applications will include deflocculants or dispersing agents to allow easy mixing or dispersion of a high solids content slip, binders and plasticiser to aid with ejection from the die.

Dispersing agents control particle surface charge (charges all particles with the same surface charge) and so avoids the formation of flocs by making the primary particles mutually repulsive. The deflocculants control the pH value (this controls the gelling of the binder with certain ions) and allows greater dispersion, a larger slurry viscosity and higher solids content. Typical defloculants used in ceramic slurries are polyelectrolytes and synthetic and natural gums.

The binder (usually Poly Vinyl Alcohol) bonds the primary particles together in the spray dried particle and gives green strength to the press body. Plasticiser is a rheological aid, this improves the flexibility of the binder films, allowing plastic deformation of spray dried granules which reduces the

amount of springback in the pressed body, which is essential to the ejection of zinc oxide press bodies from the die, otherwise catastrophic lamination or cracking will occur.

Lubricants such as stearates are frequently added to the slip to become an integral part of the powder mix. Lubricants act to increase interparticle sliding (reducing particle-particle friction and particle-die wall friction). (Cannell, D. et al; 1974). They are particularly useful for parts with high aspect ratios in order to minimise density gradients caused as a result of friction between the die wall and the powder. Zinc stearate is frequently used as a lubricant for zinc oxide varistor powders.

Anti-foaming agents reduce surface tension thereby eliminating the foam which causes the slip to be aerated which in turn increases viscosity. Small amounts of anti-foaming agents are required (typically $< 0.05\%$).

The primary purpose of a binder during spray drying is to provide enough adhesive quality and strength to stabilise the special particles produced by the atomization of the slip into dried powder form (Hoffman, E.; 1972).

The selection of a binder should ensure that it remains robust to normal processing conditions. The most popular organic binder used in ceramic processing, contain hydroxyl functions. This hydroxyl group makes the material hydrophillic and therefore unstable during aqueous processing (Pincus, A. G.; 1969). There are a number of different types of PVA with various molecular weights, and it can be partially or fully hydrolysed (Hoescht, Commercial Brochure).

The glass transition temperature is defined as the temperature or range of temperatures below which an amorphous polymer is glassy and rigid and above which it is flexible and deformable (Rosen, S.L.; 1982). The plasticing effect of Polyethylene Glycol (PEG) on PVA results in a decrease in the glass transition temperature Tg, resulting in increased deformability of the powder. Use of a plasticizer can reduce the tendency for a coating containing an organic binder to crack during drying or in the early stages of firing (Smith, T.A.). Pressing powder containing PVA plasticised with PEG will exhibit a higher density at a given pressure, but a lower green strength compared to the non-plasticized powder. This is due to the lower adhesion strength of the PEG/PVA combination.

Water also acts as a plasticizer for PVA, as with PEG, an increase in moisture content in the powder lowers the glass transition temperature and the apparent yield point. The density of the final compact increases with moisture content (Brewer, J.A. et al; 1981).

The humidity of the storage and press areas will strongly affect the moisture content of the powder. The amount of moisture absorbed per mass of powder increases with increasing organic content as PVA and PEG enhance moisture absorbtion (Di Milia, R.A. et al; 1983).

### 2.3.3 Powder Compaction

On pressing a spray dried powder, the compaction pressure applied deforms the agglomerates into a coherent compact. Significant reduction in

porosity occurs. The number of interparticle contacts increases as do the bonds formed within the pressed body (Brewer, J.A. et al; 1981).

The present work examines the consolidation of ceramic powders using uniaxial pressing inside a cylindrical die and punch. The following steps in a press profile normally exist:-

(1) Uniform filling the die with a specified weight of free flowing powder.

(2) Slow de-airing the powder in the die by the application of low pressure (< 10T) including a high initial densification rate.

(3) High pressure compaction of the powder into a desired shape, with a reduction in the volume of inter particle voids, and corresponding bulk density increase.

(4) Formation of interparticle bonds under the application of pressure at equal rates from both sides.

(5) After a dwell at high pressure, removal of the compacting pressure again at equal rates from both sides.

(6) Controlled ejection of the part from the die to ensure that no damage is caused to the green part.

Extreme care should be taken when pressing varistor powders into devices with high aspect ratios. This is to avoid mechanical damage to the parts in the green state such as laminations, end cap and ring defects. (Figure 2.16). In some cases the damage may not be evident until after the sintering process is complete. Timely detection of these problems using non destructive testing is increasingly finding popularity with techniques such as ultrasonic

testing.

In general three main stages during the densification of the compact include (1) granule fracture and filling of voids with some elastic or plastic deformation. The first stage of the compaction process forms powder into a cohesive unit with a particular shape and microstructure. High densification rate, increasing rapidly at pressures greater than 5 - 10 mPa is one feature at this point. The initial stresses are transmitted by interparticle contacts, causing granule deformation and porosity reduction. De-airing takes place, air escaping between the punch and die.

(2) Filling of the small voids and spaces by grain size reduction of the large granules or by plastic deformation (Reymer,A.P.S.; 1990).

(3) Pressures of up to 100mPa are common for high performance technical ceramics. Final compact densities of up to 60% of the theoretical maximum are common. At high pressure die wear is rapid and is also dependent on the hardness and quality of surface finish of the tooling. Punch faces are frequently polished to 2$\mu$m to ensure long tool life and quality of the pressed part (Reed, J.S.; 1987). A low compacting ratio will normally produce better compacted parts.

The compaction of spray dried agglomerates has been shown to take place in three stages. (Di Milla, R.A. et al; 1983). Figure 2.17 shows the relative density of spray dried Alumina as a function of the applied pressure up to 10 mPa applied pressure a slight increase in density occurs owing to the sliding or rearrangement of granules. Granule deformation and fracture takes place up to 100 mPa filling the relatively large intergranular interstices.

Granules yield at pressures typically of the order 1MPa when a soft and ductile binder system is used. The final stage of compaction occurs when most of the large pores among the granules have disappeared and a dense packing configuration in formed.

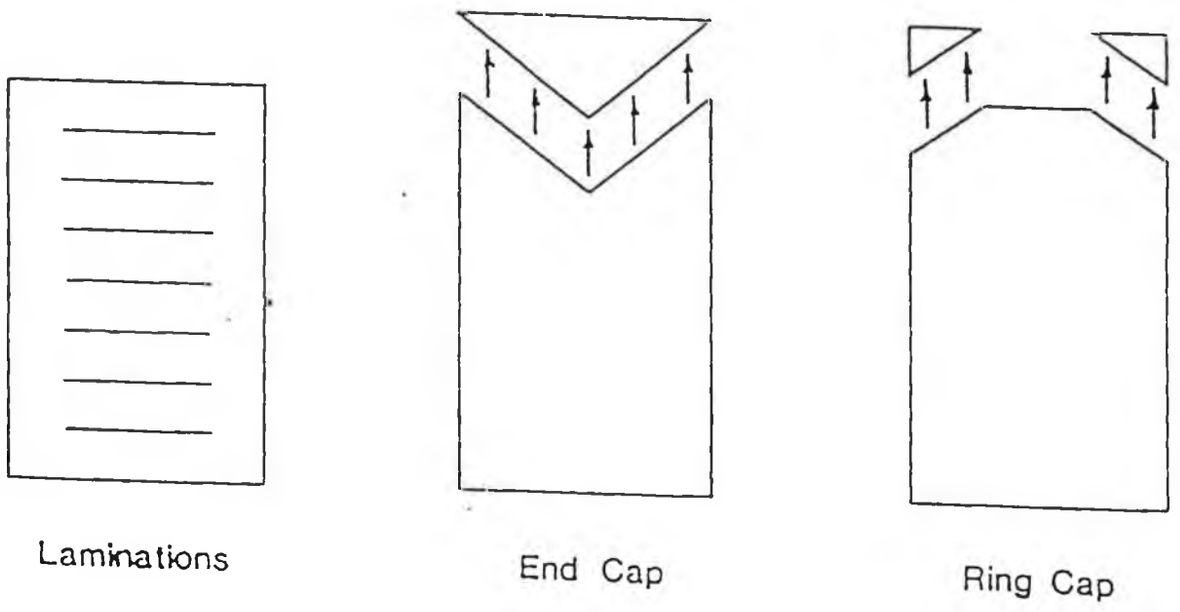


(Source O'Sullivan, F. ; 1990)

**Figure 2.16 Common defects in pressed compacts.**

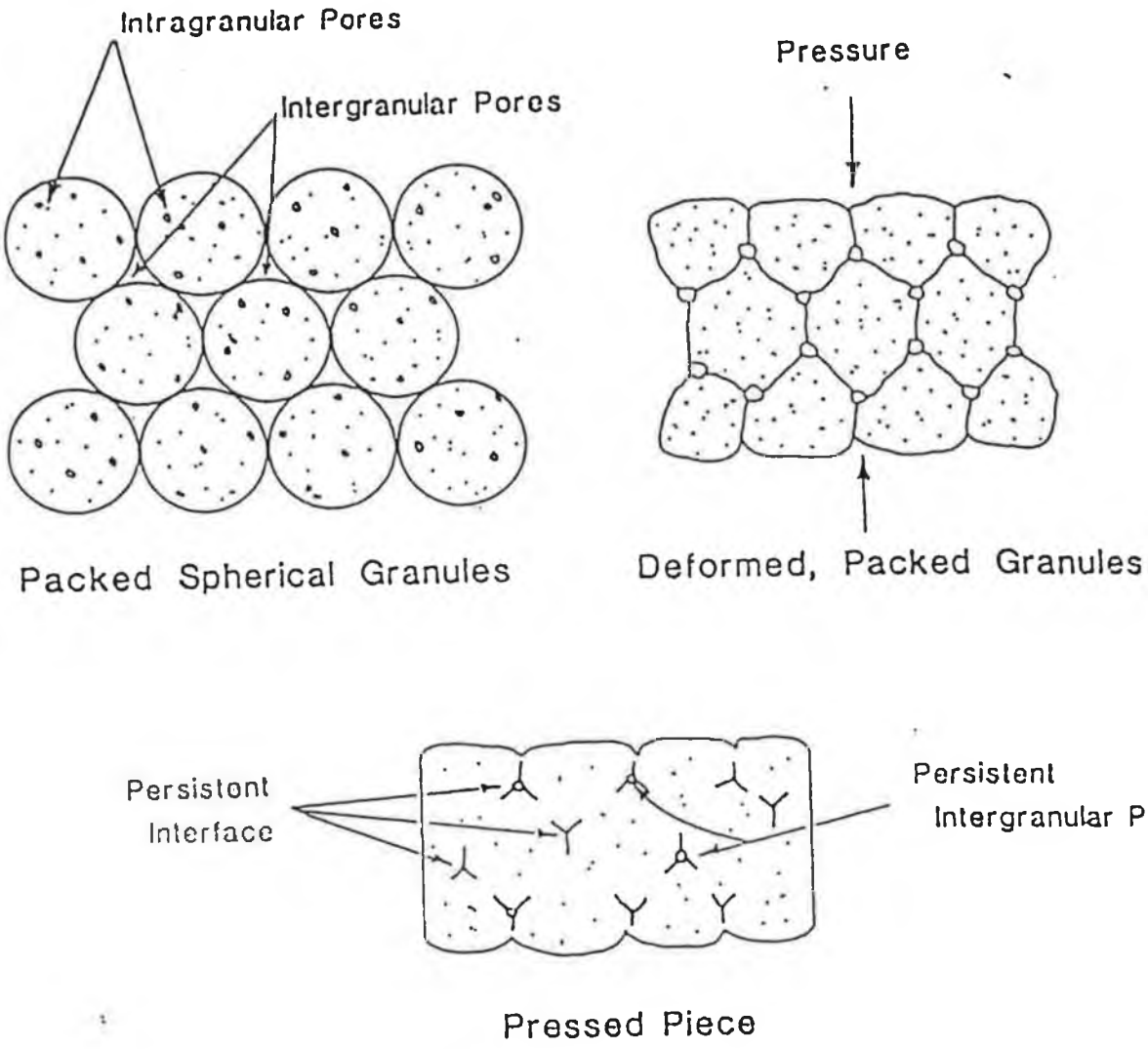


**(Source O'Sullivan, F. ; 1990)**

**Figure 2.17 - Stages in the compaction of a ceramic Powder**

Emeruwa, E. et al; 1989, studied the effect of applying ultrasonics during the pressing operation. The compaction behaviour of the ceramic powder was improved resulting in a drop in pressure required to press the part when using ultrasonics, also reduction in porosity was noted as a result of filling intergranular pores.

Nyberg, et al; 1988, studied the effects of using both PVA and latex binders on pressing performance and the green structure and sintered density of alumina particles. They found that hollow granules were formed when using PVA compared to a significantly low content of hollow granules using latex. They also found that higher densities were achieved at lower pressures using latex, and force of ejection from the punch was reduced when zinc stearate lubricant is added. After sintering the latex systems exhibit highest sintered density compared to PVA because of the large number of unsinterable pores in the PVA system.

Wang, J.; 1984, studied the effects on the binder burn out rate using conventional uniaxial die pressing and cold isostatic pressing. He found that CIP parts exhibit a lower sintered density and more porosity than conventionally pressed parts, although CIP favours higher and more uniform green density. Processing related flaws due to the delayed burnout of an organic residue or binder are more likely to occur in cold isostatically pressed powder compacts than in uniaxially pressed compacts.

Kendal, K. et al; 1986, proposed a new theory of green strength of pressed compacts. The theory explains the effects of particle packing of grain size, of powder mixing, and of environment. They found that the distribution

of large flaws in the green body remain unchanged through sintering, besides further flaws can be introduced by grain growth. In addition they proved that green bodies fail by cracking, verified by the application of the Griffith energy balance theory to green body strength. They conclude that the ceramic particles are strongly bonded to one another in the green state, at small contact areas, and that sintering is merely an expansion of the contact regions between the grains. This result has significant implications for the attainment of stronger more reliable ceramics. This work was conducted on samples of alumina and titania.

Lukasiewicz, S.L.et al; 1986, discuss the characteristics of industrially prepared spray-dried agglomerates and modes of compaction response during dry pressing. They found various sizes of craters independent of agglomerate size caused by excessively high drying temperatures. They found that when yield pressure is exceeded, agglomerates deform plastically by internal particle sliding and rearrangement into interstices. They showed that compaction of a narrowly classified sample of agglomerates at one ton the compaction response was independent of particle size. Aggregates of agglomerates retard compaction during the final stages of compaction and achievement of a narrow range of pore size. Coarse pores persist during sintering and are especially deleterious to mechanical strength. They conclude that using compaction diagrams to optimise pressing material may indicate problems arising from irregularity in organics additive mixtures, milling of aggregates and /or the spray drying process.

Dynys, F.W. et al; 1984, studied the behaviour of aggregated powders during uniaxial pressing. They found that by increasing the pressure applied the population of aggregates decreases, but they are not eliminated. This decreases the total volume porosity and corresponds to an increase in theoretical density. The presence of aggregates tends to retard the compaction rate at all stages in the compaction process.

Brewer, J.A. et al; 1985, investigated the compaction behaviour of agglomerated barium titanate and manganese zinc ferrite pressing grade powder prepared by spraying drying. Variables under consideration include % PVA and absorbed moisture. They found agglomerate yield strength more dependent on the % RH (Relative Humidity) in which the powder was stored than the % PVA added in the range 1.3 - 2%. Variation in the % RH of the stored atmosphere can produce significant variation in the powder pressability and finished part dimension at a given pressure. This in turn gave higher green strength.

## 2.4.0 Present work and its objectives

The present work involves a study of the effect of varying the comminution techniques employed to mill varistor dopants. Both dopants and zinc oxide are mixed together to form a full formulation varistor slip for spray drying. The objective of the present work is to see the effect of the commminution process on the microstructure and energy absorption capabilities of low voltage zinc oxide varistors.

The study will attempt to make improvements as suggested by

literature, to the processing of powders for zinc oxide varistor applications, using a proprietary commercial varistor formulation and conventional ceramic manufacturing process, by specifically varying the comminution techniques employed prior to spray drying at the beginning of the process. The effects on the particle size distribution of both the oxide dopants and the zinc oxide - dopant mixture, are measured and changes made to these parameters are related to the ceramic microstructure and electrical performance measured under test conditions, in an attempt to optimise end product performance effected by processing.

## CHAPTER 3 EXPERIMENTAL METHODOLOGY

## 3.1 Introduction

The present experimental work examines how a variety of commercially available comminution techniques used during the conventional ceramic manufacturing process can be implemented to prepare low voltage zinc oxide varistors. The comminution technique chosen affects the particle size distribution of both dopants and full feed formulation (zinc oxide-oxide dopant slurry) and the resultant microstructural and electrical performance characteristics. The approach taken in this study was to investigate these effects as a consequence of varying the comminution technique in an established manufacturing process on both the dopant and full feed slip for spray drying. The resulting particle size distributions are then compared to microstructural observations regarding estimated grain sizes, intergranular and intragranular porosity, bismuth oxide distribution, and electrical characteristics such as breakdown voltage, energy handling capacity, voltage reliability, residual voltages and leakage currents. This comparison is used to optimise the quality of zinc oxide varistors produced using this process.

## 3.2 EQUIPMENT USED

### 3.2.1 BALANCE

Weighing of the dopants was carried out using a Mettler PM 6100 balance capable of weighing up to 6.1kg with a resolution accuracy of 0.01g.

### 3.2.2 SHEAR MIXER

A Greaves model GM 95 (Figure 3.6) high dissolver mixer was used. The machine is designed for material batch processing capable of producing a low globule suspension of insoluble solids, including the reduction of large pre milled agglomerates.

A typical varistor composition (Matsuoka, M.; 1986) includes 97 mol% ZnO, 1 mol% $Sb_2O_3$ and 0.5 mol% each of $Bi_2O_3$, MnO, CoO, and $Cr_2O_3$. All chemicals of reagent grade are checked for trace quantities of impurities and then each additive is weighed to recipe accuracy of +\- 0.5% by weight and stored in airtight containers.

The powders for all experimental work were prepared in the laboratory and pilot line facilities.

### 3.2.3. BALL MILL

The ball mill (Photo 3.7) in the experiment comprised a variable speed roller set, with a two litre PVC jar containing a 50% by volume media charge. Rotational speed adjustment effected the cascading action required for particle size reduction. Grinding media were zirconia cylinders 10mm in diameter, 12mm long.

### 3.2.4. VIBRATORY MILL

A Sweco M18 vibratory mill (Photo 3.8) was used. The M18 grinding chamber supported on springs was bolted to the floor. An arrangement of eccentric weights driven by a 0.5kW, 50hz motor, creates a three dimensional vibration of the media at a frequency of approximately 20hz.

An air driven pump is used to recirculate the slurry in the mill. The effect is

a faster, more uniform particle size reduction. The chamber is carefully rinsed with de-ionised water after each milling cycle is completed. This helps recover the complete charge and prevents cross contamination with the next sample.

### 3.2.5 ATTRITION MILLING

A Dyno mill model KDL (Figure 3.9) was used. Attrition mill construction includes a totally enclosed stationary grinding chamber filled to 80% by volume with the chosen grinding media activated by a rotating shaft complete with agitators. The excessive heat generated is removed during the grinding operation by a water cooling jacket. The mill charge is pumped through the chamber by a peristaltic pump until the required particle size distribution is achieved. A special feature of the attrition mill is its ability to produce distributions with maximum particle sizes less than one micron. It is usual to control the attrition milling process by monitoring the number of times the charge passes through the mill chamber, product outlet temperature, pressure and motor currents. Significant care must also be taken to examine media and agitator wear rates.

### 3.2.6 TURBULA MIXER /MILL

A model T2C (Figure 3.10) laboratory Turbula mixer/mill with two litre jar, filled to 50% by volume with zirconia media was used. The Turbula is capable of producing a complex three dimensional movement causing intense turbulence and excellent mixing homogeneity.

### 3.2.7 SPRAY DRYING

A Bowen (Figure 3.11) spray drier was used to convert the full feed varistor slip into a pressing grade powder. A gas powered air heater raises the temperature

of the air flow chamber to that required to dry the atomised feed slip into granules collected in a container at the bottom of the conical drying chamber. The water evaporated is exhausted from the chamber where the entrained fine particles are separated from the air by centrifugal acceleration and discharged into a sealed jar, then the clean filtered air is discharged to the atmosphere.

### 3.2.8. POWDER PRESSING

Powder compaction into pellets was carried out using a Courtoy rotary tableting press (Figure 3.12) High grade tungsten carbide dies of diameter 7.86mm were filled with free flowing powders. Thorough cleansing of the punches and cavities are essential to prevent sample cross contamination with different types of varistor powders.

Pressed pellets were checked for weight and thickness inside a target tolerance band, parts failing to meet the desired specifications were rejected.

### 3.2.9 SINTERING

A Surefire T525 (Figure 3.13), Pot kiln manufactured by K+F Ltd, Staffordshire, UK, was used to sinter all samples which were dump loaded into Alumina saggers lined with zinc oxide liner plates to prevent cross contamination with the refractory. The kiln was equipped with a West 2054 programme control unit which has eight temperature control modules, each with four ramp and dwell stages and is capable of being linked together. A Harris proprietary temperature profile was used to sinter the varistor samples.

This sintering unit was programmed to fire the silver electrode paste applied to the sintered ceramic discs as the electrical contacts. The paste was screen printed onto both flat surfaces of the devices.

### 3.2.10 POWDER CHARACTERISATION EQUIPMENT

A Malvern model SB.08 particle sizer using laser scattering was used to measure the particle size distribution of all samples. (Figure 3.14).

This is a technique where the light from a low power helium-neon laser is used to form a collimated and monochromatic beam of light. This beam of light is known as the analyser beam and any particles present within it will scatter this laser light. The particles are introduced into the analyser beam by use of the sample cell. The set up used in this analysis was powder in liquid. The light scattered by the particles are incident onto a receiver lens, here a custom detector, in the form of 31 concentric sectors, gathers the scatterred light over a range of angles of scatter. When a particle scatters light it produces a unique light intensity. It scatters light on the detector at an angle which is related to its energies in large angles of scatter. The detector provides an electronic output signal proportional to the light energy measured over 31 separate angles of collection. The computer reads the signal and converts it into particle size data (Figure 3.1).

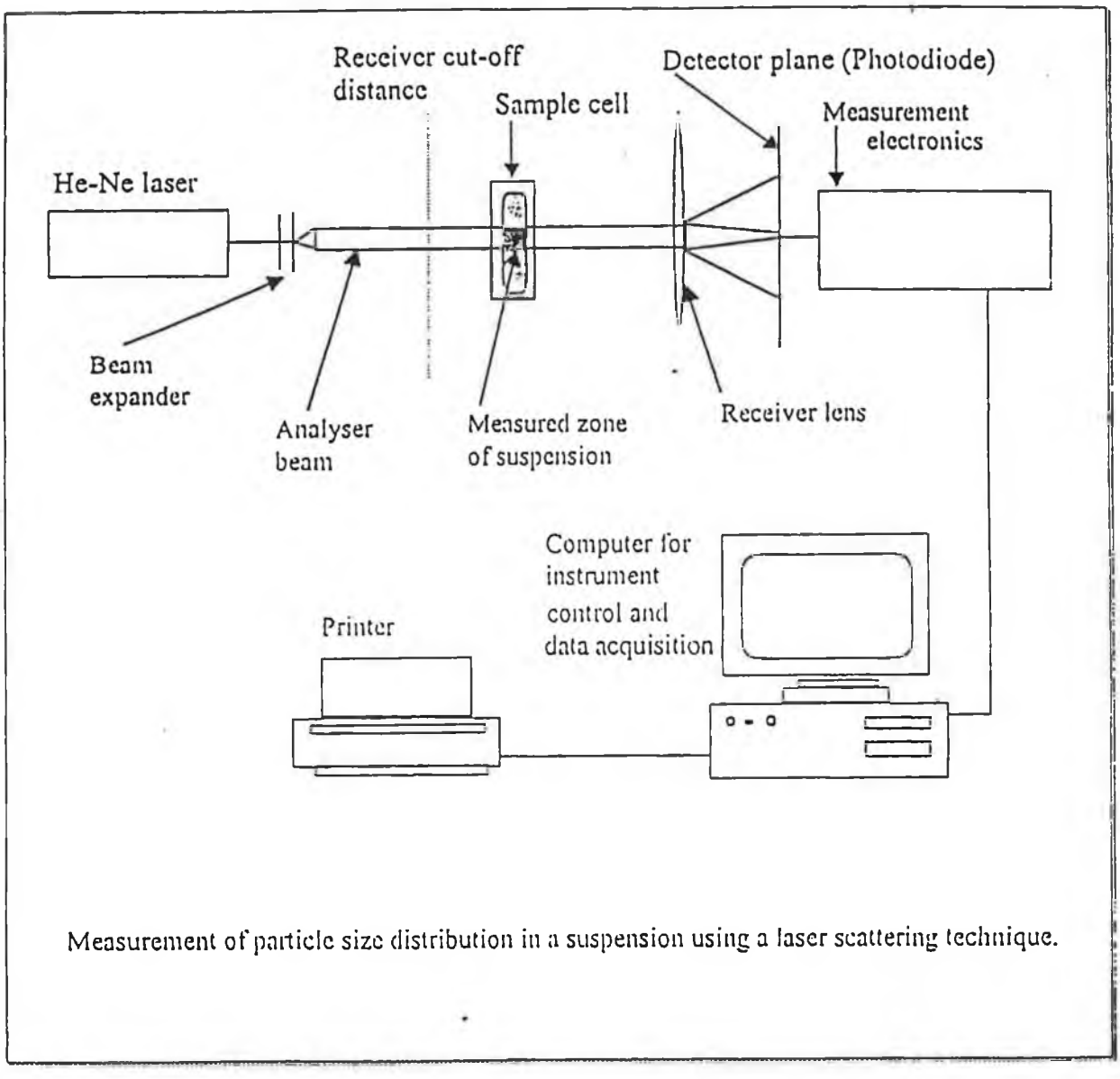


Measurement of particle size distribution in a suspension using a laser scattering technique.

**(Source: Malvern Commercial Brochure)**

**Figure 3.1 - Measurement of particle size distribution using a light scattering laser technique**

Bulk density of the agglomerated samples was measured using a graduated cylinder and the Mettler PM 6100 balance, The bulk density is then calculated according to Equation 3.1:-

Bulk density= Mass (M1)/Volume(V1) .....Equation 3.1

The samples were then placed in Quantachrome model A46 tapping machine, (Photo 3.2.10.2B) and then the tap density after 1000 taps is calculated according to Equation 3.2:-

Tap density = Mass (M2)/ Volume (V2) .....Equation 3.2

The moisture content of the powders were determined by measuring the weight loss of a 5g sample after heating it to 120°C for 1hr.

The binder content of the samples was determined by measuring the weight loss of the same 5g sample after heating it to 520°C for a further 1hr.

### 3.2.11 MICROSTRUCTURAL ANALYSIS

A Japan Electron Optics Laboratory scanning electron microscope model JSM 840 was used to examine the ceramic microstructure at high magnification. Samples are loaded into the chamber, bombarded with an electron beam focussed onto a small area of the sample, scattered electrons of several types are collected by a fixed detector and the signal fed to a Cathode Ray Tube. The beam sweeps the surface of the samples synchronously displaying a trace image of the speciment on the CRT.

In addition to the detection of secondary electrons and back scattered electrons the JSM-840 can accommodate detection of cathodoluminescence, X-rays, adsorded electrons, transmitted electrons. It can be expanded and made an electron probe X-ray microanalyser by adding energy dispersive spectrometers, allowing accurate and efficient non-destructive elemental analysis and elemental distribution study of micro areas. (Figure 3.2 Scanning electron microscope, Signals emitted from specimens).

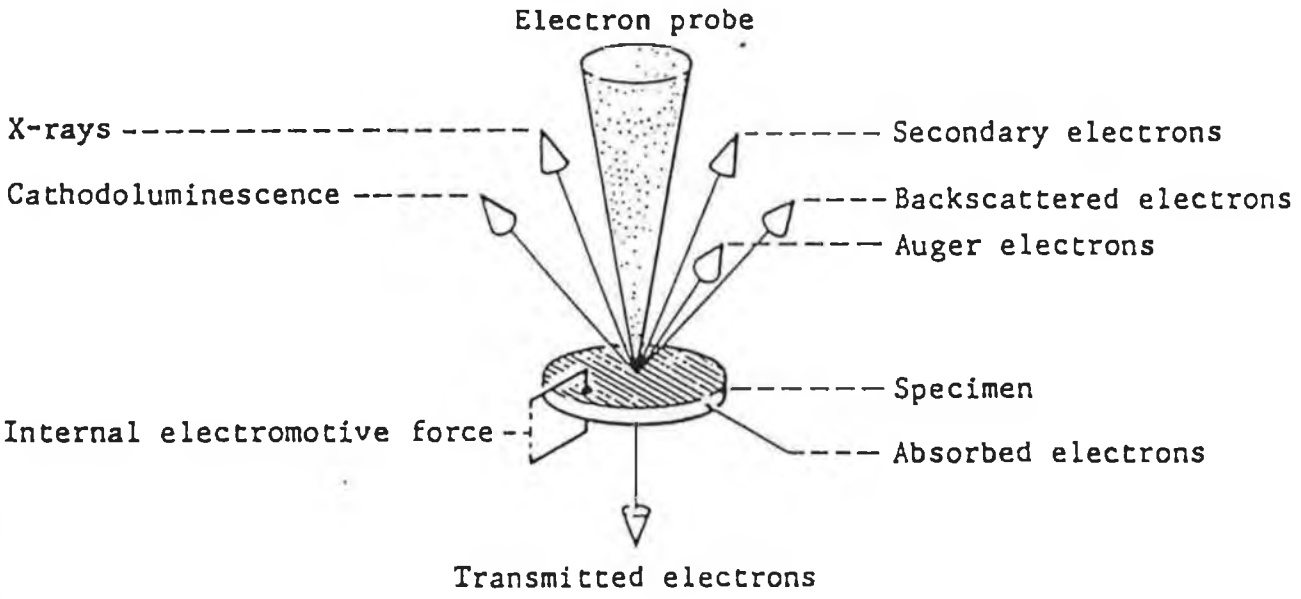


**(Source: Japan Electron Optics Laboratory)**

**Figure 3.2 Scanning electron microscope signals from specimens.**

## 3.3.0 POWDER SAMPLE PREPARATION

### 3.3.1 INTRODUCTION

The purpose of powder sample preparation was to allow a full characterisation of the effects on varistor powders and discs, caused as a result of varying the comminution techniques. To achieve this end a fully blocked, designed experiment was prepared and excecuted in the pilot manufacturing facility at Harris Ireland. The first step was to select a suitable combination of mixing-milling techniques, then translate the chosen variables into a manufacturing flowchart and produce the powders in a fully blocked designed experiment. This approach ensures that any observations made regarding different characteristics of the devices are purely the effects caused by the variables under evaluation. A manufacturing flowchart depicting the order in which the devices were constructed was then developed. (Figure 3.3).

### 3.3.2 RECIPE WEIGH UP

A total of eight powder samples were produced using the proprietary varistor formulation. Oxide dopants for each powder were individually weighed to within 1% of the target weight, then stored in clean plastic bags, the processs continued until all recipes were completed and the bags then labelled and sealed. The weights of organics and zinc oxide were also weighed for each of the eight samples in a similiar manner. To ensure blocking the experiment at this stage all elemental ingredients were selected from the same manufacturers lot number.

| Lot Size each group | Flowchart | | Sampling from each of the 8 groups |
|---|---|---|---|
| | ZnO plus Dopant Weigh up | | |
| | Milling Dopants | → | 5g ea for particle size analysis |
| 25 kg | ZnO Dopant Mixing | → | 5g ea for particle size analysis |
| 25 kg | Spray Drying | → | 1 kg ea for moisture, binder, bulk, tap density |
| 200 pcs | Pressing | → | 10 pcs ea for height, weight check |
| 190 | Sintering | → | 2 pcs ea for microstructure evaluation |
| 188 | Assembly | | |
| 90 | Test | → | 50 pcs ea for Vnom testing<br>10 pcs ea for maximum rated voltage test.<br>10 pcs ea for energy, clamp voltage at peak current |
| | ↓ | | 10 pc ea for energy at rated voltage. |
| | Unused samples retained for future analysis | | |

**Subscript Notation for 8 samples**

| Sample # | Milling Dopants | Mixing Dopants ZnO |
|---|---|---|
| T-T | Turbula | Turbula |
| T-S | Turbula | Shear |
| B-B | Ball | Ball |
| B-S | Ball | Shear |
| V-A | Vibro | Attrition |
| V-S | Vibro | Shear |
| A-A | Attrition | Attrition |
| A-S | Attrition | Shear |

**Figure 3.3 - Flowchart showing lot sizes and notations for each of the eight groups of powders, including samples taken for testing during the process**

### 3.3.2 RECIPE

A total of eight samples were produced using the proprietary varistor formulation. Oxide dopants for each powder were individually weighed to within 1% of the target weight, then stored in clean plastic bags, the process continued until all recipes were completed and the bags then labelled and sealed. The organics and zinc oxide were also weighed for each of the eight samples in a similar manner.

To ensure blocking out the effects of any variables at this stage, all elemental ingredients were selected from the same manufacturers lot number, and stored under the same conditions, for similar durations.

### 3.3.3 MIXING/MILLING VARIABLES

This study examines the effects of varying the dopant - ZnO milling/mixing combination used during the powder manufacturing process, on the particle size distribution of dopants and the dopant-ZnO mixture, microstructural and electrical characteristics of the discs prepared using this proprietary varistor formulation. Over twenty combinations are possible with the equipment being evaluated. However, it is impractical to consider evaluation of such a large number of samples, so eight combinations most favourable for scaling up into this production environment have been chosen from the grouping matrix of Figure 3.4. The exception being the turbula technique which was included as the poorest form of comminution used in the evaluation.

| ZNO DOPANT MIXING/ MILLING | DOPANT MILLING | | | | |
|---|---|---|---|---|---|
| | | Turbula (T) | Ball (B) | Vibro (V) | Attrition (A) |
| | Turbula (T) | T-T | | | |
| | Ball (B) | | B-B | | |
| | Vibro (V) | | | | |
| | Attrition (A) | | | V-A | A-A |
| | Shear (S) | T-S | B-S | V-S | A-S |
| | | | | | |

**Figure 3.4: Milling/Mixing Matrix Grouping**

The cells in the above matrix contain a two letter notation, the first letter serves to identify the dopant milling technique used, the second identifies the technique used to mix or mill the dopants and zinc oxide together. Once again to ensure blocking extraneous variables from the experiment during these stages, the work was carried out using all raw materials from the same manufacturers lot number, all equipment was thoroughly cleaned to prevent cross contamination, and milling times carefully monitored. Dopants are milled first in order to ensure the desired size distribution prior to addition to the zinc oxide.

### 3.3.3.1 Sample preparation by Turbula Processing

All samples with first subscript T were milled in a laboratory scale turbula mill complete with 2l jar filled to 50% by volume with zirconia media as described in 3.3.2.1. Dopants were loaded into the jar and wet milled for 6 hours in 800ml of deionised water. To control viscosity of the charge, 50g of defloculant was added. At the end of each milling run a (5g) sample from each charge was taken and marked with subscript T for particle size distribution analysis. In all two dopant samples were turbula milled.

In the samples with second subscript T the premilled dopants and ZnO slip were mixed in a production scale turbula, complete with 45l sealed plastic drum, loaded with 10kg of zirconia media to aid mixing. The samples were wet milled in a suspension with 6.7l of deionised water for one hour to produce the full formula varistor grade slips for spray drying. A 5g sample of the slip was taken for particle size analysis and labelled with the notation already described.

### 3.3.3.2 Sample Preparation by Ball Milling

The dopants for all samples with first subscript "B" were wet ball milled for six hours in 800 ml of deionised water. Dopants were loaded into the jar and placed on the rotating rollers causing the cascading action necessary for particle size reduction. Viscosity of the charge in the grinding chamber was controlled by adding 40g of deflocculent. A 5g sample from each charge was removed for particle size distribution analysis using the

Malvern light scattering laser. Care was taken to ensure the grinding chamber was clean and free from contaminants before and after use.

In the samples with second subscript "B" the pre milled dopants and ZnO slip were mixed in a production scale 60l ball mill. The grinding chamber was charged to 50% by weight with zirconia media, 6.7l of deionised water and mixed for one hour prior to spray drying. Mix viscosity was controlled by adding 50g of deflocculent to the charge. A 5g sample of the slip was labelled and stored for particle size analysis.

#### 3.3.3.3 Sample preparation by Vibro Milling

The dopants from all samples with first subscript "V" were wet milled in the M18 vibro mill for 6 hours in 5l of deionised water. Viscosity of the mix was controlled by adding 40g of deflocculent to the charge. A 5g sample from each charge was retained for particle size analysis. Care was taken to ensure the grinding chamber was clean and free from contamination before and after use.

In samples with second subscript "V" the pre milled dopants and ZnO slip were wet mixed together in the M18 vibro mill for 1 hour to produce the full formula varistor slip with a viscosity controlled by the addition of 40g of deflocculent, followed by spray drying. A 5g sample of each charge was retained for particle size analysis.

#### 3.3.3.4 Sample preparation by Attrition Milling

All dry powder dopants marked with first subscript "A" were dispersed into 2l of deionised water using the Greaves shear mixer for 1 hour. The suspension was then circulated by a perstaltic pump, through the attrition mill for 2 hours. Mix viscosity was controlled by the addition of 40g of deflocculent. A 5g sample of the charge was retained after milling for particle size distribution analysis. After dopant milling, the charge was transferred directly to the ZnO mixing stage.

All samples with second subscript "A" premilled dopants and zinc oxide were mixed in the attrition mill for 60 minutes in 5l of deionised water to produce the full formula varistor slip, ready for spray drying. A 5g sample was retained for particle size distribution analysis.

### 3.3.4 CONVERSION OF SLIP TO POWDER : SPRAY DRYING

The eight slips were spray dried in the Bowen pilot line spray drier, in each producing 25kg of a fine free flowing pressing grade varistor powder. Care was taken to ensure the drying chamber, all pumps, pipes and tanks were clean before and after use, so avoiding sample cross contamination. Each slip was pumped at 20 Bar through to the atomising nozzle, where it was discharged into the preheated chamber where the outlet temperature was controlled at 125°C. The powder was collected in a sealed container underneath the drier. The outlet drying temperature was carefully chosen for the production of zinc oxide varistor powder, so that no damage or loss

of binder occured during the drying cycle, this will ensure pressability of the powder. Also varistor powder must have well rounded spherical agglomerates of uniform size distribution of ensure uniform die filling, this is guaranteed by careful maintenance of a constant pumping pressure (20 Bar). Care was also taken to avoid boiling off the organics added to the slip in doing so, catastrophic defects such as pinholes left by binder burn out from the sintered press body were avoided.

### 3.4.0 POWDER TESTING

Samples at various stages of the powder manufacturing process were retained for analysis as follows:

### 3.4.1 DOPANT AND SLIP PARTICLE SIZE DISTRIBUTION

A 0.1g sample of the dopants were suspended in 20ml of deionised water and ultrasonically agitated for 5 minutes to breakdown agglomerates. This suspension was then transferred to a pre cleaned cell containing pure deionised water and then was used to reference focus the laser beam. The particle size distribution for each comminution technique was calculated and a hard copy taken. The same procedure was used to measure the particle size distribution of the full formula varistor powder.

### 3.4.2 BULK AND TAP DENSITY MEASUREMENTS

The bulk density for each powder sample was measured by pouring the free

flowing powder into graduated cylinder to the 250ml level. Taring the scales with the empty cylinder and filling, allows direct read out of the weight of powder in the given volume. These figures were recorded and substituted in to Equation 3.1 giving the actual values of bulk density in g/cc. After bulk density, the same samples were then placed on a Quantachrome tapping machine, given 1000 taps and the new volume occupied by the previously recorded mass of powder is noted, the figures substituted into Equation 3.2 giving tap density (g/cc) for each sample.

### 3.4.3 MOISTURE AND ORGANIC CONTENTS

A 5g sample of each powder was placed in Aluminium containers and placed into an oven at 120°C for one hour to remove absorbed moisture. The weight loss as a result was then recorded and the % moisture content for each powder calculated. The same samples were then placed into a kiln at 520°C for a further one hour to remove the organics added during processing. The weight loss as a result was then recorded and the % organic content for each powder calculated and recorded. Care was taken to ensure no interference between the % moisture and % organics during this analysis. All data is recorded in Appendix 1a.

## 3.5.0 DISC FABRICATION

The electrical characteristics of a varistor are primarily the result of the powder formulation. However the breakdown voltage for any given varistor is controlled by voltage gradient and the distances between the electrodes. The energy

capability is determined by the volume of the part. All samples were pressed to a target thickness of 1.8mm. For each powder 200 pieces were pressed. The mean and standard deviation for all pressed parts was recorded. Pressed part diameters were 7.86mm. After pressing the parts were loaded into saggars lined with ZnO plates so the pressed discs avoid contamination by touching alumina. The saggar complete with all samples was then loaded into a K&F kiln, the parts are then sintered using a proprietary temperature profile, control of the peak temperature and time giving the final breakdown voltage of the devices.

The devices are then silver electroded, fitted with leads and finally completely encapsulated with an epoxy resin based insulating material. The parts are now ready for electrical testing.

### 3.6.0 MICROSTRUCTURE ANALYSIS

Taking two discs from each pressed lot, each was cut using a diamond saw and the section mounted in resin. After grinding and polishing, the mount was chemically etched to highlight the ceramic grain structure. The surface for observation was coated with a thin gold palladium layer and then examined using the scanning electron microscope. Average grain size for the samples was calculated using the line count method. In addition, observations were made regarding the shape and size of pores, zinc oxide grain and bismuth deposits. Photographs at x500 magnification for each sample were taken to allow a comparison of the observed microstructure with electrical performance data.

## 3.7.0 ELECTRICAL TESTING

### 3.7.1 Breakdown Voltage

The breakdown voltage of a 50 pc sample from each disc lot was measured at a current density of 1mA/cm$^2$ on the Keithley 237 impulse generator. The data was recorded and loaded into a purpose designed software package to calculate statistical information including average breakdown voltage, and the % variance of the sample breakdown voltage.

### 3.7.2 Maximum Rated Residual Voltage

The performance of the samples in terms of maximum rated energy capability is measured by selecting the maximum rated current (5A) and applying at the 10$\mu$s/1000$\mu$s impulse waveform. The clamping voltage of a ten piece sample from every lot was recorded and the average energy capability for the lot determined by calculating the area under the current time by substitution into the Equation 3.3,

$$\text{Energy absorbed @ 5A} = V_C \times I_{\text{Applied}} \times 1.405 \times 10^{-3} \quad \text{Equation 3.3}$$

Data is recorded in Appendix 1C. The waveform rises to peak current in 10$\mu$s and decays to 50% in 1000$\mu$s (Figure 3.5). Ref. Harris Semiconductor Databook, 1993.

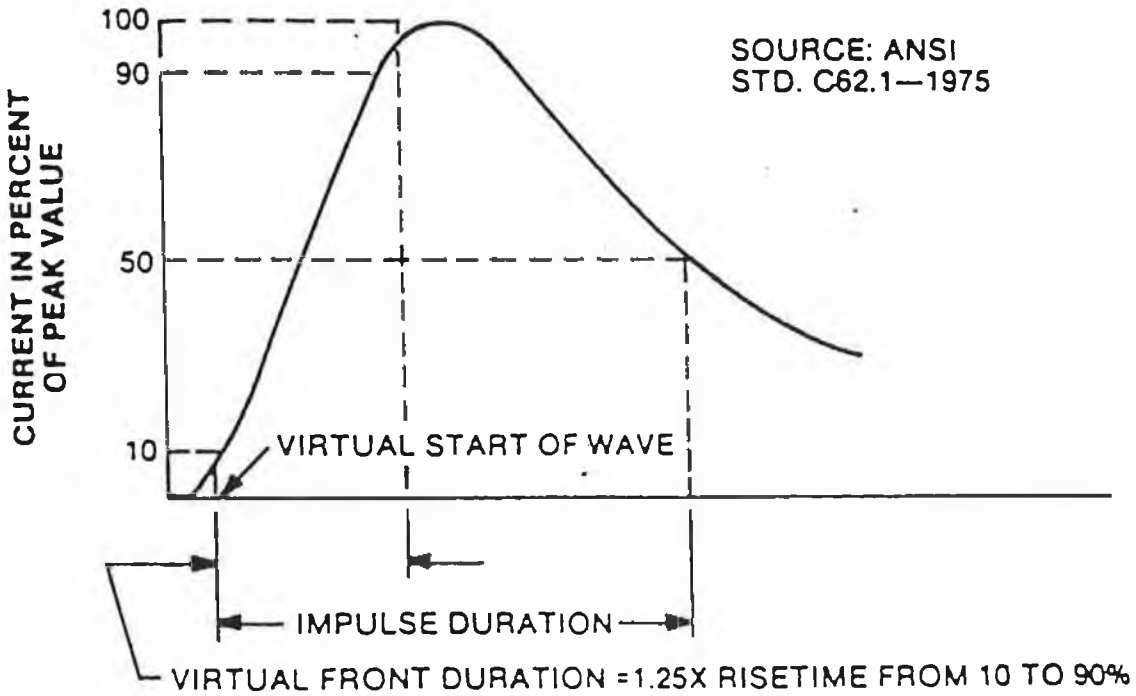


**Figure 3.5 - Definition of Pulse Current Waveform**

The clamping voltage at 5A must fall within the specification rated by current industrial standards for commercially available varistors of the type used in this work. Varistors are rated for a maximum pulse energy surge that results in a varistor voltage shift less than $\pm 10\%$ from the initial value. To this effect, the reference voltage (Vnom) at current density of $1mA/cm^2$ for the 10 pcs from every sample are recorded. Statistics regarding the mean and standard deviation are calculated followed by reference voltage check again. The % voltage shift at $1mA/cm^2$ are then calculated for each of the ten pieces of all the samples. The data for the pre clamp voltage @ 5A, post clamp voltage @ 5A and corresponding % voltage shift between

these two sets of measurements is calculated and recorded. All data is then recorded into Appendix 1d.

### 3.7.3 Energy Capability and Clamp Voltage at Peak Current

Clamping voltage of ten devices from each sample at the peak current rating of 250A generated in an 8$\mu$s/20$\mu$s impulse waveform are measured. The waveform rises to 250A in 8$\mu$s and decays to 50% of its maximum value in 20$\mu$s. Data on the clamp voltage at 250A is recorded in Appendix 1e. Once again the pre and post peak current test breakdown voltage must remain within $\pm$10% of the original values. Data on the clamp voltage @ 250A is recorded in Appendix 1e, data on pre and post breakdown voltages, % shifts in Appendix 1f. The energy capability of the parts is calculated by substituting the clamping voltage measured at 250A into Equation 3.4 and the information for the average energy capability of a ten piece disc sample for each powder recorded in Appendix 1g.

### 3.7.4 Maximum Clamp Voltage at Rated Energy

The maximum clamping voltage at the energy rated for these devices is determined by first calculating the current that must be applied. Substituting into Equation 3.4.

Rearranging $$I_{Applied} = \frac{\text{Rated Energy}}{1.405 \times 10^{-3} \times \text{Rated } V_{Clamp}}$$ Equation 3.4

(Source Harris Semiconductor, 1993)

This current is applied to ten discs from every sample and the actual clamping voltage at this current/energy applied is recorded in Appendix 1H. These values must be below the maximum rated for the devices in the Harris Semiconductor Manual. Reference voltage at breakdown current of $1mA/cm^2$ before and after clamp voltage testing at the rated energy must remain within $\pm 10\%$ of the original value. This data is summarised in Appendix 1I.

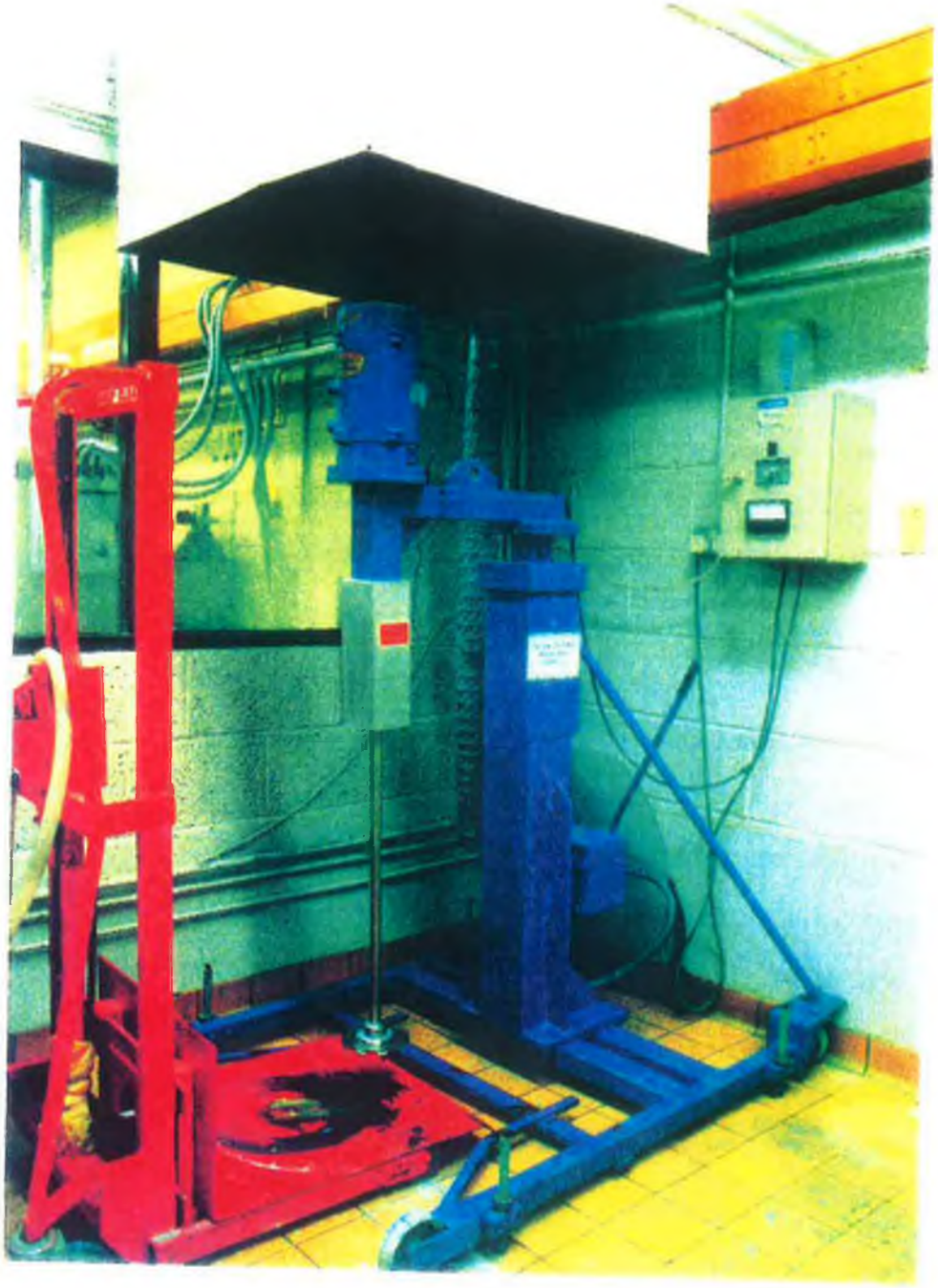

**Figure 3.6 Greaves model GM 95 High Shear Mixer**

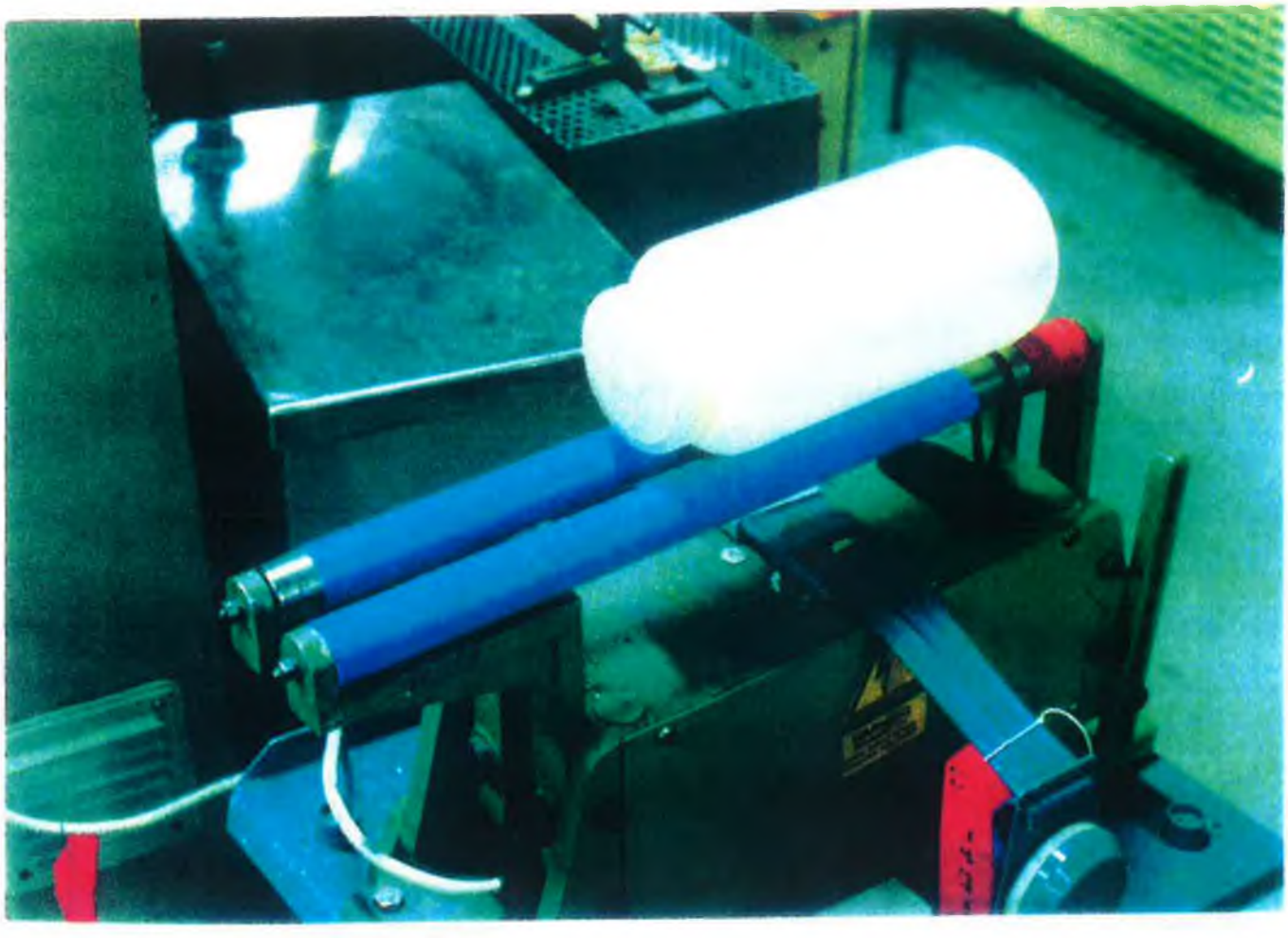

Figure 3.7 - Ball Mill apparatus used

**Figure 3.8 M18 Vibratory Mill Courtesy Sweco Inc.**

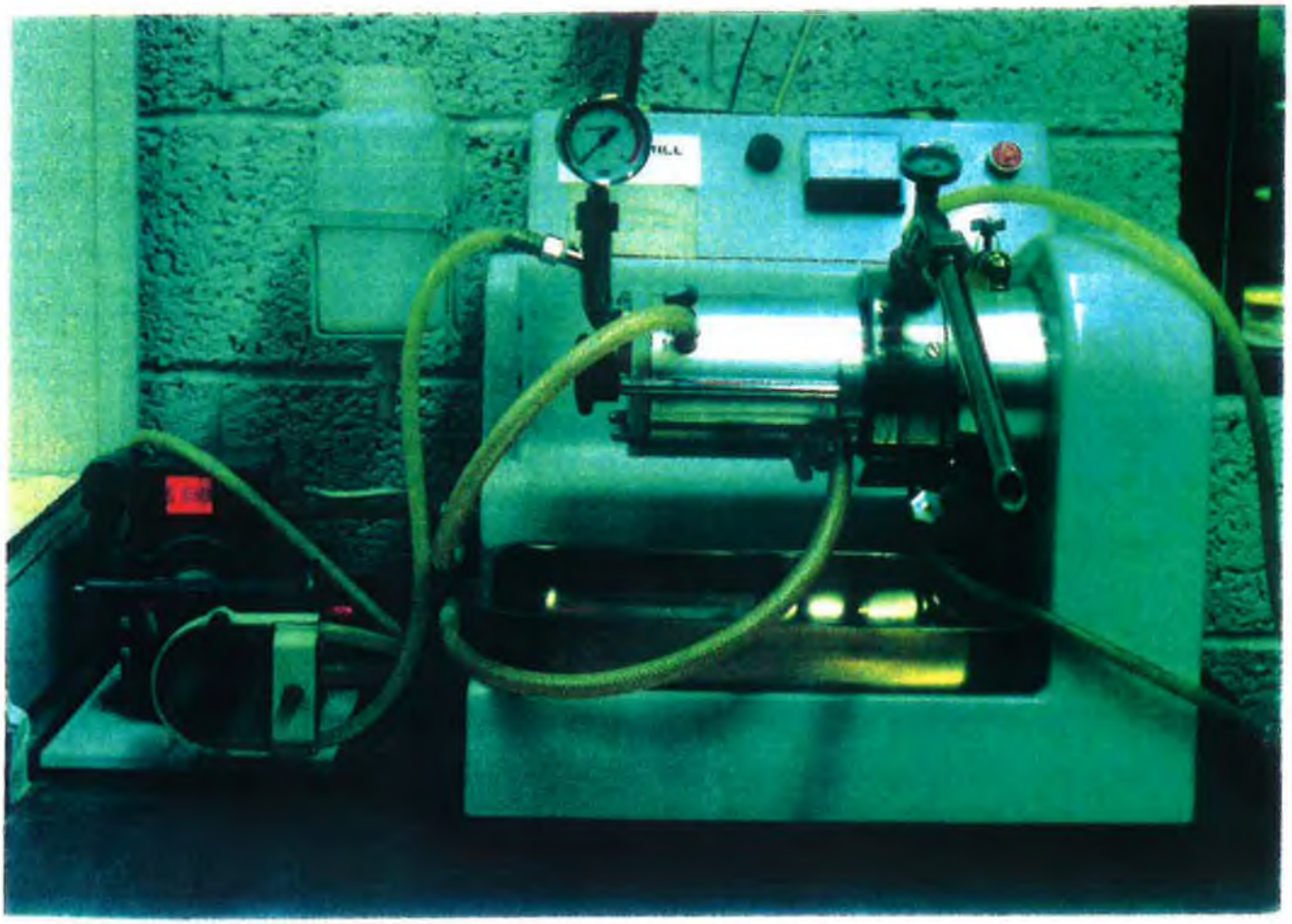

**Figure 3.9 Dnyo Mill Type KDL**

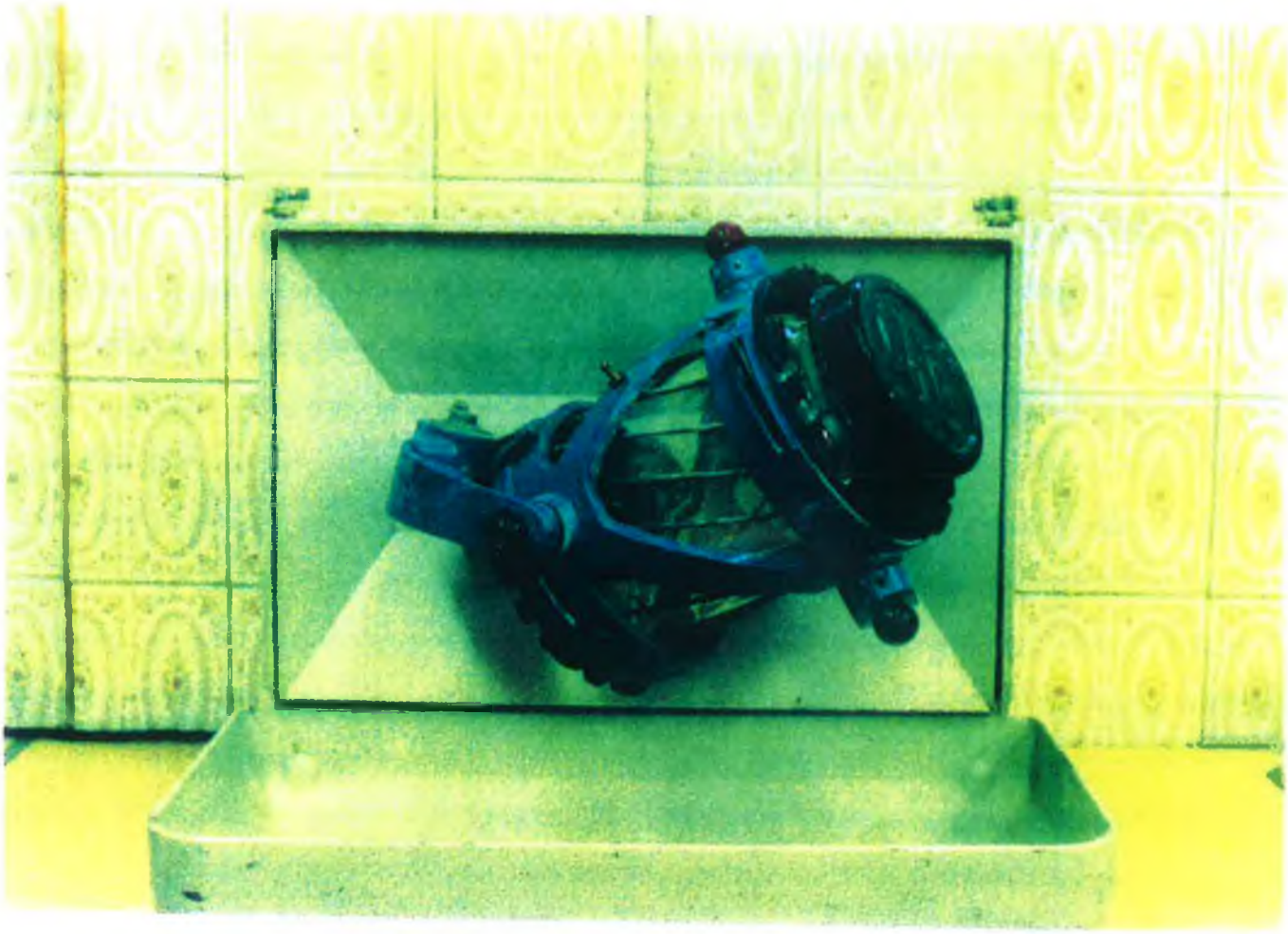

**Figure 3.10 W.A. Bachofen Model T2C Turbula**

**Figure 3.11 Bowen Spray Drier**

**Figure 3.12 Courtoy Rotary Tableting Press**

**Figure 3.13 Surefire T525 K+F Kiln**

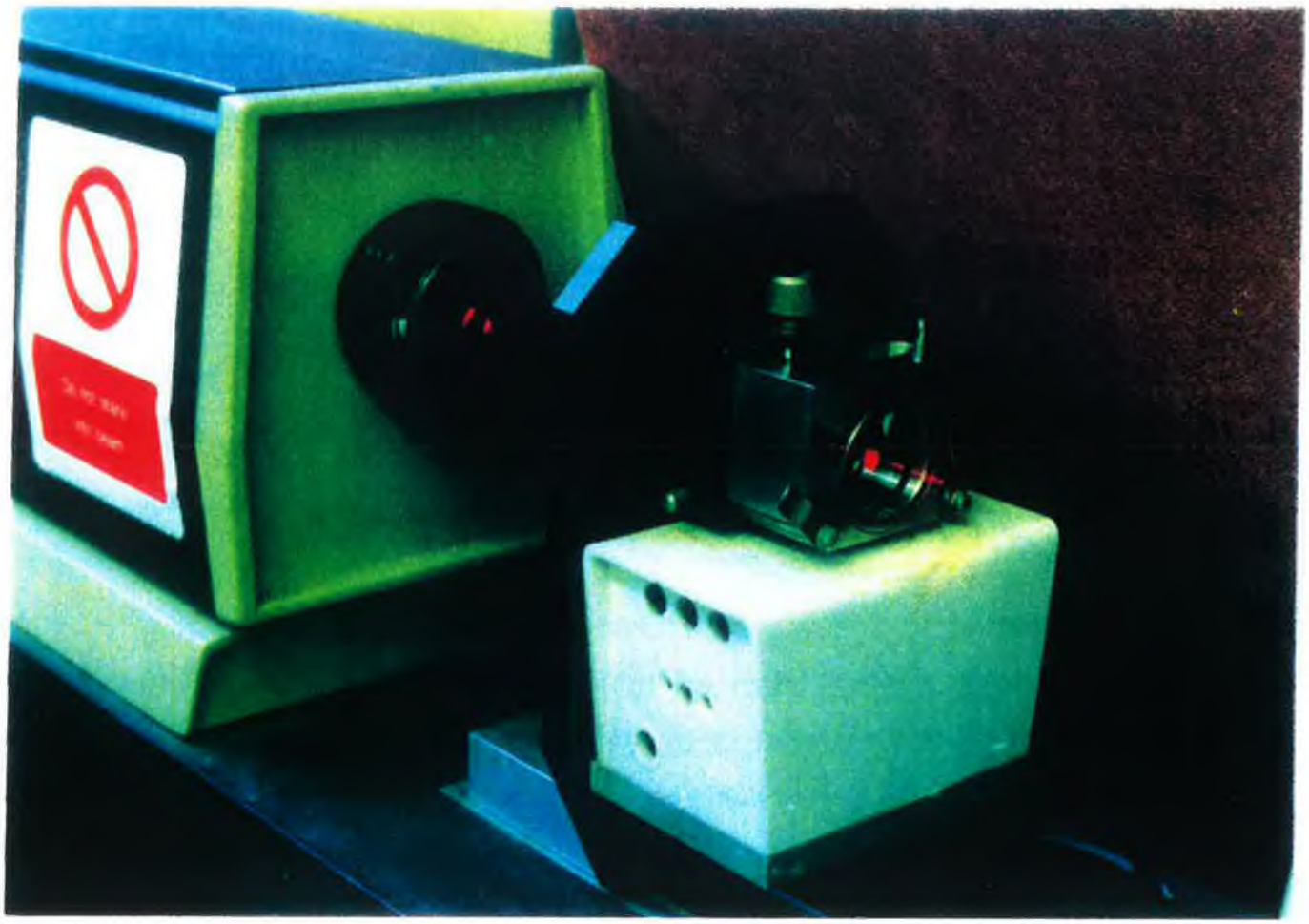

**Figure 3.14 - Malvern SB-08**

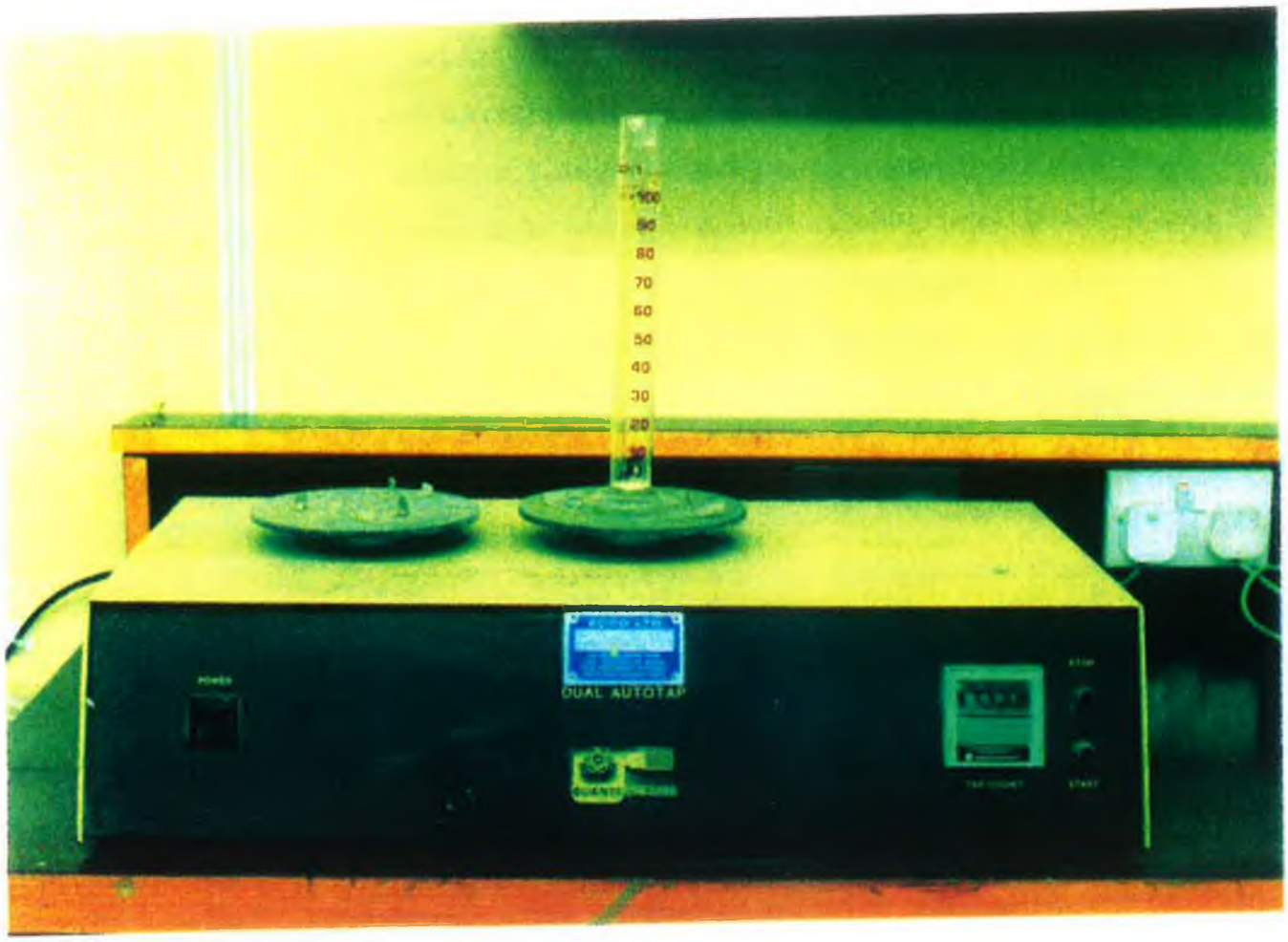


**Figure 3.15 Quantachrome model A46 tapping machine**


**Figure 3.16 Keithley 237 Surge Generator**

## Chapter Four - Test results and discussion

## 4.1 Introduction

The particle size distribution of oxide dopants mixed into the zinc oxide slip prior to spray drying is critical to the final microstructure and electrical properties of the sintered varistor. Homogenous distribution of all elements in the slip is essential for uniform diffusion of dopants around the zinc oxide grain. Non uniformity reduces energy capability performance and introduces product variability resulting from poor processing. Comminution in the form of milling is the only process step used in this conventional ceramic processing route to ensure particle size homogeneity of oxide dopants before the irreversible pressing and sintering reaction takes place.

This work evaluates the efficiency of four milling techniques on the oxide dopants of a proprietary varistor formulation and compares the subsequent electrical properties of the devices with observations made regarding disc microstructure and particle size distribution during powder processing. The eight powder samples have been routinely checked for bulk and tap density and moisture content after spray drying. The devices are electrically characterised to determine their breakdown voltage at a current density of $1mA/cm^2$ and statistical determination of the coefficient of variation of the breakdown voltages calculated as a means of evaluating the engineering yield to target of the sample. The effect of press thickness variation for each of the samples has been removed by calculating the actual voltage per unit length for each of the device samples. Results are tabulated in the Appendix.

## 4.2 Comparison of Milling Technique versus Dopant Particle Size Distribution

### 4.2.1 Results

Particle size analysis of the eight samples were carried out using a light scattering laser, and particle size data collected by a control computer. The distribution was electronically decoded from the sample laser signal and plots for the samples are recorded in Figures 4.1A to 4.1F.

### 4.2.2 Discussion

A comparison of the particle size distribution produced using the four milling techniques is summarised in Table 4.1

| Milling Technique | Particle Size ($\mu$m) | | | Max Size |
|---|---|---|---|---|
| | 10% (less than) | 50% (less than) | 90% (less than) | |
| Ball | 0.87 | 4.90 | 7.47 | 10.8 |
| Turbula | 0.87 | 4.39 | 7.19 | 10.8 |
| Vibro | 0.72 | 1.86 | 5.18 | 7.49 |
| Attrition | 0.48 | 0.97 | 1.88 | 2.71 |

**Table 4.1: Particle size distribution summary for oxide Dopant milling samples**

Average particle sizes of 1$\mu$m are ideal for the production of homogeneous varistor powders using the conventional ceramic processing route. Analysis of data presented in Table 4.1 indicated attrition milling is the most efficient technique of the four evaluated, producing an average size distribution of 0.97$\mu$m. Vibro milling has an average 1.86$\mu$m with turbula 4.39$\mu$m and ball milling 4.9$\mu$m.

An important observation regarding milling time is that the attrition mill process reduced the charge to the distribution in two hours compared to six hours for all others. This characteristic offers significant advantages when scaling a particle size reduction technique into full scale production.

The superior performance of the attrition technique is again reflected by the tight particle size distribution produced. One disadvantage is the extra operation required to suspend the charge in a wet media in order to pump it through the mill. Figure 4.2 graphically compares the distribution of particles produced by each technique.

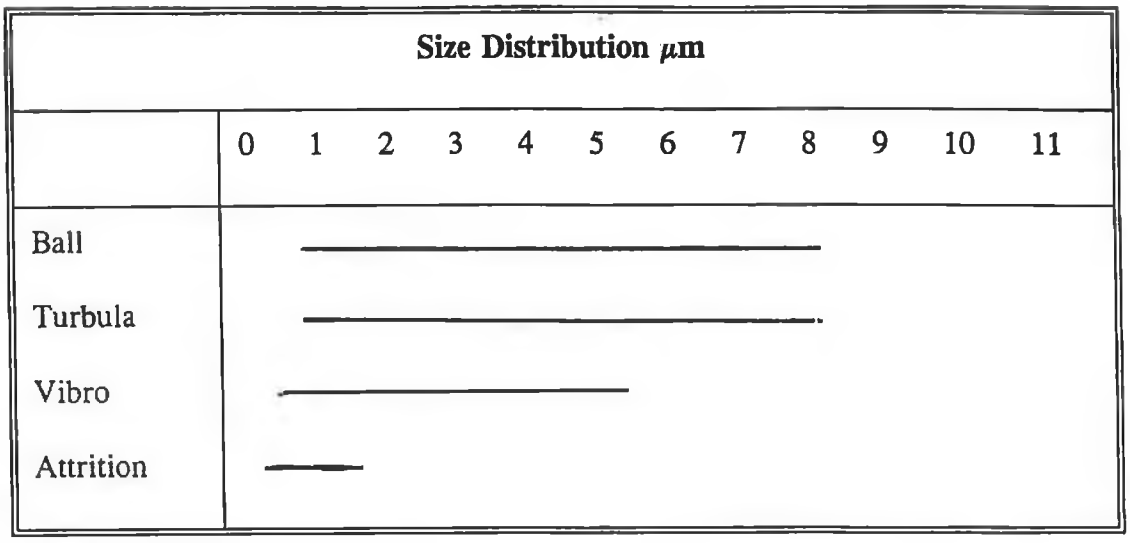


**Figure 4.2: Comparison of Dopant particle distribution by comminution technique.**

Next to attrition milling, vibro produces the tightest distribution, followed by ball and turbula as the only technique capable of size reduction into the ultrafine or $< 1\mu$m size range. This observation should be reflected where attrition is used to mix dopants and zinc oxide together in Section 4.4 and in both electrical performance and microstructure.

15 Feb 1994 3:42 pm

MALVERN Instruments SB.0B

Sample 1 additives. b-s 23m Milling experiment. DMcA.
Sample of slurry into 20 mls water.Ultrasonic 5 mins,3 drops Nopcosant 000005408
Beaker, Test sample of this solution.

1978 pil 1JP337

| High Size | Under % | High Size | Under % | High Size | Under % | High Size | Under % | High Size | Under % | High Size | Under % | Span 1.35 |
|---|---|---|---|---|---|---|---|---|---|---|---|---|
| 118 | 100 | 53.3 | 100 | 24.0 | 100 | 10.8 | 100 | 4.84 | 49.6 | 2.18 | 30.8 | D[4,3] 4.19µm |
| 110 | 100 | 49.5 | 100 | 22.3 | 100 | 10.0 | 99.9 | 4.50 | 47.5 | 2.03 | 30.3 | |
| 102 | 100 | 46.1 | 100 | 20.7 | 100 | 9.31 | 99.9 | 4.19 | 46.7 | 1.88 | 30.1 | D[3,2] 1.84µm |
| 95.2 | 100 | 42.8 | 100 | 19.3 | 100 | 8.66 | 99.4 | 3.89 | 46.2 | 1.75 | 29.9 | |
| 88.6 | 100 | 39.8 | 100 | 17.9 | 100 | 8.05 | 96.2 | 3.62 | 45.4 | 1.63 | 29.4 | |
| 82.4 | 100 | 37.0 | 100 | 16.7 | 100 | 7.49 | 90.3 | 3.37 | 43.9 | 1.51 | 28.1 | D[v,0.9] 7.47µm |
| 76.6 | 100 | 34.4 | 100 | 15.5 | 100 | 6.97 | 82.6 | 3.13 | 41.9 | 1.41 | 26.1 | |
| 71.2 | 100 | 32.0 | 100 | 14.4 | 100 | 6.48 | 74.3 | 2.91 | 39.4 | 1.31 | 23.4 | |
| 66.2 | 100 | 29.8 | 100 | 13.4 | 100 | 6.02 | 66.1 | 2.71 | 36.5 | 1.22 | 20.5 | D[v,0.1] 0.87µm |
| 61.6 | 100 | 27.7 | 100 | 12.5 | 100 | 5.60 | 59.0 | 2.52 | 33.9 | | | |
| 57.3 | 100 | 25.8 | 100 | 11.6 | 100 | 5.21 | 53.3 | 2.34 | 32.0 | | | |

| | | | |
|---|---|---|---|
| Source = :Sample | Beam length = 14.3 mm | Model indp | D[v,0.5] 4.90µm |
| | Log. Diff. = 3.520 | | |
| Focal length = 63 mm | Obscuration = 0.2844 | Volume Conc. = 0.0014% | |
| Presentation = pil | Volume distribution | Sp.S.A 3.2606 m²/cc. | |

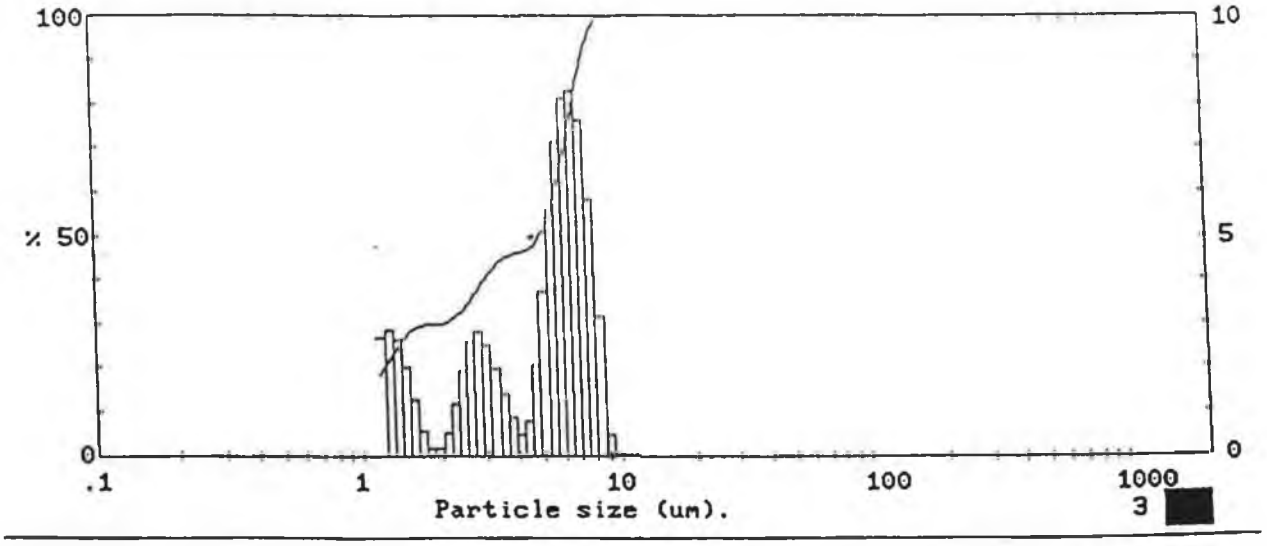


HARRIS IRELAND

Figure 4.1A - particle size analysis for dopants B-S (Ball - Shear)

15 Feb 1994 3:34 pm

MALVERN Instruments SB.0B

Sample 7 additives. t-s 23m Milling experiment. DMcA.
Sample of slurry into 20 mls water.Ultrasonic 5 mins,3 drops Nopcosant 000005405
Beaker, Test sample of this solution.

1978 pil 1JP337

| High Size | Under % | High Size | Under % | High Size | Under % | High Size | Under % | High Size | Under % | High Size | Under % | Span 1.44 |
|---|---|---|---|---|---|---|---|---|---|---|---|---|
| 118 | 100 | 53.3 | 100 | 24.0 | 100 | 10.8 | 100 | 4.84 | 53.0 | 2.18 | 32.8 | D[4,3] 3.96µm |
| 110 | 100 | 49.5 | 100 | 22.3 | 100 | 10.0 | 99.9 | 4.50 | 50.5 | 2.03 | 32.1 | |
| 102 | 100 | 46.1 | 100 | 20.7 | 100 | 9.31 | 99.9 | 4.19 | 49.5 | 1.88 | 31.9 | |
| 95.2 | 100 | 42.8 | 100 | 19.3 | 100 | 8.66 | 99.7 | 3.89 | 49.0 | 1.75 | 31.6 | D[3,2] 1.77µm |
| 88.6 | 100 | 39.8 | 100 | 17.9 | 100 | 8.05 | 97.9 | 3.62 | 48.0 | 1.63 | 30.9 | |
| 82.4 | 100 | 37.0 | 100 | 16.7 | 100 | 7.49 | 93.4 | 3.37 | 46.5 | 1.51 | 29.5 | |
| 76.6 | 100 | 34.4 | 100 | 15.5 | 100 | 6.97 | 87.1 | 3.13 | 44.3 | 1.41 | 27.3 | D[v,0.9] 7.19µm |
| 71.2 | 100 | 32.0 | 100 | 14.4 | 100 | 6.48 | 79.6 | 2.91 | 41.7 | 1.31 | 24.5 | |
| 66.2 | 100 | 29.8 | 100 | 13.4 | 100 | 6.02 | 71.6 | 2.71 | 38.7 | 1.22 | 21.4 | |
| 61.6 | 100 | 27.7 | 100 | 12.5 | 100 | 5.60 | 63.9 | 2.52 | 36.1 | | | D[v,0.1] 0.87µm |
| 57.3 | 100 | 25.8 | 100 | 11.5 | 100 | 5.21 | 57.4 | 2.34 | 34.1 | | | |

| | | | |
|---|---|---|---|
| Source = :Sample | Beam length = 14.3 mm | Model indp | D[v,0.5] 4.39µm |
| | Log. Diff. = 3.496 | | |
| Focal length = 63 mm | Obscuration = 0.3269 | Volume Conc. = 0.0016% | |
| Presentation = pil | Volume distribution | Sp.S.A 3.3901 m²/cc. | |

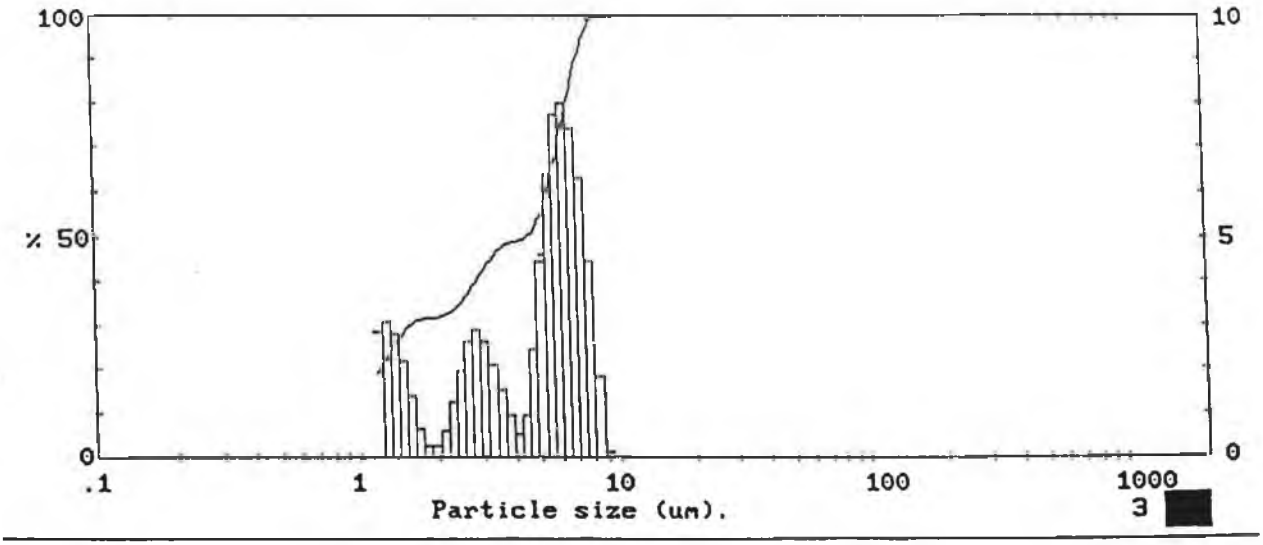


HARRIS IRELAND

**Figure 4.1B - Particle size analysis for dopants T-S (Turbula - Shear)**

15 Feb 1994 3:06 pm

MALVERN Instruments SB.0B

Sample 4 additives. b-b 23m Milling experiment. DMcA.
Sample of slurry into 20 mls water.Ultrasonic 5 mins,3 drops Nopcosant 000005398
Beaker, Test sample of this solution.

1978 pil 1JP337

| High Size | Under % | High Size | Under % | High Size | Under % | High Size | Under % | High Size | Under % | High Size | Under % | Span 1.43 |
|---|---|---|---|---|---|---|---|---|---|---|---|---|
| 118 | 100 | 53.3 | 100 | 24.0 | 100 | 10.8 | 99.1 | 4.84 | 51.1 | 2.18 | 32.3 | D[4,3] 4.20µm |
| 110 | 100 | 49.5 | 100 | 22.3 | 100 | 10.0 | 98.8 | 4.50 | 48.8 | 2.03 | 31.6 | |
| 102 | 100 | 46.1 | 100 | 20.7 | 100 | 9.31 | 98.1 | 4.19 | 47.8 | 1.88 | 31.1 | |
| 95.2 | 100 | 42.8 | 100 | 19.3 | 100 | 8.66 | 96.6 | 3.89 | 47.1 | 1.75 | 30.8 | D[3,2] 1.83µm |
| 88.6 | 100 | 39.8 | 100 | 17.9 | 100 | 8.05 | 93.5 | 3.62 | 46.0 | 1.63 | 30.0 | |
| 82.4 | 100 | 37.0 | 100 | 16.7 | 100 | 7.49 | 88.7 | 3.37 | 44.4 | 1.51 | 28.5 | |
| 76.6 | 100 | 34.4 | 100 | 15.5 | 100 | 6.97 | 82.6 | 3.13 | 42.4 | 1.41 | 26.3 | D[v,0.9] 7.52µm |
| 71.2 | 100 | 32.0 | 100 | 14.4 | 100 | 6.48 | 75.6 | 2.91 | 40.1 | 1.31 | 23.4 | |
| 66.2 | 100 | 29.8 | 100 | 13.4 | 99.9 | 6.02 | 68.2 | 2.71 | 37.6 | 1.22 | 20.3 | |
| 61.6 | 100 | 27.7 | 100 | 12.5 | 99.7 | 5.60 | 61.1 | 2.52 | 35.3 | | | D[v,0.1] 0.89µm |
| 57.3 | 100 | 25.8 | 100 | 11.6 | 99.4 | 5.21 | 55.2 | 2.34 | 33.6 | | | |

| | | | |
|---|---|---|---|
| Source = :Sample | Beam length = 14.3 mm | Model indp | D[v,0.5] 4.70µm |
| | Log. Diff. = 3.197 | | |
| Focal length = 63 mm | Obscuration = 0.3420 | Volume Conc. = 0.0018% | |
| Presentation = pil | Volume distribution | So.S.A 3.2798 m²/cc. | |

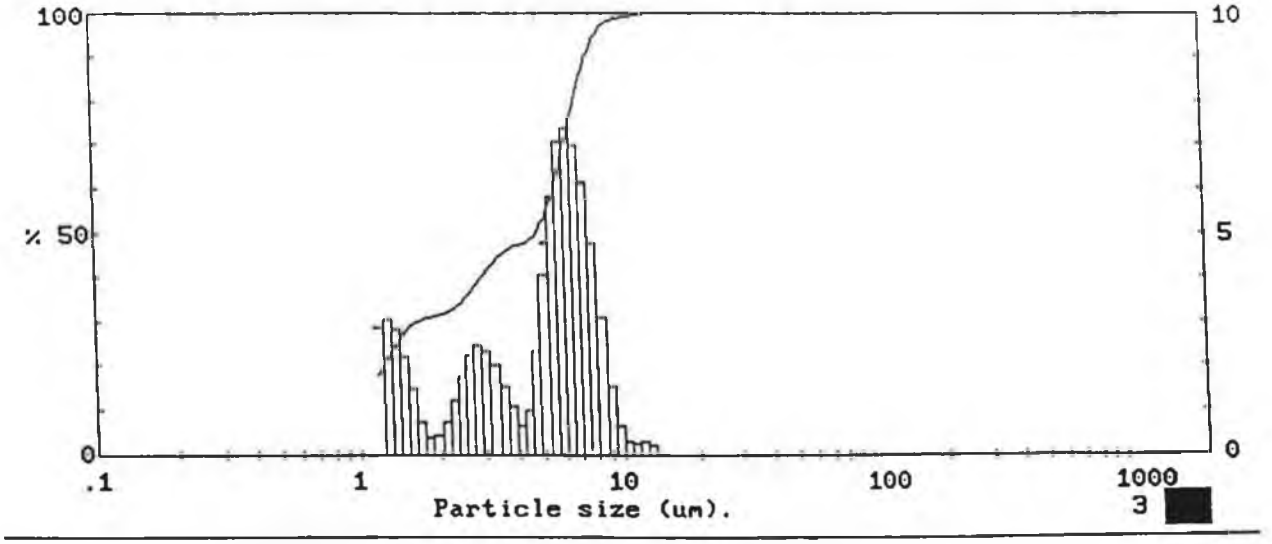


HARRIS IRELAND

**Figure 4.1C - Particle size analysis for dopants B-B (Ball - Ball)**

15 Feb 1994 2:39 pm

MALVERN Instruments SB.0B

Sample 6.additives. v-s 23m Milling experiment. DMcA.
Sample of slurry into 20 mls water.Ultrasonic 5 mins,3 drops Napcosant 000005391
Beaker, Test sample of this solution.

1978 pil 1JP337

| High Size | Under % | High Size | Under % | High Size | Under % | High Size | Under % | High Size | Under % | High Size | Under % | Span 2.40 |
|---|---|---|---|---|---|---|---|---|---|---|---|---|
| 118 | 100 | 53.3 | 100 | 24.0 | 100 | 10.8 | 100 | 4.84 | 86.2 | 2.18 | 55.1 | D[4,3] 2.42µm |
| 110 | 100 | 49.5 | 100 | 22.3 | 100 | 10.0 | 100 | 4.50 | 82.3 | 2.03 | 52.7 | |
| 102 | 100 | 46.1 | 100 | 20.7 | 100 | 9.31 | 100 | 4.19 | 78.6 | 1.88 | 50.3 | |
| 95.2 | 100 | 42.8 | 100 | 19.3 | 100 | 8.66 | 100 | 3.89 | 75.3 | 1.75 | 48.0 | D[3,2] 1.29µm |
| 88.6 | 100 | 39.8 | 100 | 17.9 | 100 | 8.05 | 100 | 3.62 | 72.6 | 1.63 | 45.3 | |
| 82.4 | 100 | 37.0 | 100 | 16.7 | 100 | 7.49 | 100 | 3.37 | 70.1 | 1.51 | 42.2 | |
| 76.6 | 100 | 34.4 | 100 | 15.5 | 100 | 6.97 | 99.8 | 3.13 | 67.8 | 1.41 | 38.7 | D[v,0.9] 5.18µm |
| 71.2 | 100 | 32.0 | 100 | 14.4 | 100 | 6.48 | 99.2 | 2.91 | 65.4 | 1.31 | 34.9 | |
| 66.2 | 100 | 29.8 | 100 | 13.4 | 100 | 6.02 | 97.3 | 2.71 | 62.8 | 1.22 | 30.9 | |
| 61.6 | 100 | 27.7 | 100 | 12.5 | 100 | 5.60 | 94.1 | 2.52 | 60.1 | | | D[v,0.1] 0.72µm |
| 57.3 | 100 | 25.8 | 100 | 11.6 | 100 | 5.21 | 90.3 | 2.34 | 57.6 | | | |

| | | | |
|---|---|---|---|
| Source = :Sample | Beam length = 14.3 mm | Model indp | D[v,0.5] 1.86µm |
| | Log. Diff. = 3.413 | | |
| Focal length = 63 mm | Obscuration = 0.2317 | Volume Conc. = 0.0008% | |
| Presentation = pil | Volume distribution | Sp.S.A 4.5480 m²/cc. | |

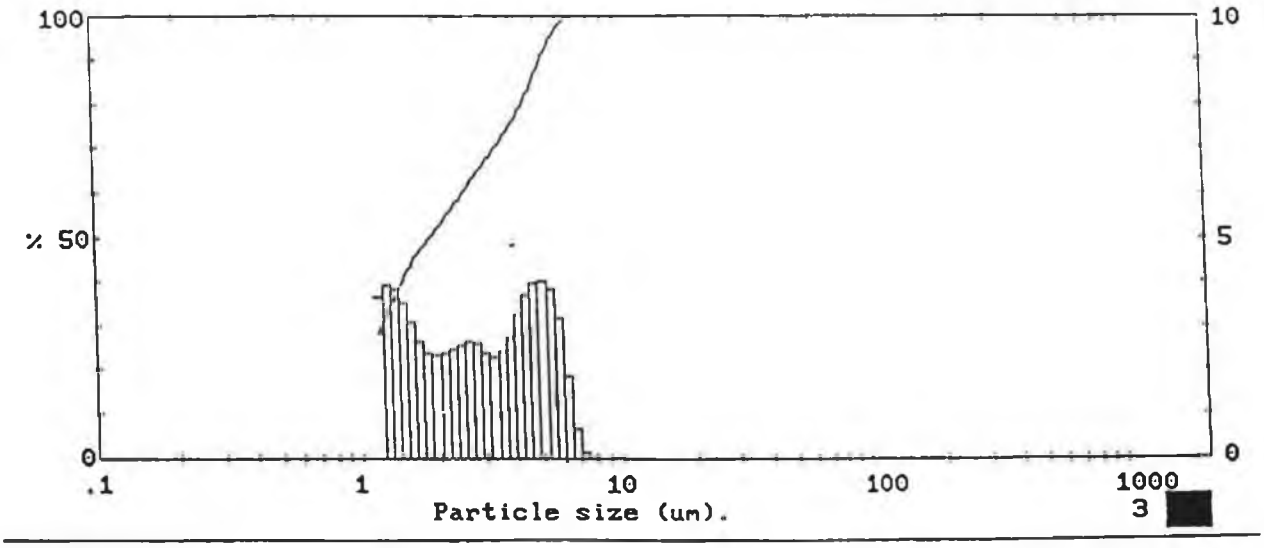


HARRIS IRELAND

Figure 4.1D - Particle size analysis for dopants V-S (Vibro - Shear)

15 Feb 1994 3:20 pm

MALVERN Instruments SB.0B

Sample 7 additives. a-s 23m Milling experiment. DMcA.
Sample of slurry into 20 mls water.Ultrasonic 5 mins,3 drops Nopcosant 000005401
Beaker, Test sample of this solution.

1978 pil 1JP337

| High Size | Under % | High Size | Under % | High Size | Under % | High Size | Under % | High Size | Under % | High Size | Under % | Span 1.45 |
|---|---|---|---|---|---|---|---|---|---|---|---|---|
| 118 | 100 | 53.3 | 100 | 24.0 | 100 | 10.8 | 100 | 4.84 | 100 | 2.18 | 97.7 | D[4,3] 1.03µm |
| 110 | 100 | 49.5 | 100 | 22.3 | 100 | 10.0 | 100 | 4.50 | 100 | 2.03 | 94.7 | |
| 102 | 100 | 46.1 | 100 | 20.7 | 100 | 9.31 | 100 | 4.19 | 100 | 1.88 | 90.3 | |
| 95.2 | 100 | 42.8 | 100 | 19.3 | 100 | 8.66 | 100 | 3.89 | 100 | 1.75 | 84.7 | D[3,2] 0.81µm |
| 88.6 | 100 | 39.8 | 100 | 17.9 | 100 | 8.05 | 100 | 3.62 | 100 | 1.63 | 78.8 | |
| 82.4 | 100 | 37.0 | 100 | 16.7 | 100 | 7.49 | 100 | 3.37 | 100 | 1.51 | 73.5 | |
| 76.6 | 100 | 34.4 | 100 | 15.5 | 100 | 6.97 | 100 | 3.13 | 100 | 1.41 | 69.0 | D[v,0.9] 1.88µm |
| 71.2 | 100 | 32.0 | 100 | 14.4 | 100 | 6.48 | 100 | 2.91 | 100 | 1.31 | 65.4 | |
| 66.2 | 100 | 29.8 | 100 | 13.4 | 100 | 6.02 | 100 | 2.71 | 100 | 1.22 | 62.1 | |
| 61.6 | 100 | 27.7 | 100 | 12.5 | 100 | 5.60 | 100 | 2.52 | 99.9 | | | D[v,0.1] 0.48µm |
| 57.3 | 100 | 25.8 | 100 | 11.6 | 100 | 5.21 | 100 | 2.34 | 99.3 | | | |

| | | | |
|---|---|---|---|
| Source = | :Sample | Beam length = 14.3 mm | Model indp |
| | | Log. Diff. = 4.721 | |
| Focal length = | 63 mm | Obscuration = 0.6604 | Volume Conc. = 0.0020% |
| Presentation = | pil | Volume distribution | Sp.S.A 7.3926 m²/cc. |

D[v,0.5] 0.97µm

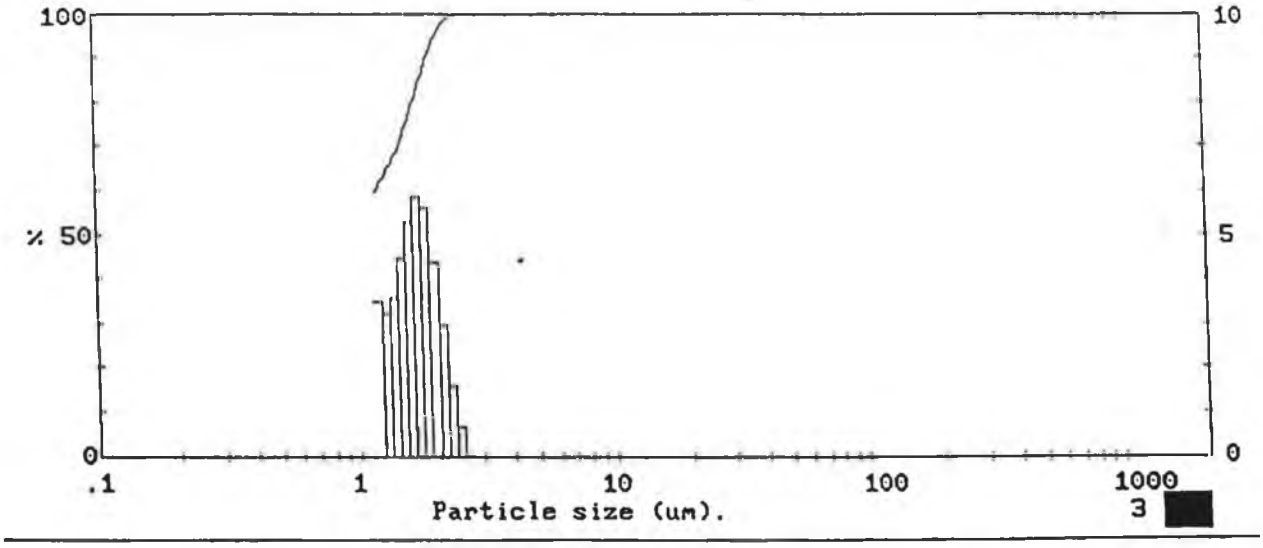


HARRIS IRELAND

Figure 4.1E - Particle size analysis for dopants A-S (Attrition - Shear)

15 Feb 1994 12:49 pm

MALVERN Instruments SB.0B

Sample 8.additives. A-A 23m Milling experiment. DMcA.
Sample of slurry into 20 mls water.Ultrasonic 5 mins,3 drops Nopcosant 000005386
Beaker, Test sample of this solution.

1978 pil 1JP337

| High Size | Under % | High Size | Under % | High Size | Under % | High Size | Under % | High Size | Under % | High Size | Under % | Span 1.43 |
|---|---|---|---|---|---|---|---|---|---|---|---|---|
| 118 | 100 | 53.3 | 100 | 24.0 | 100 | 10.8 | 100 | 4.84 | 100 | 2.18 | 99.3 | D[4,3] 0.97µm |
| 110 | 100 | 49.5 | 100 | 22.3 | 100 | 10.0 | 100 | 4.50 | 100 | 2.03 | 97.7 | |
| 102 | 100 | 46.1 | 100 | 20.7 | 100 | 9.31 | 100 | 4.19 | 100 | 1.88 | 94.3 | |
| 95.2 | 100 | 42.8 | 100 | 19.3 | 100 | 8.66 | 100 | 3.89 | 100 | 1.75 | 88.9 | D[3,2] 0.79µm |
| 88.6 | 100 | 39.8 | 100 | 17.9 | 100 | 8.05 | 100 | 3.62 | 100 | 1.63 | 82.7 | |
| 82.4 | 100 | 37.0 | 100 | 16.7 | 100 | 7.49 | 100 | 3.37 | 100 | 1.51 | 77.0 | |
| 76.6 | 100 | 34.4 | 100 | 15.5 | 100 | 6.97 | 100 | 3.13 | 100 | 1.41 | 72.3 | D[v,0.9] 1.77µm |
| 71.2 | 100 | 32.0 | 100 | 14.4 | 100 | 6.48 | 100 | 2.91 | 100 | 1.31 | 68.7 | |
| 66.2 | 100 | 29.8 | 100 | 13.4 | 100 | 6.02 | 100 | 2.71 | 100 | 1.22 | 65.5 | |
| 61.6 | 100 | 27.7 | 100 | 12.5 | 100 | 5.60 | 100 | 2.52 | 100 | | | D[v,0.1] 0.47µm |
| 57.3 | 100 | 25.8 | 100 | 11.6 | 100 | 5.21 | 100 | 2.34 | 99.9 | | | |

| | | | |
|---|---|---|---|
| Source = :Sample | Beam length = 14.3 mm | Model indp | D[v,0.5] 0.91µm |
| | Log. Diff. = 4.162 | | |
| Focal length = 63 mm | Obscuration = 0.2090 | Volume Conc. = 0.0004% | |
| Presentation = pil | Volume distribution | Sp.S.A 7.6350 $m^2/cc$. | |

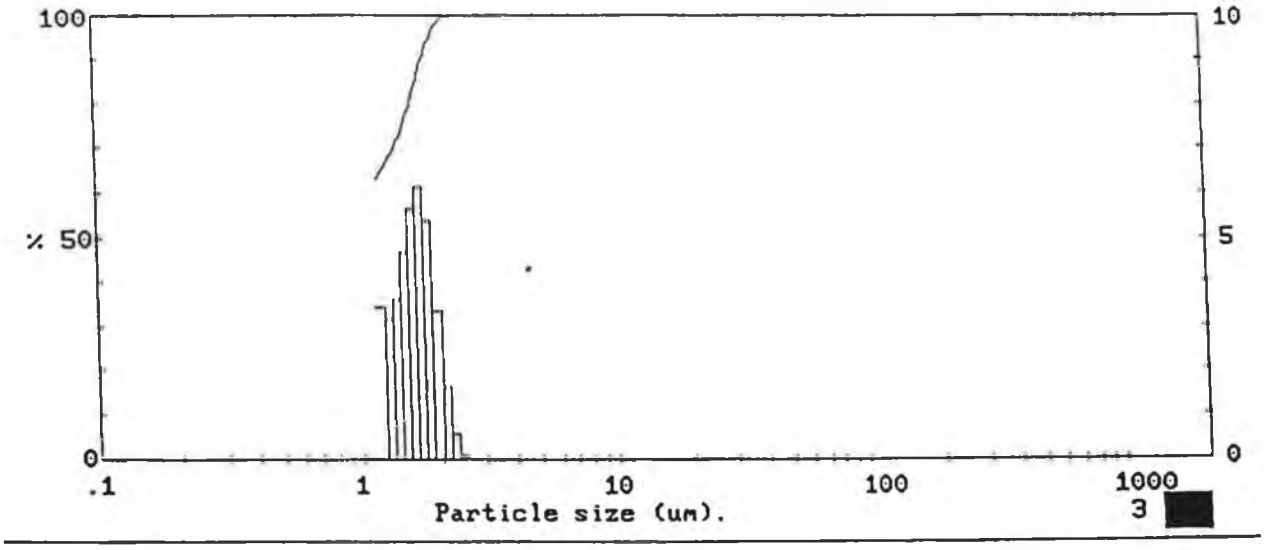


HARRIS IRELAND

**Figure 4.1F - Particle size analysis for dopants A-A (Attrition - Attrition)**

## 4.3 Comparison of Milling-Mixing Combination on Full Feed Slip Particle Size Distribution

### 4.3.1 Results

The particle size distribution for the eight slips were measured by electronically decoding the sample laser signal generated by the Malvern particle analyser. Figures 4.5A to 4.5H represent the particle size distribution plots of the slips.

### 4.3.2 Discussion

The particle size distributions produced by the eight mix-mill combinations for each spray dry slip are summarised. The original zinc oxide slips have particle size distribution averages of 0.5$\mu$m addition of dopants with distributions per Figure 4.2 gives the result of Table 4.2. Average particle size distributions less than one micron, with maximum values $<5\mu$m are desirable at this stage. Samples V-A and A-A give the tightest distribution for all slips. This again demonstrates the enhanced capability of the attrition mill compared to all the techniques in producing ultra fine particle size distributions.

| Mix/Mill Combination | Sizes of Particles $\mu$m % less than | | | |
|---|---|---|---|---|
| | **10%** | **50%** | **90%** | **100%** |
| T-T | 0.57 | 1.16 | 2.57 | 6.97 |
| T-S | 0.47 | 0.97 | 2.03 | 6.02 |
| B-B | 0.47 | 0.93 | 1.91 | 3.89 |
| B-S | 0.47 | 0.88 | 1.86 | 4.84 |
| V-A | 0.46 | 0.85 | 1.69 | 2.52 |
| V-S | 0.47 | 0.89 | 1.94 | 4.84 |
| A-A | 0.46 | 0.87 | 1.79 | 2.49 |
| A-S | 0.46 | 0.86 | 1.81 | 3.89 |

**Table 4.2: Particle size distributions for all mix/mill combinations used to mix both dopants and zinc oxide together**

Comparing A-A to A-S, it is evident that further size reduction takes place with a second milling action as opposed to simply shear mixing. This same observation can be made for samples B-B vs. B-S, V-A vs. V-S, and T-T vs. T-S.

The range of particle size distributions may be grouped as shown in Figure 4.4.

| Mix Mill Combination | Size Distribution $\mu$m | |
|---|---|---|
| | 0 1 2 3 4 5 6 | |
| T-T | | Range 1 |
| T-S | | |
| B-B | | Range 2 |
| B-S | | |
| V-S | | |
| A-S | | |
| V-A | | Range 3 |
| A-A | | |

**Figure 4.4: Grouping the full formulation slip samples into similiar size distribution range.**

In the analysis of both microstructure and electrical performance, the uniformity of processing at this stage should be reflected in both microstructural uniformity and a comparable difference in energy absorption capability. Samples with the widest particle size range (range 1) should have lower overall energy capability compared to slips with the tighter distributions (range 3). Differences in both the size and distribution of Bismuth around zinc oxide grains should be evident from SEM analysis and photographs.

16 Feb 1994 12:14 pm

MALVERN Instruments SB.0B

Sample 6, powder slurry. v-s. Milling experiment. DMcA.
Sample of slurry into 20 mls water.Ultrasonic 5 mins,3 drops Nopcosant 000005437
Beaker, Test sample of this solution.

1978 pil 1JP337

| High Size | Under % | High Size | Under % | High Size | Under % | High Size | Under % | High Size | Under % | High Size | Under % | Span 1.65 |
|---|---|---|---|---|---|---|---|---|---|---|---|---|
| 118 | 100 | 53.3 | 100 | 24.0 | 100 | 10.8 | 100 | 4.84 | 100 | 2.18 | 94.0 | D[4,3] |
| 110 | 100 | 49.5 | 100 | 22.3 | 100 | 10.0 | 100 | 4.50 | 99.9 | 2.03 | 91.7 | 1.01µm |
| 102 | 100 | 46.1 | 100 | 20.7 | 100 | 9.31 | 100 | 4.19 | 99.7 | 1.88 | 88.8 | |
| 95.2 | 100 | 42.8 | 100 | 19.3 | 100 | 8.66 | 100 | 3.89 | 99.6 | 1.75 | 85.5 | D[3,2] |
| 88.6 | 100 | 39.8 | 100 | 17.9 | 100 | 8.05 | 100 | 3.62 | 99.3 | 1.63 | 82.0 | 0.78µm |
| 82.4 | 100 | 37.0 | 100 | 16.7 | 100 | 7.49 | 100 | 3.37 | 99.0 | 1.51 | 78.6 | |
| 76.6 | 100 | 34.4 | 100 | 15.5 | 100 | 6.97 | 100 | 3.13 | 98.7 | 1.41 | 75.2 | D[v,0.9] |
| 71.2 | 100 | 32.0 | 100 | 14.4 | 100 | 6.48 | 100 | 2.91 | 98.3 | 1.31 | 71.9 | 1.94µm |
| 66.2 | 100 | 29.8 | 100 | 13.4 | 100 | 6.02 | 100 | 2.71 | 97.9 | 1.22 | 68.4 | |
| 61.6 | 100 | 27.7 | 100 | 12.5 | 100 | 5.60 | 100 | 2.52 | 97.1 | | | D[v,0.1] |
| 57.3 | 100 | 25.8 | 100 | 11.6 | 100 | 5.21 | 100 | 2.34 | 95.8 | | | 0.47µm |

| | | | |
|---|---|---|---|
| Source = :Sample | Beam length = 14.3 mm | Model indp | D[v,0.5] |
| | Log. Diff. = 3.384 | | 0.89µm |
| Focal length = 63 mm | Obscuration = 0.4098 | Volume Conc. = 0.0010% | |
| Presentation = pil | Volume distribution | Sp.S.A 7.7300 m²/cc. | |

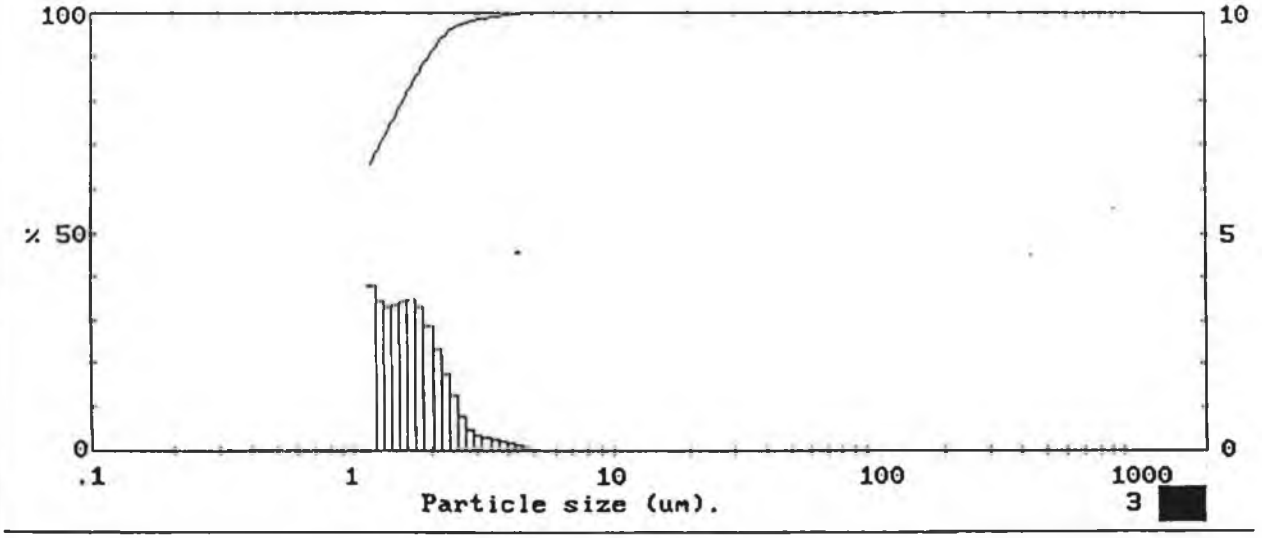


HARRIS IRELAND

**Figure 4.5A - Particle size analysis on full feed slip V-S (Vibro-Shear)**

MALVERN Instruments SB.0B

Sample 5 Powder. v-a 23m Milling experiment. DMcA.
Sample of slurry into 20 mls water.Ultrasonic 5 mins,3 drops Nopcosant 000005394
Beaker, Test sample of this solution.

1978 pil 1JP337

| High Size | Under % | High Size | Under % | High Size | Under % | High Size | Under % | High Size | Under % | High Size | Under % | Span 1.46 |
|---|---|---|---|---|---|---|---|---|---|---|---|---|
| 118 | 100 | 53.3 | 100 | 24.0 | 100 | 10.8 | 100 | 4.84 | 100 | 2.18 | 99.4 | D[4,3] 0.89µm |
| 110 | 100 | 49.5 | 100 | 22.3 | 100 | 10.0 | 100 | 4.50 | 100 | 2.03 | 98.2 | |
| 102 | 100 | 46.1 | 100 | 20.7 | 100 | 9.31 | 100 | 4.19 | 100 | 1.88 | 95.8 | |
| 95.2 | 100 | 42.8 | 100 | 19.3 | 100 | 8.66 | 100 | 3.89 | 100 | 1.75 | 92.1 | D[3,2] 0.74µm |
| 88.6 | 100 | 39.8 | 100 | 17.9 | 100 | 8.05 | 100 | 3.62 | 100 | 1.63 | 87.7 | |
| 82.4 | 100 | 37.0 | 100 | 16.7 | 100 | 7.49 | 100 | 3.37 | 100 | 1.51 | 83.4 | |
| 76.6 | 100 | 34.4 | 100 | 15.5 | 100 | 6.97 | 100 | 3.13 | 100 | 1.41 | 79.5 | D[v,0.9] 1.69µm |
| 71.2 | 100 | 32.0 | 100 | 14.4 | 100 | 6.48 | 100 | 2.91 | 100 | 1.31 | 76.0 | |
| 66.2 | 100 | 29.8 | 100 | 13.4 | 100 | 6.02 | 100 | 2.71 | 100 | 1.22 | 72.6 | |
| 61.6 | 100 | 27.7 | 100 | 12.5 | 100 | 5.60 | 100 | 2.52 | 100 | | | D[v,0.1] 0.46µm |
| 57.3 | 100 | 25.8 | 100 | 11.6 | 100 | 5.21 | 100 | 2.34 | 99.9 | | | |

| | | | |
|---|---|---|---|
| Source = | :Sample | Beam length = 14.3 mm | Model indp |
| | | Log. Diff. = 3.891 | D[v,0.5] 0.85µm |
| Focal length = | 63 mm | Obscuration = 0.3288 | Volume Conc. = 0.0007% |
| Presentation = | pil | Volume distribution | Sp.S.A 8.0727 m²/cc. |

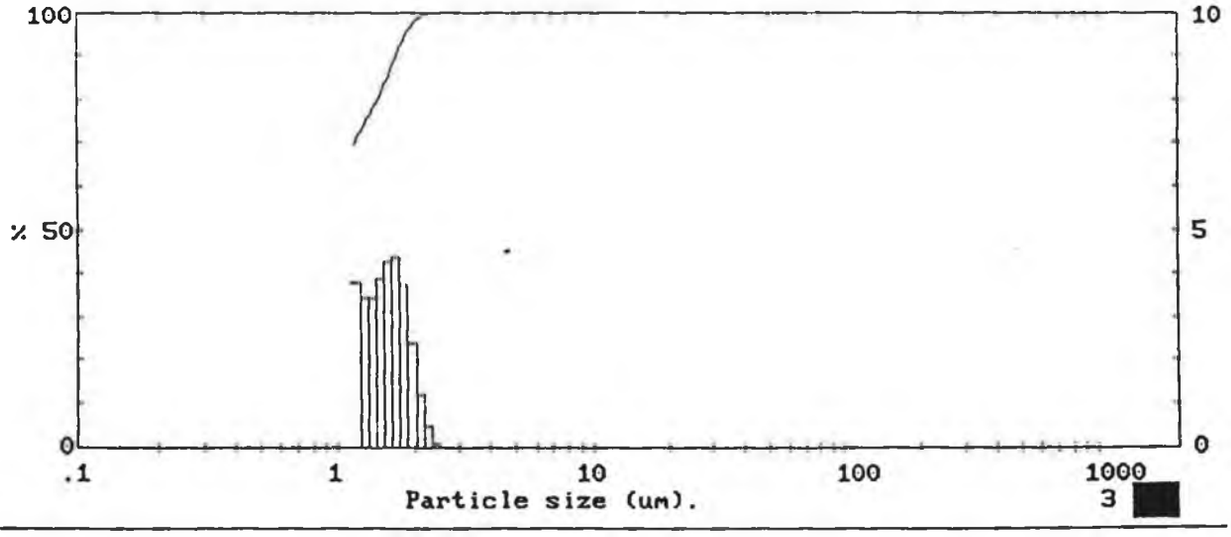


HARRIS IRELAND

**Figure 4.5B - Particle size analysis on full feed slip V-A (Vibro-Attrition)**

MALVERN Instruments SB.0B

Sample 2, powder slurry. t-t. Milling experiment. DMcA.
Sample of slurry into 20 mls water.Ultrasonic 5 mins,3 drops Nopcosant 000005449
Beaker, Test sample of this solution.

1978 pil 1JP337

| High Size | Under % | High Size | Under % | High Size | Under % | High Size | Under % | High Size | Under % | High Size | Under % | Span 1.72 |
|---|---|---|---|---|---|---|---|---|---|---|---|---|
| 118 | 100 | 53.3 | 100 | 24.0 | 100 | 10.8 | 100 | 4.84 | 97.9 | 2.18 | 86.6 | D[4,3] 1.31µm |
| 110 | 100 | 49.5 | 100 | 22.3 | 100 | 10.0 | 100 | 4.50 | 97.1 | 2.03 | 84.6 | |
| 102 | 100 | 46.1 | 100 | 20.7 | 100 | 9.31 | 100 | 4.19 | 96.3 | 1.88 | 82.3 | D[3,2] 0.88µm |
| 95.2 | 100 | 42.8 | 100 | 19.3 | 100 | 8.66 | 100 | 3.89 | 95.4 | 1.75 | 79.6 | |
| 88.6 | 100 | 39.8 | 100 | 17.9 | 100 | 8.05 | 100 | 3.62 | 94.6 | 1.63 | 76.1 | |
| 82.4 | 100 | 37.0 | 100 | 16.7 | 100 | 7.49 | 100 | 3.37 | 93.7 | 1.51 | 71.7 | D[v,0.9] 2.57µm |
| 76.6 | 100 | 34.4 | 100 | 15.5 | 100 | 6.97 | 99.9 | 3.13 | 92.9 | 1.41 | 66.4 | |
| 71.2 | 100 | 32.0 | 100 | 14.4 | 100 | 6.48 | 99.8 | 2.91 | 91.9 | 1.31 | 60.5 | |
| 66.2 | 100 | 29.8 | 100 | 13.4 | 100 | 6.02 | 99.5 | 2.71 | 90.9 | 1.22 | 54.3 | D[v,0.1] 0.57µm |
| 61.6 | 100 | 27.7 | 100 | 12.5 | 100 | 5.60 | 99.1 | 2.52 | 89.7 | | | |
| 57.3 | 100 | 25.8 | 100 | 11.6 | 100 | 5.21 | 98.6 | 2.34 | 88.3 | | | |

| | | | |
|---|---|---|---|
| Source = :Sample | Beam length = 14.3 mm | Model indp | D[v,0.5] 1.16µm |
| | Log. Diff. = 3.223 | | |
| Focal length = 63 mm | Obscuration = 0.4118 | Volume Conc. = 0.0011% | |
| Presentation = pil | Volume distribution | Sp.S.A 6.7864 m²/cc. | |

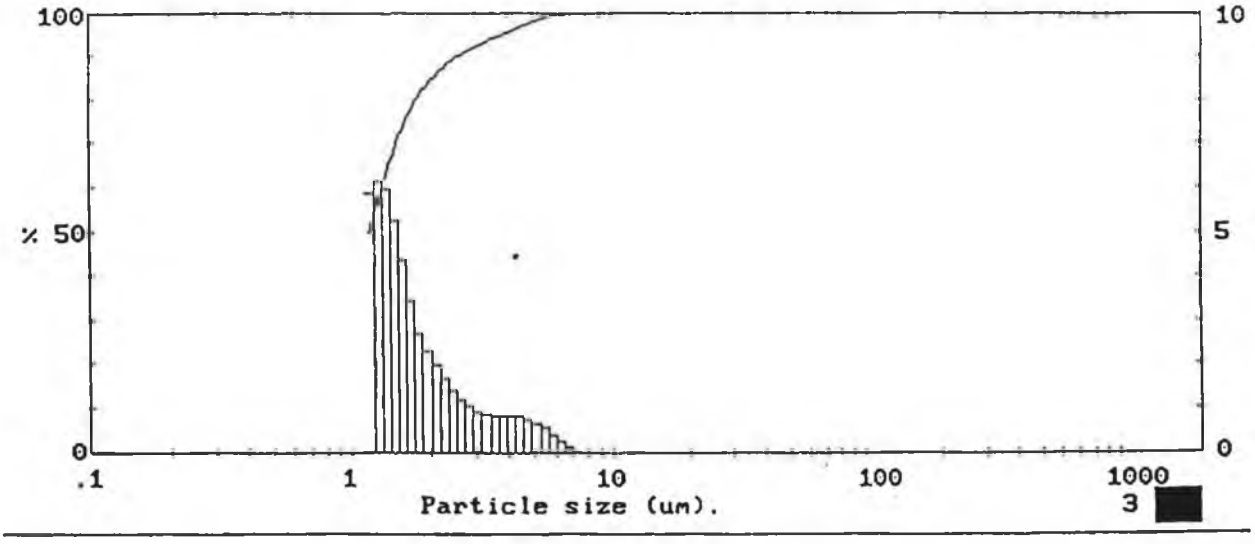


HARRIS IRELAND

Figure 4.5C - Particle size analysis on full feed slip 1-1 (Turbula-Turbula)

16 Feb 1994 12:27 pm

MALVERN Instruments SB.0B

Sample 6, powder slurry. t-s. Milling experiment. DMcA.
Sample of slurry into 20 mls water.Ultrasonic 5 mins,3 drops Nopcosant 000005440
Beaker, Test sample of this solution.

1978 pil 1JP337

| High Size | Under % | High Size | Under % | High Size | Under % | High Size | Under % | High Size | Under % | High Size | Under % | Span 1.74 |
|---|---|---|---|---|---|---|---|---|---|---|---|---|
| 118 | 100 | 53.3 | 100 | 24.0 | 100 | 10.8 | 100 | 4.84 | 99.3 | 2.18 | 92.2 | D[4,3] 1.07µm |
| 110 | 100 | 49.5 | 100 | 22.3 | 100 | 10.0 | 100 | 4.50 | 98.8 | 2.03 | 90.0 | |
| 102 | 100 | 46.1 | 100 | 20.7 | 100 | 9.31 | 100 | 4.19 | 98.3 | 1.88 | 87.3 | D[3,2] 0.78µm |
| 95.2 | 100 | 42.8 | 100 | 19.3 | 100 | 8.66 | 100 | 3.89 | 97.8 | 1.75 | 84.2 | |
| 88.6 | 100 | 39.8 | 100 | 17.9 | 100 | 8.05 | 100 | 3.62 | 97.3 | 1.63 | 81.0 | D[v,0.9] 2.03µm |
| 82.4 | 100 | 37.0 | 100 | 16.7 | 100 | 7.49 | 100 | 3.37 | 97.0 | 1.51 | 77.7 | |
| 76.6 | 100 | 34.4 | 100 | 15.5 | 100 | 6.97 | 100 | 3.13 | 96.6 | 1.41 | 74.4 | D[v,0.1] 0.47µm |
| 71.2 | 100 | 32.0 | 100 | 14.4 | 100 | 6.48 | 100 | 2.91 | 96.2 | 1.31 | 71.2 | |
| 66.2 | 100 | 29.8 | 100 | 13.4 | 100 | 6.02 | 100 | 2.71 | 95.8 | 1.22 | 67.8 | D[v,0.5] 0.90µm |
| 61.6 | 100 | 27.7 | 100 | 12.5 | 100 | 5.60 | 99.8 | 2.52 | 95.0 | | | |
| 57.3 | 100 | 25.8 | 100 | 11.6 | 100 | 5.21 | 99.6 | 2.34 | 93.8 | | | |

Source = :Sample
Focal length = 63 mm
Presentation = pil
Beam length = 14.3 mm
Log. Diff. = 3.170
Obscuration = 0.3420
Volume distribution
Model indp
Volume Conc. = 0.0008%
Sp.S.A 7.6489 m²/cc.

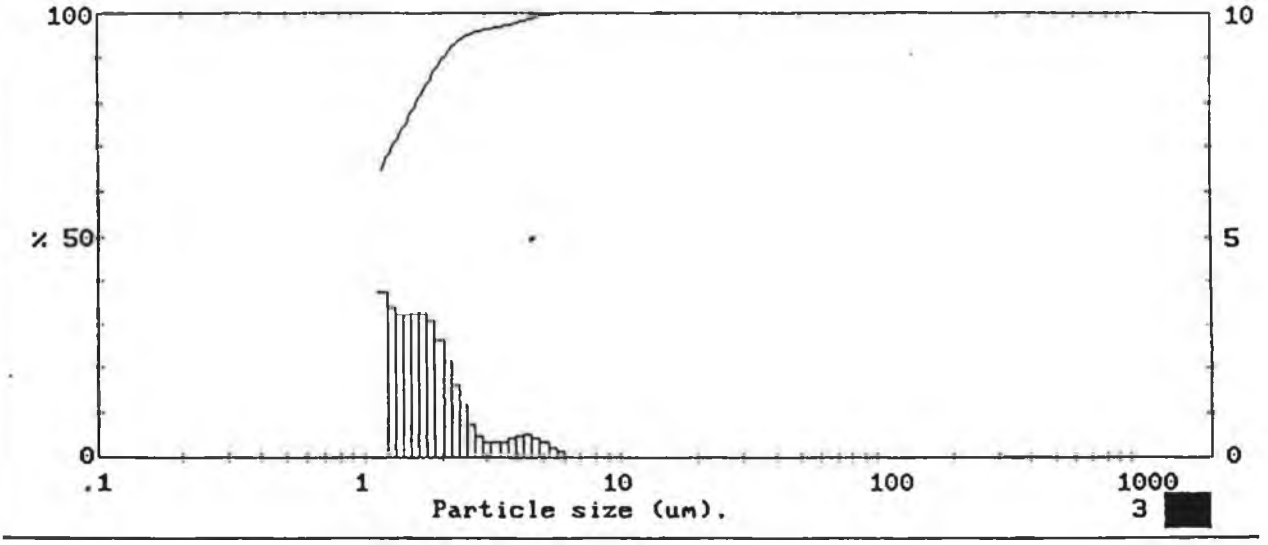


HARRIS IRELAND

**Figure 4.5D - Particle size analysis on full feed slip T-S (Turbula-Shear)**

MALVERN Instruments SB.0B

Sample 4, powder slurry. b-b. Milling experiment. DMcA.
Sample of slurry into 20 mls water.Ultrasonic 5 mins,3 drops Nopcosant 000005434
Beaker, Test sample of this solution.

1978 pil 1JP337

| High Size | Under % | High Size | Under % | High Size | Under % | High Size | Under % | High Size | Under % | High Size | Under % | Span 1.54 |
|---|---|---|---|---|---|---|---|---|---|---|---|---|
| 118 | 100 | 53.3 | 100 | 24.0 | 100 | 10.8 | 100 | 4.84 | 100 | 2.18 | 95.9 | D[4,3] 1.01µm |
| 110 | 100 | 49.5 | 100 | 22.3 | 100 | 10.0 | 100 | 4.50 | 100 | 2.03 | 93.0 | |
| 102 | 100 | 46.1 | 100 | 20.7 | 100 | 9.31 | 100 | 4.19 | 100 | 1.88 | 89.3 | D[3,2] 0.79µm |
| 95.2 | 100 | 42.8 | 100 | 19.3 | 100 | 8.66 | 100 | 3.89 | 100 | 1.75 | 84.9 | |
| 88.6 | 100 | 39.8 | 100 | 17.9 | 100 | 8.05 | 100 | 3.62 | 99.9 | 1.63 | 80.3 | D[v,0.9] 1.91µm |
| 82.4 | 100 | 37.0 | 100 | 16.7 | 100 | 7.49 | 100 | 3.37 | 99.8 | 1.51 | 75.9 | |
| 76.6 | 100 | 34.4 | 100 | 15.5 | 100 | 6.97 | 100 | 3.13 | 99.8 | 1.41 | 72.0 | D[v,0.1] 0.47µm |
| 71.2 | 100 | 32.0 | 100 | 14.4 | 100 | 6.48 | 100 | 2.91 | 99.7 | 1.31 | 68.5 | |
| 66.2 | 100 | 29.8 | 100 | 13.4 | 100 | 6.02 | 100 | 2.71 | 99.6 | 1.22 | 65.1 | D[v,0.5] 0.93µm |
| 61.6 | 100 | 27.7 | 100 | 12.5 | 100 | 5.60 | 100 | 2.52 | 99.1 | | | |
| 57.3 | 100 | 25.8 | 100 | 11.6 | 100 | 5.21 | 100 | 2.34 | 97.9 | | | |

| | | |
|---|---|---|
| Source = :Sample | Beam length = 14.3 mm | Model indp |
| | Log. Diff. = 3.277 | |
| Focal length = 63 mm | Obscuration = 0.2581 | Volume Conc. = 0.0006% |
| Presentation = pil | Volume distribution | Sp.S.A 7.5557 m²/cc. |

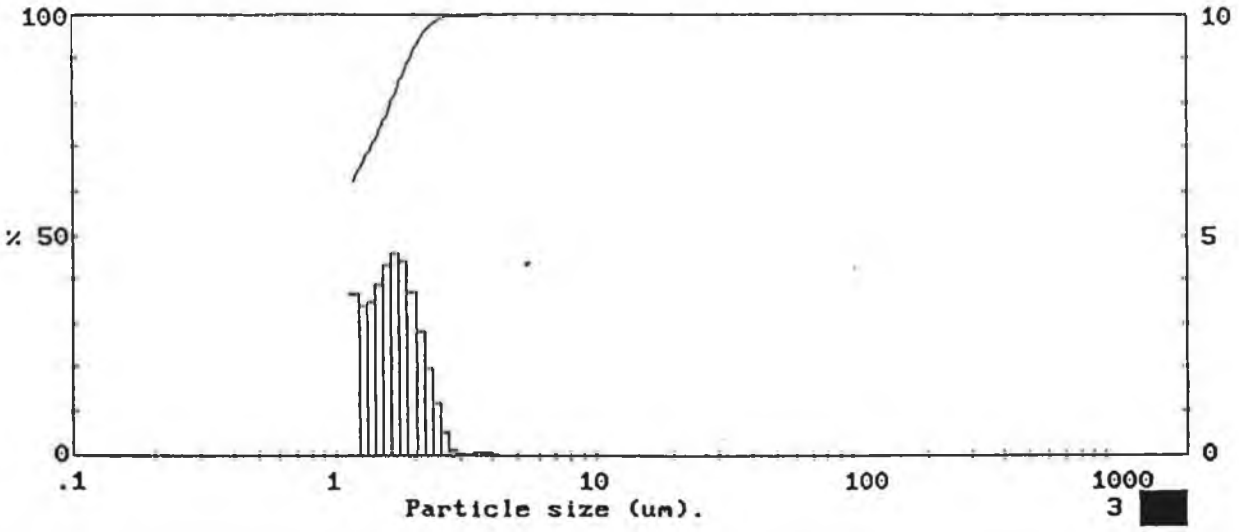


HARRIS IRELAND

**Figure 4.5E - Particle size analysis on full feed slip B-B (Ball-Ball)**

Sample 6, powder slurry. b-s. Milling experiment. DMcA.
Sample of slurry into 20 mls water.Ultrasonic 5 mins,3 drops Nopcosant 000005441
Beaker, Test sample of this solution.

1978 pil 1JP337

| High Size | Under % | High Size | Under % | High Size | Under % | High Size | Under % | High Size | Under % | High Size | Under % | Span 1.58 |
|---|---|---|---|---|---|---|---|---|---|---|---|---|
| 118 | 100 | 53.3 | 100 | 24.0 | 100 | 10.8 | 100 | 4.84 | 100 | 2.18 | 95.3 | D[4,3] 0.98µm |
| 110 | 100 | 49.5 | 100 | 22.3 | 100 | 10.0 | 100 | 4.50 | 99.9 | 2.03 | 93.3 | |
| 102 | 100 | 46.1 | 100 | 20.7 | 100 | 9.31 | 100 | 4.19 | 99.7 | 1.88 | 90.5 | D[3,2] 0.77µm |
| 95.2 | 100 | 42.8 | 100 | 19.3 | 100 | 8.66 | 100 | 3.89 | 99.6 | 1.75 | 87.0 | |
| 88.6 | 100 | 39.8 | 100 | 17.9 | 100 | 8.05 | 100 | 3.62 | 99.4 | 1.63 | 83.3 | |
| 82.4 | 100 | 37.0 | 100 | 16.7 | 100 | 7.49 | 100 | 3.37 | 99.2 | 1.51 | 79.6 | D[v,0.9] 1.86µm |
| 76.6 | 100 | 34.4 | 100 | 15.5 | 100 | 6.97 | 100 | 3.13 | 98.9 | 1.41 | 76.1 | |
| 71.2 | 100 | 32.0 | 100 | 14.4 | 100 | 6.48 | 100 | 2.91 | 98.7 | 1.31 | 72.7 | |
| 66.2 | 100 | 29.8 | 100 | 13.4 | 100 | 6.02 | 100 | 2.71 | 98.3 | 1.22 | 69.2 | D[v,0.1] 0.47µm |
| 61.6 | 100 | 27.7 | 100 | 12.5 | 100 | 5.60 | 100 | 2.52 | 97.7 | | | |
| 57.3 | 100 | 25.8 | 100 | 11.6 | 100 | 5.21 | 100 | 2.34 | 96.8 | | | |

| | | | |
|---|---|---|---|
| Source = :Sample | Beam length = 14.3 mm | Model indp | D[v,0.5] 0.88µm |
| | Log. Diff. = 3.296 | | |
| Focal length = 63 mm | Obscuration = 0.5822 | Volume Conc. = 0.0016% | |
| Presentation = pil | Volume distribution | Sp.S.A 7.8009 m²/cc. | |

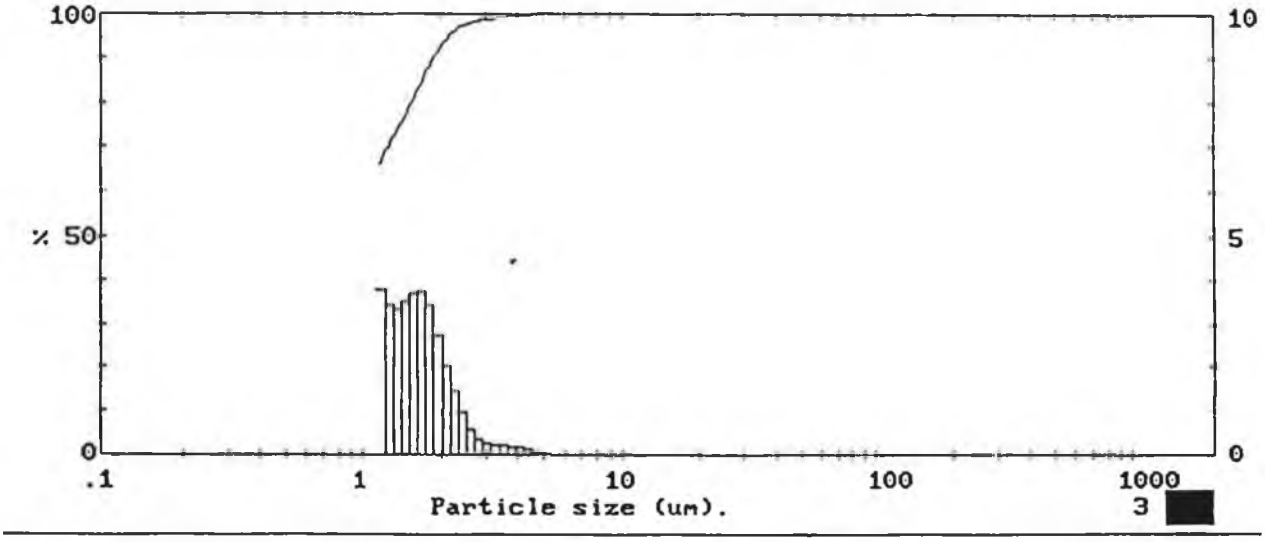


HARRIS IRELAND

**Figure 4.5F - Particle size analysis on full feed slip B-S (Ball-Shear)**

16 Feb 1994 12:53 pm

MALVERN Instruments SB.0B

Sample 7, powder slurry. a-s. Milling experiment. DMcA.
Sample of slurry into 20 mls water.Ultrasonic 5 mins,3 drops Nopcosant 000005452
Beaker, Test sample of this solution.

1978 pil 1JP337

| High Size | Under % | High Size | Under % | High Size | Under % | High Size | Under % | High Size | Under % | High Size | Under % | Span 1.56 |
|---|---|---|---|---|---|---|---|---|---|---|---|---|
| 118 | 100 | 53.3 | 100 | 24.0 | 100 | 10.8 | 100 | 4.84 | 100 | 2.18 | 96.4 | D[4,3] 0.94µm |
| 110 | 100 | 49.5 | 100 | 22.3 | 100 | 10.0 | 100 | 4.50 | 100 | 2.03 | 94.4 | |
| 102 | 100 | 46.1 | 100 | 20.7 | 100 | 9.31 | 100 | 4.19 | 100 | 1.88 | 91.7 | D[3,2] 0.76µm |
| 95.2 | 100 | 42.8 | 100 | 19.3 | 100 | 8.66 | 100 | 3.89 | 99.9 | 1.75 | 88.5 | |
| 88.6 | 100 | 39.8 | 100 | 17.9 | 100 | 8.05 | 100 | 3.62 | 99.8 | 1.63 | 84.9 | |
| 82.4 | 100 | 37.0 | 100 | 16.7 | 100 | 7.49 | 100 | 3.37 | 99.7 | 1.51 | 81.4 | D[v,0.9] 1.81µm |
| 76.6 | 100 | 34.4 | 100 | 15.5 | 100 | 6.97 | 100 | 3.13 | 99.6 | 1.41 | 78.0 | |
| 71.2 | 100 | 32.0 | 100 | 14.4 | 100 | 6.48 | 100 | 2.91 | 99.5 | 1.31 | 74.6 | |
| 66.2 | 100 | 29.8 | 100 | 13.4 | 100 | 6.02 | 100 | 2.71 | 99.3 | 1.22 | 71.1 | D[v,0.1] 0.46µm |
| 61.6 | 100 | 27.7 | 100 | 12.5 | 100 | 5.60 | 100 | 2.52 | 98.8 | | | |
| 57.3 | 100 | 25.8 | 100 | 11.6 | 100 | 5.21 | 100 | 2.34 | 97.9 | | | |

| | | | |
|---|---|---|---|
| Source = | :Sample | Beam length = 14.3 mm | Model indp |
| | | Log. Diff. = 3.499 | D[v,0.5] 0.86µm |
| Focal length = | 63 mm | Obscuration = 0.5523 | Volume Conc. = 0.0014% |
| Presentation = | p:1 | Volume distribution | Sp.S.A 7.9346 m²/cc. |

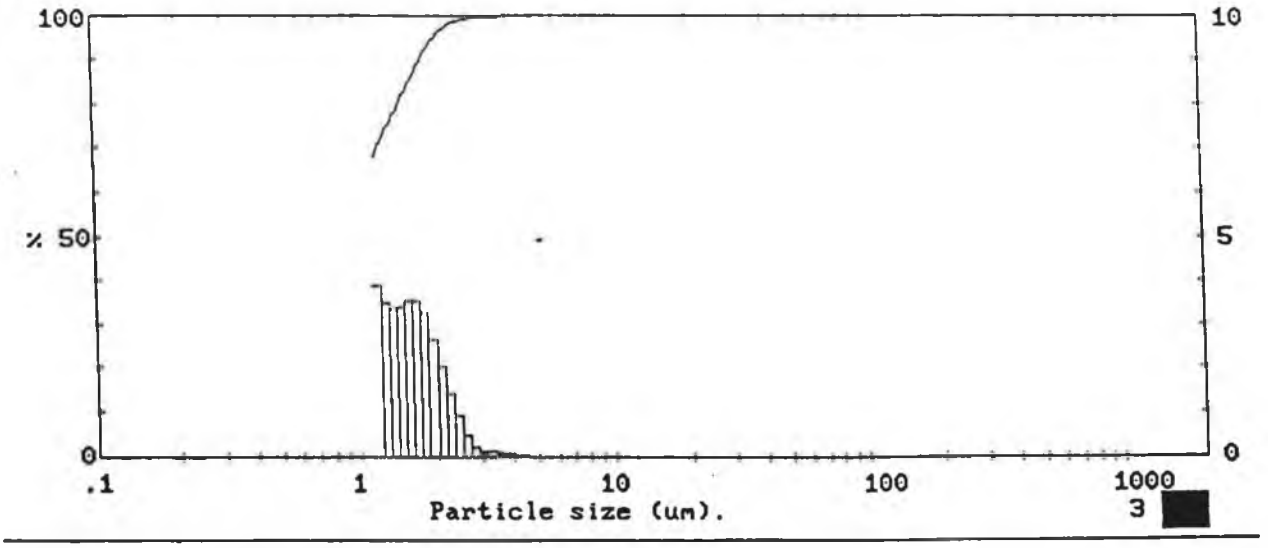


HARRIS IRELAND

**Figure 4.5G - Particle size analysis on full feed slip A-S (Attrition-Shear)**

16 Feb 1994 12:14 pm

MALVERN Instruments SB.0B

Sample 6, powder slurry. v-s. Milling experiment. DMcA.
Sample of slurry into 20 mls water.Ultrasonic 5 mins,3 drops Nopcosant 000005437
Beaker, Test sample of this solution. Marguerite.

1978 pil 1JP337

| High Size | Under % | High Size | Under % | High Size | Under % | High Size | Under % | High Size | Under % | High Size | Under % | Span 1.65 |
|---|---|---|---|---|---|---|---|---|---|---|---|---|
| 118 | 100 | 53.3 | 100 | 24.0 | 100 | 10.8 | 100 | 4.84 | 100 | 2.18 | 94.0 | D[4,3] 1.01µm |
| 110 | 100 | 49.5 | 100 | 22.3 | 100 | 10.0 | 100 | 4.50 | 99.9 | 2.03 | 91.7 | |
| 102 | 100 | 46.1 | 100 | 20.7 | 100 | 9.31 | 100 | 4.19 | 99.7 | 1.88 | 88.8 | D[3,2] 0.78µm |
| 95.2 | 100 | 42.8 | 100 | 19.3 | 100 | 8.66 | 100 | 3.89 | 99.6 | 1.75 | 85.5 | |
| 88.6 | 100 | 39.8 | 100 | 17.9 | 100 | 8.05 | 100 | 3.62 | 99.3 | 1.63 | 82.0 | |
| 82.4 | 100 | 37.0 | 100 | 16.7 | 100 | 7.49 | 100 | 3.37 | 99.0 | 1.51 | 78.6 | D[v,0.9] 1.94µm |
| 76.6 | 100 | 34.4 | 100 | 15.5 | 100 | 6.97 | 100 | 3.13 | 98.7 | 1.41 | 75.2 | |
| 71.2 | 100 | 32.0 | 100 | 14.4 | 100 | 6.48 | 100 | 2.91 | 98.3 | 1.31 | 71.9 | |
| 66.2 | 100 | 29.8 | 100 | 13.4 | 100 | 6.02 | 100 | 2.71 | 97.9 | 1.22 | 68.4 | D[v,0.1] 0.47µm |
| 61.6 | 100 | 27.7 | 100 | 12.5 | 100 | 5.60 | 100 | 2.52 | 97.1 | | | |
| 57.3 | 100 | 25.8 | 100 | 11.6 | 100 | 5.21 | 100 | 2.34 | 95.8 | | | |

| | | | |
|---|---|---|---|
| Source = :Sample | Beam length = 14.3 mm | Model indp | D[v,0.5] 0.89µm |
| | Log. Diff. = 3.384 | | |
| Focal length = 63 mm | Obscuration = 0.4098 | Volume Conc. = 0.0010% | |
| Presentation = pil | Volume distribution | Sp.S.A 7.7300 m²/cc. | |

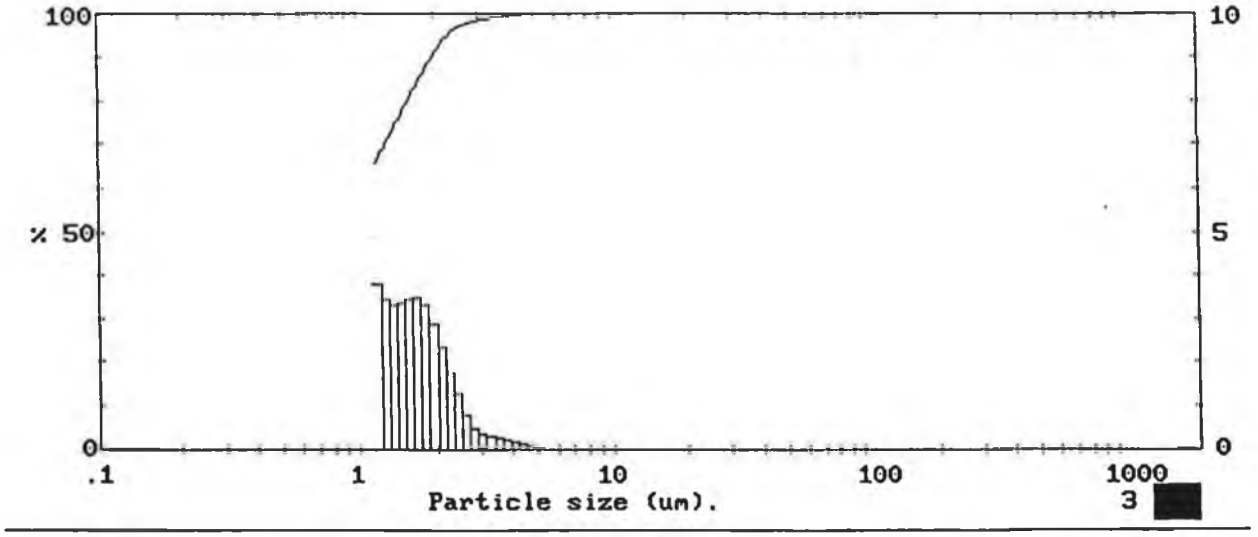


HARRIS IRELAND

**Figure 4.5H : Particle Size Analysis on full feed slip A-A (Attrition-Attrition)**

## 4.4 Disc Microstructure Analysis

### 4.4.1 Results

A scanning electron microscope was used to examine the microstructure of the samples at X500 magnification. Measurements of maximum and minimum grain size were taken, in addition observations were made regarding disc intragranular and intergranular porosity.

Photographs of the eight samples are contained from Figures 4.6A to 4.6H, also Table 4.2 summarises the main mechanical features of the sintered microstructure.

### 4.4.2 Discussion

In sample T-T, Figure 4.6A it was observed that grain size distribution was in the range of 40$\mu$m, with an average estimated at 50$\mu$m, representing 20 grains per millimetre. The porosity was primarily intragranular, but the intergranular pores were largest in the range from 5$\mu$m to 20$\mu$m. The Bismuth phase was evident at the grain boundaries, it was neither uniform in size nor distribution around the zinc oxide grains. It is this characteristic that may cause non uniform conduction within the disc body and hence the phenomenon known as hot spots. In sample T-S Figure 4.6B, microstructural appearance is similar to T-T, however its average grain size

distribution is closer to 60$\mu$m.

Sample B-B, Figure 4.6C shows grains ranging in size from 20$\mu$m to 80$\mu$m with an average 40$\mu$m or estimated 25 grains/millimetre. The grains were clearly irregular in shape. Porosity again was primarily intragranular but the intergranular pores were larger, in the size range 5$\mu$m to 30$\mu$m. The Bismuth phase was evident at the grain boundaries. Samples B-S, Figure 4.6D was very similar in appearance to B-B, with the exception that the intergranular porosity was smaller, in the range of 5$\mu$m to 20$\mu$m.

Sample V-S, Figure 4.6E shows irregularly shaped grains in the size range 60$\mu$m to 80$\mu$m with a low level of intragranular porosity compared to the turbula milled and ball milled samples. The intergranular pores were more clearly defined and in the size range 5 to 20$\mu$m. The Bismuth phase was visibly uniform at all grain boundaries, in sample V-A, Figure 4.6F the grain size distribution ranged from 60$\mu$m to 100$\mu$m with an average size of 80$\mu$m.

Sample A-A, Figure 4.6G showed irregular shaped grains in the size range 20$\mu$m to 80$\mu$m with an average of 40$\mu$m or 25 grains per millimetre. Porosity was again primarily intragranular with some longer intergranular pores in the range 5$\mu$m to 20$\mu$m. The Bismuth phase was evidently uniformly distributed around the zinc oxide grain. Samples A-S, Figure 4.6H was similar to A-A, however long narrow intergranular pores

were observed up to 40$\mu$m in length. Throughout the disc microstructure areas of both high porosity and dense grain growth were evident.

General observations regarding the microstructure of all the varistors shows that relatively large zinc oxide grains are the predominant plase. These are interspersed with a Bismuth rich phase at the grain boundaries which creates the varistor action. A high degree of uniform density in all samples was visible, with comparably similar degrees of porosity.

Estimates of the grain barrier voltage were made for all the samples based on the breakdown voltage measured at 1mA/cm$^2$ normalised to the voltage per millimetre and substituted into Equation 4.1

$$\text{grain barrier voltage} = \frac{\text{Voltage/Millimetre}}{\text{Average grain size}} \qquad \text{Equation 4.1}$$

Results are summarized under the electrical performance of the parts in Appendix A1.

| Mix/Mill Combination | Grain Size $\mu$m | | | | Porosity | | | Comments Bismuth Content |
|---|---|---|---|---|---|---|---|---|
| | Min | Avg | Max | Range | Intrag-granular present X not present | Inter-granular $\mu$m | | |
| | | | | | | Min | Max | |
| T-T | 40 | 50 | 100 | 60 | ✓ | 5 | 20 | Not uniform |
| T-S | 40 | 60 | 100 | 60 | ✓ | 5 | 20 | " |
| B-B | 20 | 40 | 80 | 60 | ✓ | 5 | 30 | More Uniform |
| B-S | 20 | 40 | 80 | 60 | ✓ | 5 | 20 | " |
| V-A | 60 | 40 | 100 | 40 | ✓ | 5 | 20 | " |
| V-S | 60 | 50 | 80 | 20 | ✓ | 5 | 20 | " |
| A-A | 20 | 40 | 80 | 60 | ✓ | 5 | 20 | Most Uniform |
| A-V | 20 | 40 | 80 | 60 | ✓ | 5 | 40 | " |
| A-S | 30 | 50 | 80 | 50 | ✓ | 5 | 20 | " |

**Table 4.2 : Main Mechanical observation regarding the microstructure of the sintered parts.**

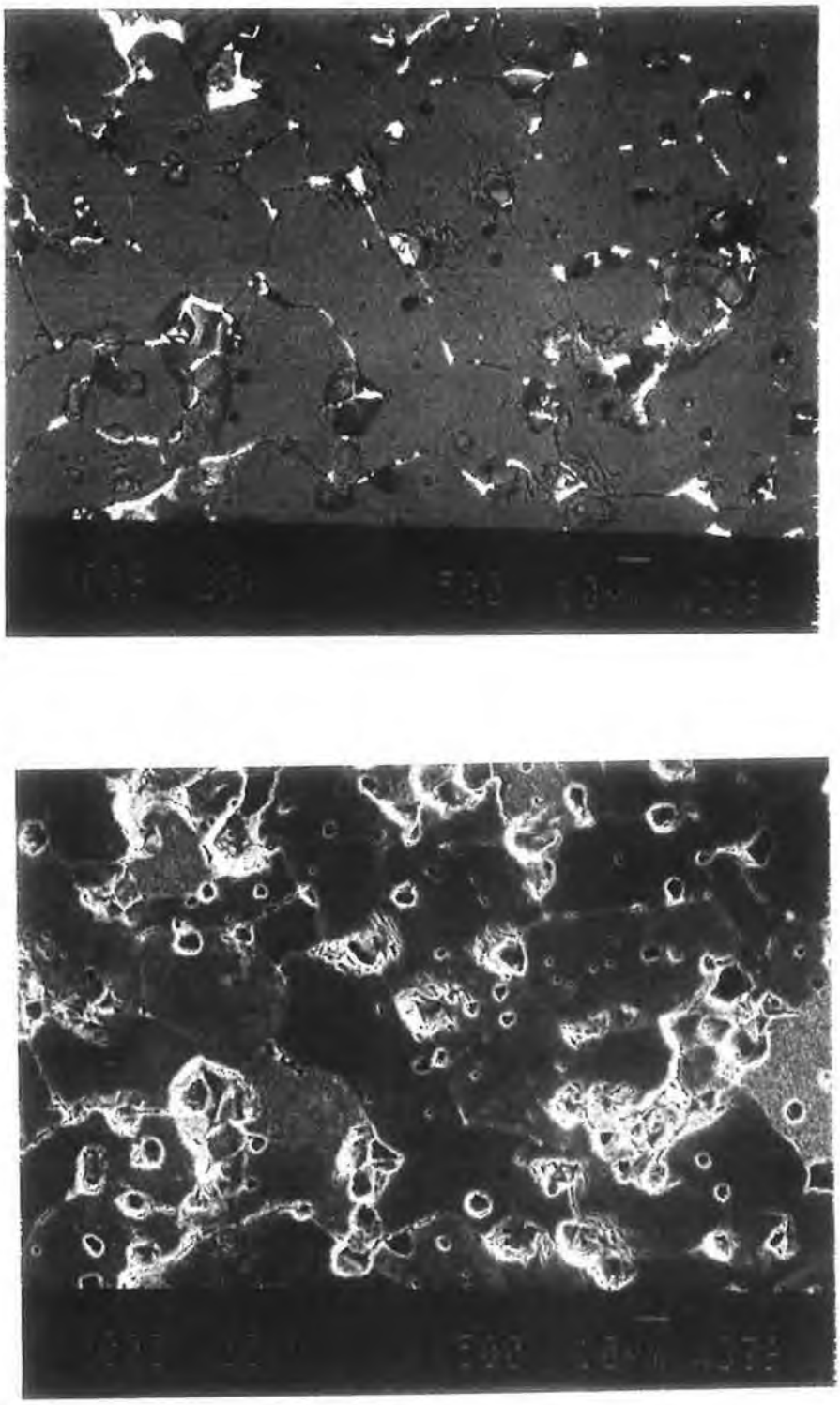

Figure 4.6A - SEM Micrograph, sample T-T (Turbula-Turbula)

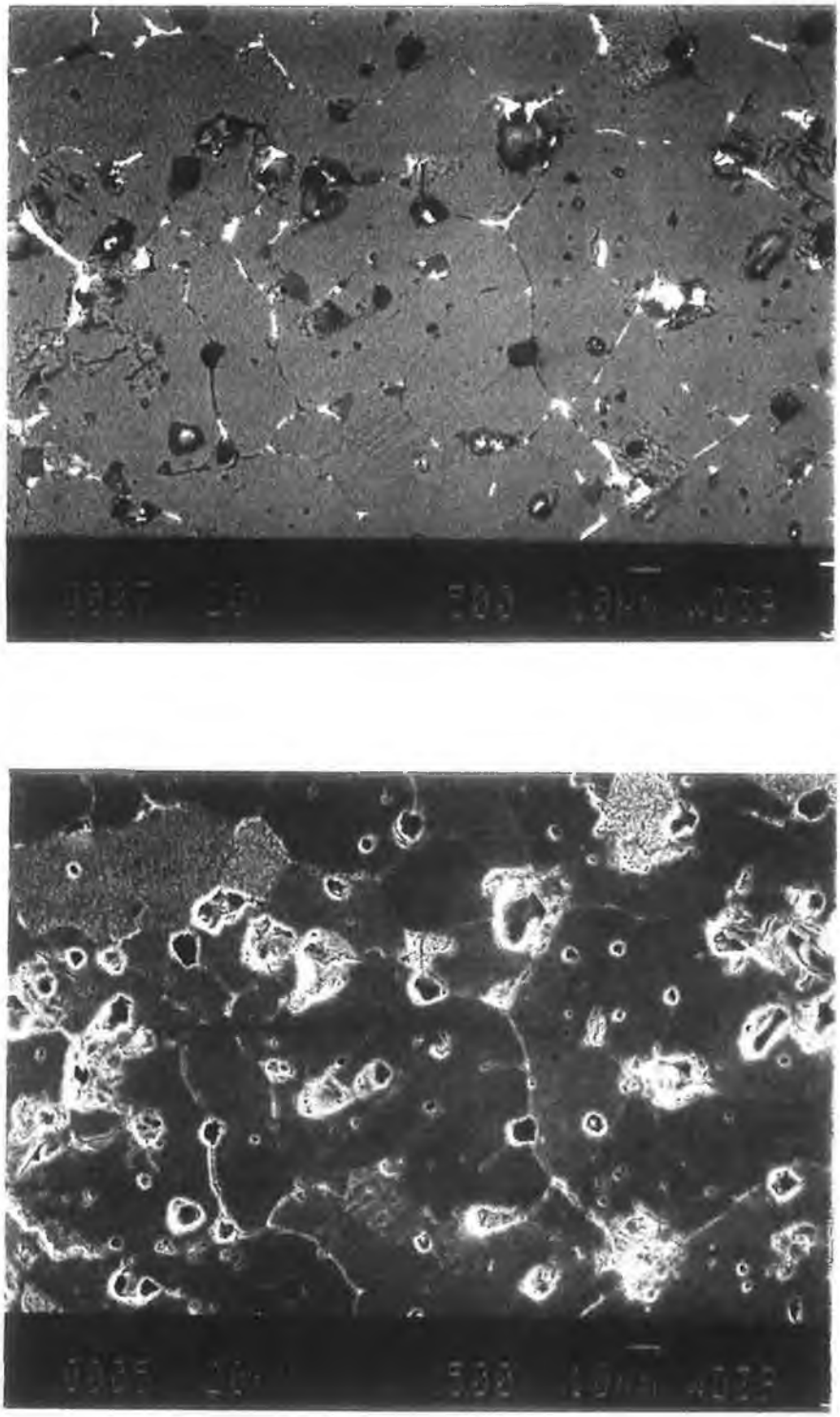

Figure 4.6B - SEM Micrograph, sample T-S (Turbula-Shear)

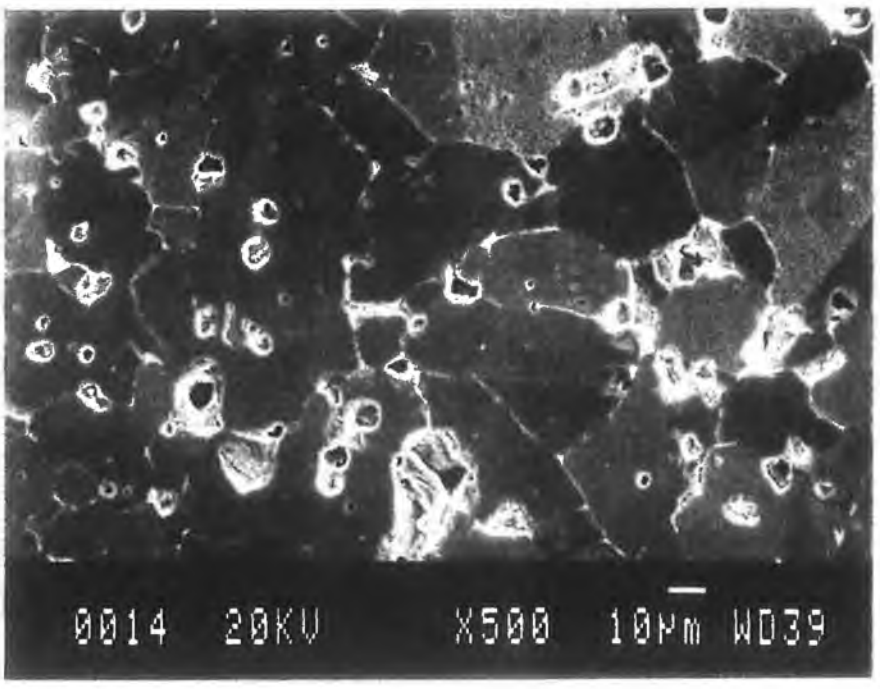


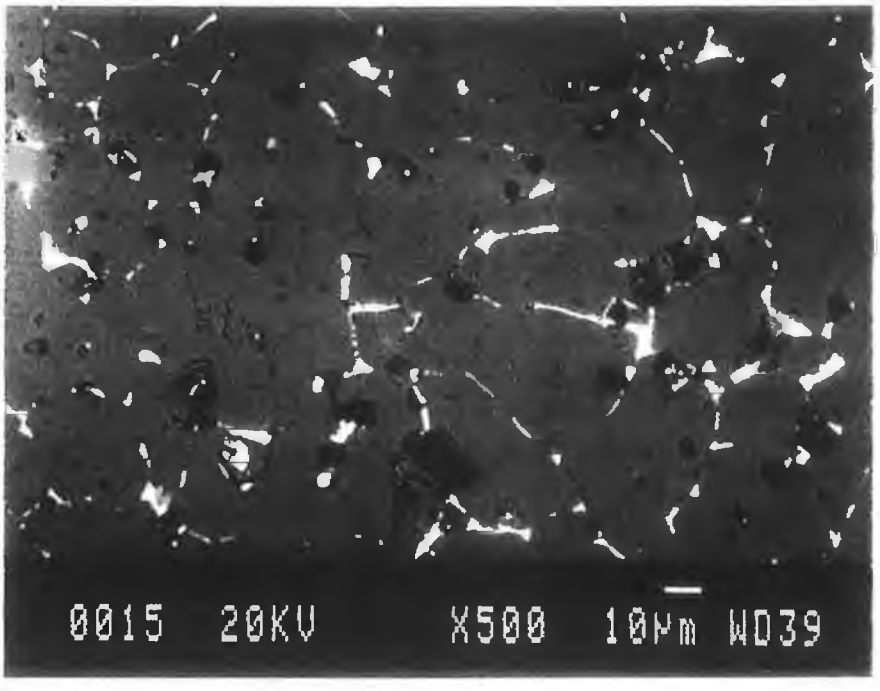


Figure 4.6C - SEM Micrograph, sample B-B (Ball-Ball)

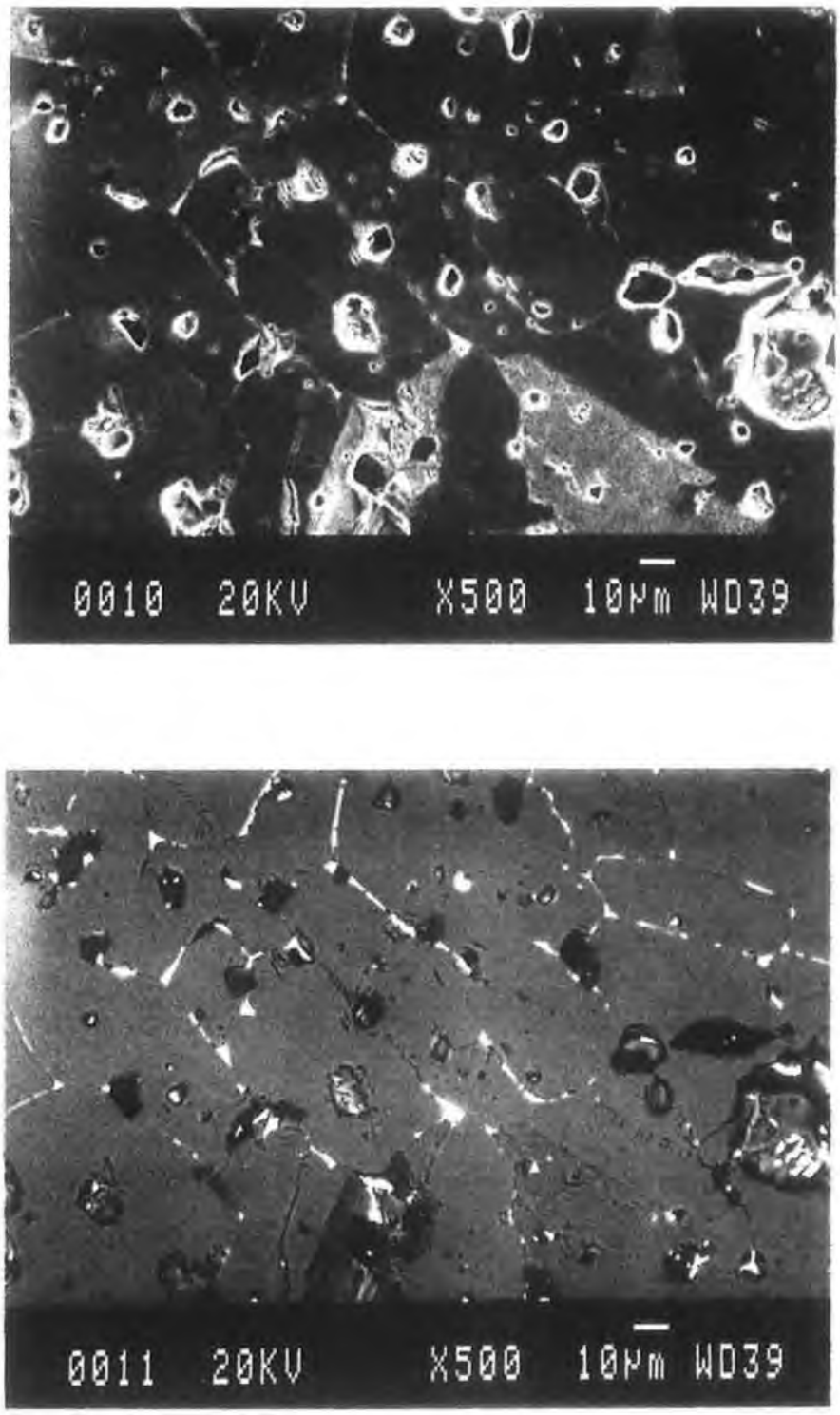


Figure 4.6D - SEM Micrograph, sample B-S (Ball-Shear)

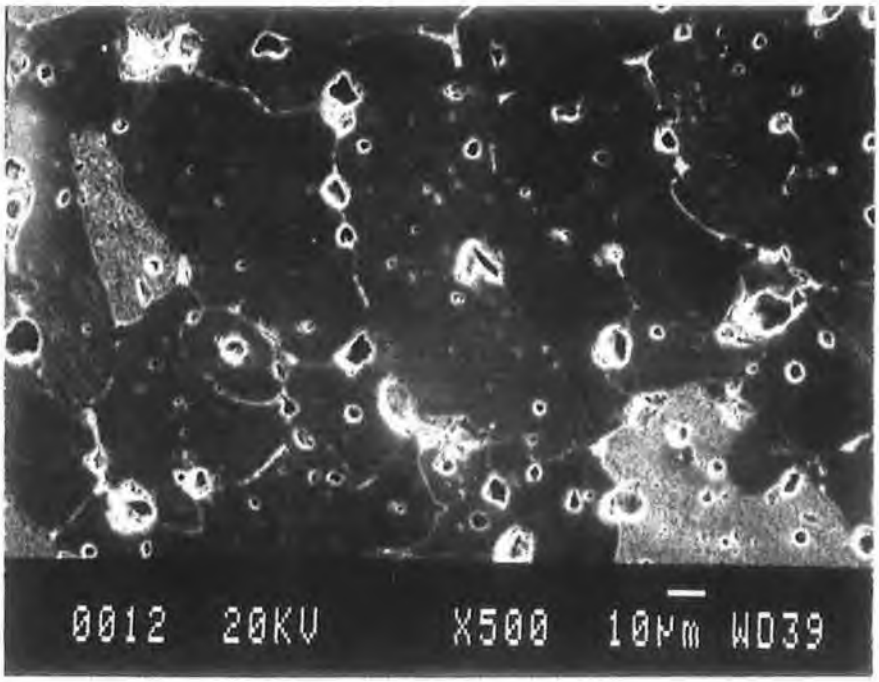


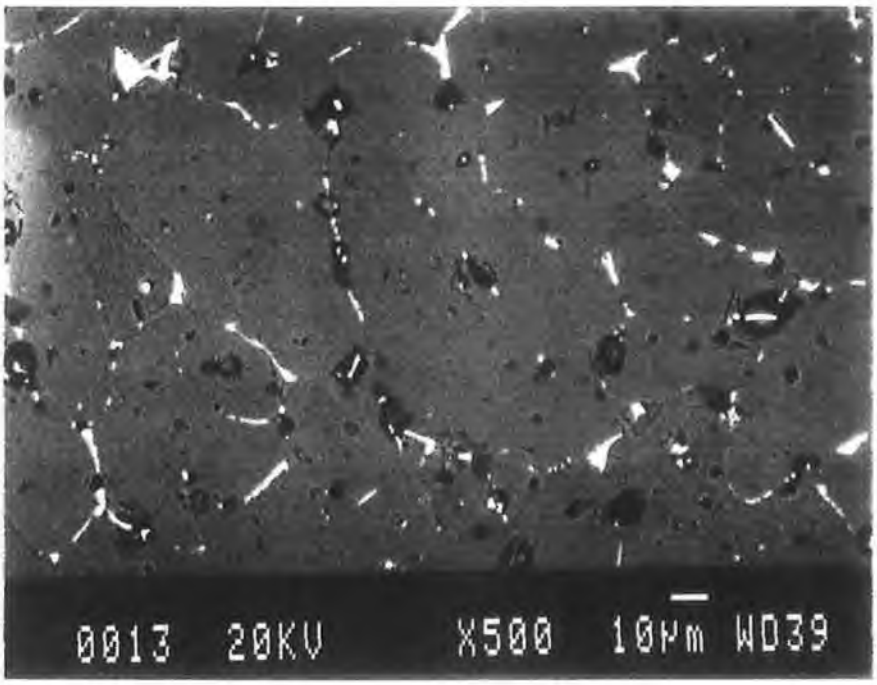


**Figure 4.6E - SEM Micrograph, sample V-A (Vibro-Attrition)**

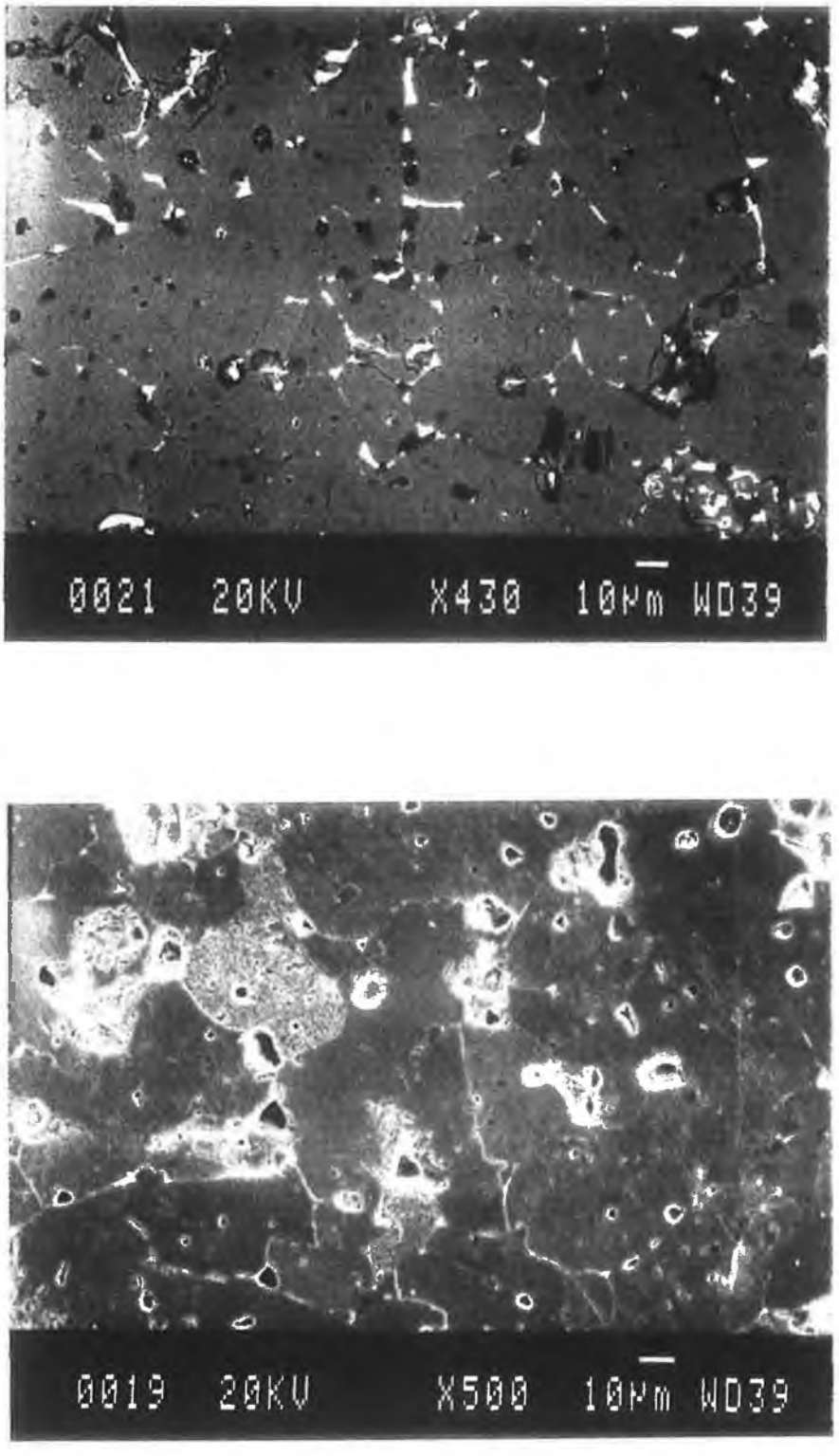


Figure 4.6F - SEM Micrograph, sample A-A (Attrition-Attrition)

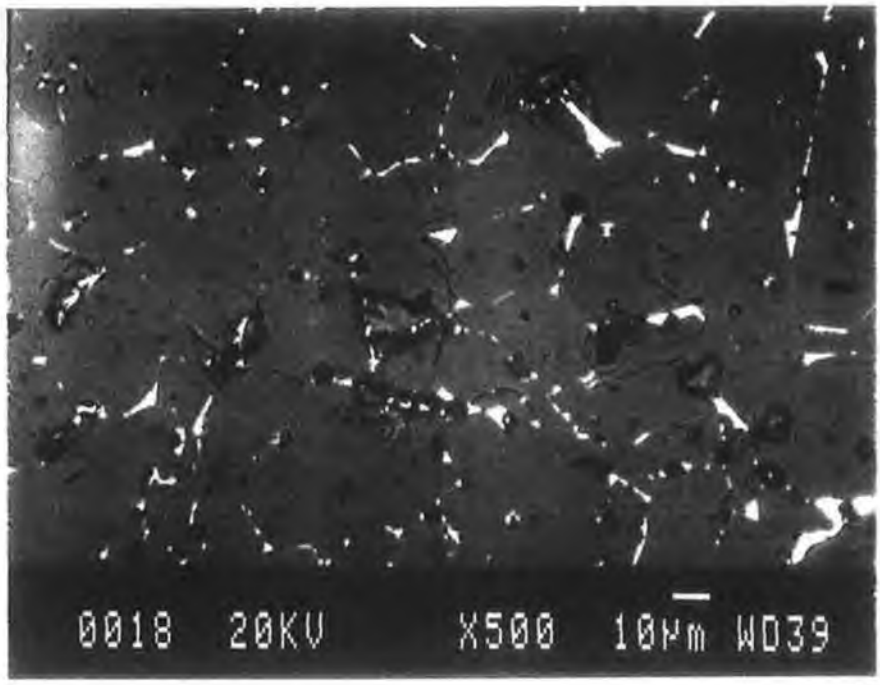


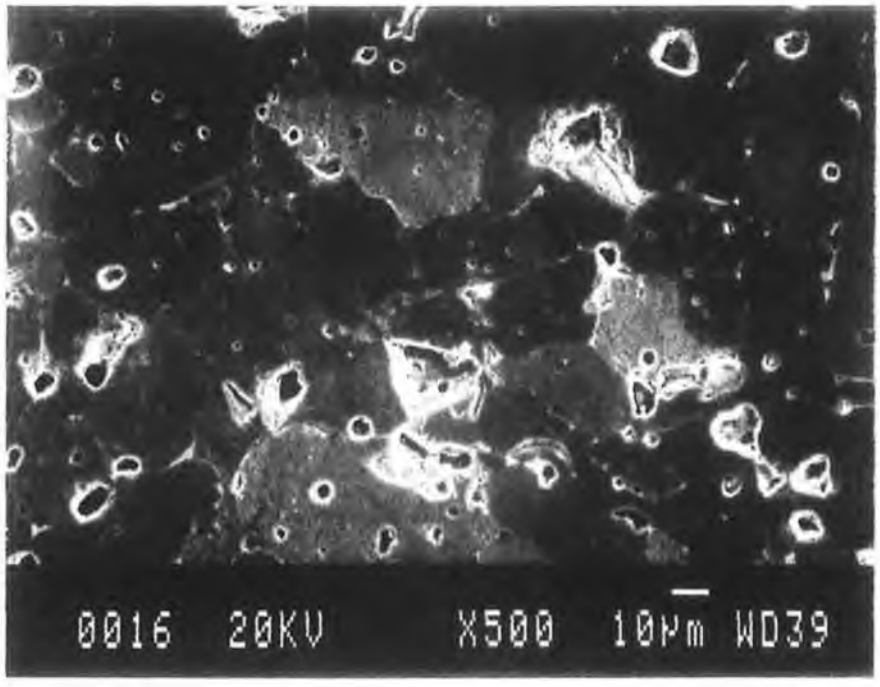


**Figure 4.6G - SEM Micrograph, sample A-S (Attrition-Shear)**

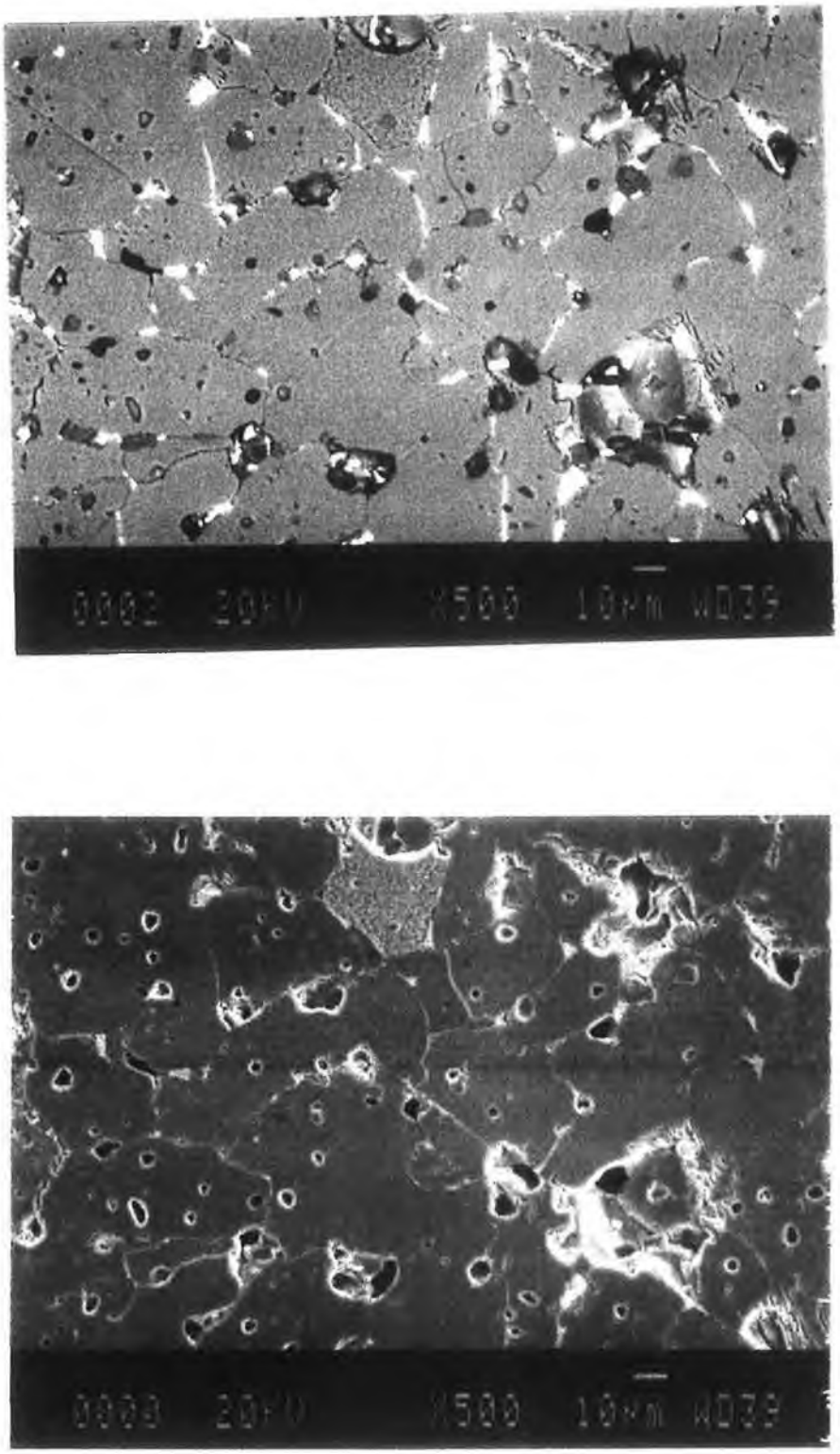

Figure 4.6H - SEM Micrograph, sample A-V (Attrition-Vibro)

### 4.5.1 Electrical Performance Analysis

All measurements taken regarding the electrical performance of all varistors are summarised in Appendix. The key results are shown in tabulated form in Table 4.3.

| Powder Type | Breakdown Voltage @ 1mA | Clamp Voltage @ 5A | % Max Clamp Voltage Shift | Clamp Voltage @ 250A | % Clamp voltage shift | Energy (J) Absorbed @ 250A | Average Clamp Voltage @ 1.8J | % Voltage Shift @ 1.8J | Estimated Grain Barrier Voltage | Leakage Current (nA) @ 23.5V | | Values |
|---|---|---|---|---|---|---|---|---|---|---|---|---|
| | | | | | | | | | | Fwd | Rev | |
| T-S | 56 | 89 | 0.58 | 159 | 2.3 | 56.2 | 80.9 | 0.74 | 1.83 | 37 | 45 | 18.3 |
| T-T | 44 | 82 | 0.61 | 151 | 2.6 | 53.1 | 78.1 | 6.2 | 2.25 | 44 | 27 | 28.3 |
| B-S | 55 | 79 | 0.94 | 162 | 3.6 | 56.9 | 79.2 | 1.0 | 1.83 | 36 | 21 | 26.3 |
| B-B | 54 | 73 | 0.39 | 157 | 7.1 | 55.2 | 78.5 | 0.7 | 1.8 | 43 | 27 | 28.2 |
| V-A | 52 | 70 | 0.4 | 144 | 1.8 | 50.6 | 75.1 | 0.6 | - | 38 | 25 | 28.6 |
| V-S | 53 | 85 | 0.4 | 149 | 0.9 | 52.3 | 77.4 | 0.39 | - | 41 | 23 | 18.1 |
| A-S | 54 | 73 | 8.04 | 158 | 7.2 | 55.2 | 78.5 | 0.7 | 1.8 | 43 | 27 | 28.2 |
| A-A | 52 | 82 | 0.2 | 149 | 1.7 | 52.6 | 75.4 | 1.39 | 1.83 | 48 | 29 | 18.5 |

**Table 4.3 : Electrical Performance Results**

### 4.5.2 Discussion

The purpose of this work is to compare the effect of powder processing techniques on both the microstructure and energy absorption capability of a diameter 7mm zinc oxide varistor for low voltate applications. To facilitate this, energy absorption during the application of a $10_{\mu s}/1000_{\mu s}$ waveform of 250A was calculated using the Equation 4.2.

(J) Energy Absorbed = $V_{Clamp}$ x $I_{Applied}$ x 1.405 x 103 Equation 4.2

where $V_{Clamp}$ - Clamp voltage measured at the applied current of 250A

(Source Harris Semiconductor, 1993)

A lower energy actually absorbed at this peak current is indicated by a lower recorded clamp voltage, and hence better varistor action. It also indicates the ability of the part to absorb higher energies This work sets out to demonstrate that the closer the particle size distribution of a varistor slip approximates to an average of 1$\mu$m what the best microstructural and electrical properties will be achieved. The variable chosen to achieve this end is the comminution technique employed to mill/mix dopants and zinc oxide together. Thus the lower and tighter the particle size distribution of the elements achieved prior to spray drying and sintering should also give the best electrical performance capability and reliability. Table 4.4 summarised the data comparing the range of energy absorbed by the eight samples produced using the four milling techniques with the particle size distribution of the dopants.

| | | ENERGY ABSORPTION RANGE (JOULES) | | | | | | | | | | | | | | | |
|---|---|---|---|---|---|---|---|---|---|---|---|---|---|---|---|---|---|
| PSD Range Ref | Powder Sample | 47 | 48 | 49 | 50 | 51 | 52 | 53 | 54 | 55 | 56 | 57 | 58 | 59 | 60 | 61 | 62 |
| 1 | T - S | | | | | | | | | | | | | | | | |
| 1 | T - T | | | | | | | | | | | | | | | | |
| 2 | B - S | | | | | | | | | | | | | | | | |
| 2 | B - B | | | | | | | | | | | | | | | | |
| 3 | V - A | | | | | | | | | | | | | | | | |
| 2 | V - S | | | | | | | | | | | | | | | | |
| 2 | A - S | | | | | | | | | | | | | | | | |
| 3 | A - A | | | | | | | | | | | | | | | | |

**Table 4.4 - Distribution of energy absorption capability @ 250A for all samples**

It is clear that the best energy absorption capability for a given current (250A) is demonstrated by sample V-A, also given its dopant particle size distribution is amongst the lowest produced. In contrast the poorest energy absorption performance is demonstrated by sample B-S where the particle size distributions are amongst the highest produced. There is a difference of 12% between the mean values of V-A and B-S of the amount of energy dissipated as a 10$\mu$s/1000$\mu$s pulse of current at 250A was applied to the devices.

Another interesting observation is that in all cases where a milling action is used to mix the dopants and zinc oxide together, the average energy absorption capability improves. Table 4.5 compares the results.

| Powder Type | Average Energy Absorbed (J) | % Improvement |
|---|---|---|
| B-S<br>B-B | 56.9<br>55.2 | 3% |
| V-S<br>V-V | 52/3<br>50.6 | 4.5% |
| A-S<br>A-A | 55.2<br>52.6 | 4.9% |

**Table 4.5 - Energy Capability improvement using a second milling operation as opposed to simply shear mixing**

Another observation of the varistor action at the peak current is the stability of the current-voltage characteristic that is required to remain within a $\pm 10\%$ tolerance of part voltage after experiencing the electrical stress as a result of the current surge applied. From the results of Appendix 1g it is clear that the max % shift of clamping voltage recorded at 250A does not exceed the $\pm 10\%$ value for any of the samples, in addition no pattern emerges regarding impaired particle size distribution of dopants or slip versus voltage stability. This holds true for voltage shifts also recorded at 5A and the rated current.

The nonlinear coefficient $\alpha$ (reference figure 1.1) of a ZnO varistor is a most important parameter of the devices. The $\alpha$ value reaches a maximum in the breakdown region of operation, and it is important to know how the $\alpha$ value relates to the range of currents over which the device is expected to operate. The $\alpha$ values for all the samples, and the slope of the V-I curve have been evaluated by substituting currents at two levels into Equation 4.3

$$\alpha = \frac{\text{Log } (I_2/I_1)}{\text{Log } (V_2/V_1)} \qquad \text{Equation 4.3}$$

where $V_2 > V_1$ and $I_2 > I_1$)

The results are summarised in Appendix A1. Currents $I_2 = 250A$ and $I_1 = 1x10^{-3}A$, voltages used to calculate the $\alpha$ values in the breakdown region associated with voltage $V_2$ at 250A and $V_1$ at 1mA. Values for $\alpha$ in most varistor applications normally range between 25 and 50. The typical $\alpha$ value

for this formulation at this current ratio is 15. Actual values of $\alpha$ measured for the 8 device samples range from 13.6 to 28.6 at a current ratio I2 /I1 = $250/1x10^{-3}$. The higher the value of $\alpha$ the better the device.

The average values of the forward and reverse leakage currents at rated 23.5V for the part are summarised below in Appendix I1. For most power applications the steady state operating voltage is between 70-80% of the breakdown voltage at a current density $1mA/cm_2$. The average leakage currents for all devices fabricated in this experiment are all within the desired range, and there are no conclusions to be drawn regarding the influence of the mix/mill techniques on the leakage current. Factors known to influence leakage current include applied voltage and varistor formulation.

The breakdown voltages at an applied specified current density of $1mA/cm^3$ were measured. There were no obvious significant differences in these values.

Estimates of the grain barrier voltage were calculated from the reference voltage and average grain size estimated during SEM microstructural analysis. No conclusions can be drawn from this because of the difficulty associated with accurate grain size measurement there is a wide variation in breakdown voltage for all samples which are known to be between 2-3V per barrier for this proprietary formula.

Leakage currents for the samples were measured and results included in Appendix I1. This characteristic of ZnO varistor is important since it determines the amount of watt loss (or power consumed as part of the circuit) that a varistor is expected to generate upon application of a steady state operating voltage. The amount of leakage current determines the magnitude of the steady state operating voltage that the device can accept without generating an excessive amount of heat due to the flow of current. The heat generated by the steady state or operating voltage will also affect the life expectancy of a varistor.

## Chapter 5 - Conclusions and recommendations for future work

5.1 Dopant Milling Systems

5.2 Dopant Zinc Oxide Mixing Milling Systems.

# CHAPTER 5: Conclusions and recommendations for future work

## 5.1 Dopant Milling Systems

It was found that the attrition mill technique was the most efficient of all comminution techniques employed during this experiment. In terms of both the time required to achieve a particle size distribution and the efficiency of the process in achieving a tight particle size distribution, the attrition mill is superior when used to reduce particle size of varistor dopants and zinc oxide. The next most efficent process is the vibratory mill. Here particle size distributions close to those achieved during attrition milling can be achieved, but they are significantly better than those produced by either the ball or turbula mills. These observations have been made on the work carried out on both the varistor dopants and the full formulation slip.

During the analysis of the disc microstructure, particular emphasis was paid to any correlation that could be made between the comminution technique employed during dopant milling and the range of grain sizes actually achieved in the sintered ceramic. The goal during sintering of a varistor body is to achieve a tight and homogenous grain size distribution without the growth of excessively large grains which can impair the electrical performance of the devices. However no clear pattern emerges from the data derived during the analysis regarding the influence of the milling techniques employed for either the dopants nor the full formulation slip on the grain size distribution achieved during sintering. However the uniformity of bismuth deposits around the zinc oxide boundaries which became progressively more uniform in size

as the efficiency of the milling technique employed became higher. Best results were achieved when both the attrition and the vibratory mills were used to reduce dopant particle size distribution compared to those achieved using the ball and turbula mills.

Another interesting conclusion of this work is the improved average energy absorption capability of the vibratory - attrition mill combination compared to the conventional ball mill - shear mixer combination . Examination of the average energy absorption capability at 250A shows the low particle size distribution of dopants and full feed slip generated by the V-A combination to perform 12% better in terms of energy absorption capability versus the B-S configuration. It should be noted that the energy absorption capability of all devices produced when powder samples were milled to prepare the full feed slip as opposed to simply shear mixing that in all cases the energy absorption capability of the devices were improved by 3 - 4.5%.

No noticeable difference in the reliability of the devices was seen between any of the samples tested, in all cases the voltage returned to within +/- 10% of the rated value at the current density of 1mA/cm2 ,on testing after the application of an 8us/20us current pulse, in addition none of the processing techniques employed show any significant change to the leakage currents measured at the rated voltage.

## 5.2 RECOMMENDATIONS FOR FUTURE WORK

This work has tried to improve on the particle size distributions of dopants and zinc oxides achieved using a variety of commercially availble

comminution techniques. It has been shown that improvements in the range and scale of reductions made can have a significant influence on the energy absorption capability of varistor devices and the distribution of dopants around zinc oxide grains during the sintering process. To further extend the scope of this observation, the production of zinc oxide devices using Sol-Gel technology would perhaps yield usefull results, where submicron sized particles as small as 0.04 microns can be produced compared to the best available conventional technique.

Another area that may yield usefull results is a study of the effects the cooling rate during the sintering cycle has on the microstructure of zinc oxide varistors, and in particular to the phases formed by the chemically reacted oxides around the zinc oxide grains. This thesis has interpretted results in terms of the simple functional microstructure used to determine the varistor voltage, particularly data regarding the grain size distribution, and general comments regarding the distribution of bismuth deposits around the zinc oxide grains.

To further the understanding of zinc oxide varistor operation, it would be usefull to extend the scope of this work to allow a more in depth interpretation of the microstructural characteristics of the devices to include relative volume fraction of zinc oxide , spinel and bismuth rich phases.

## REFERENCES


Anhydro Ltd. (Commercial Brochure)

DK-2860 Soborg, Denmark.

"Spray Drying Processing Plants"

Asokan T, Iyengar G.N.K., Nagabhushana G.R.

"Studies on microstructure and density of sintered zinc oxide based non linear resistors".

Journal of Materials Science, 22, June 1987, 2229 - 2236.

Austin M, Sonder E,

"The effect of oxidising and reducing atmospheres at elevated temperatures on the electrical properties of zinc oxide varistors"

J.Appl.Phys.54 (6), June 1983.

Bagster D.F., Roberts A.W. (1985)

"The Effect of Large Particles in the Flow Properties of Powder"

Powder Tehcnology, 43, p.11-17

Belcher D.W., Smith D.A. and Cook E.M.

"Design and Use of Spray Dryers, Design and Costs"

Bowen Engineering Inc.

Bowen Engineering Inc. (Commercial Brochure)

Somerville, New Jersey.

"Spray Drying of Ceramics for Pressing Operations"

Brewer J.A., Moore R.H. and Reed J.S. (1981)

"Effect of Relative Humidity on the Compaction of Barium Titanate and Manganese Zinc Ferrite containing PCA"

Ceramic Bulletin, P.214-217, 60 (2)

Bowen L.J., Avella F.J.

"Microstructure, Electrical properties, and failure prediction in low clamping voltage zinc oxide varistors".

J.Appl.Phys.54 (5), May 1983.

Cannell D. and Triag P.

Ceramic Transactions, the American Ceramic Society.

"Processing of Electronic Ceramics"

(Not dated)

Cerra H, Rusworm W,

"Microstructure and crystal structure of Bismuth oxide phases in zinc oxide varistor ceramics".

J.Amer.Cer.Soc, Vol 72 , No 7, p522-529, 1988.

Chemical Engineers Handbook (1985)

DiMilia R.A. and Reed J.S. (1985)

"Dependance of Compaction of the Glass Transition Temperature of the Binder Phase"

Ceramic Bulletin (62)4 P.484-488

Dynys F.W. and Halloran J.W.,

"Compaction of Aggregated Alumina Powder"

Journal of American Ceramic Society. Vol. 66 no. 9, 1983 P.655-659

Eda K,

"Destruction mechanism of zinc oxide varistors due to high currents".

J.Appl,Phys. 56 (10) 15 November 1984.

Eda K,

"Discovery of zinc oxide varistors and their progress for two decades- Progress in fabrication technology of zinc oxide varistors"

Ceramic transactions, The American ceramic society, not dated.

Emeruwa, E., Jarrige J and Hexmain J. (June 1989)

"Ferrite Powder Compaction with Ultrasonic Assistance"

Proceedings 1st European Ceramic Society and Exhibition "Science of Ceramics 15"

Maastricht (WL)

Falk L.K.L., Olssen E, Dunlop and Osterlund,

"The microstructure of an zinc oxide varistor material".

J.Mater.Sci. 20 (1985) 4091 - 4098.

Frey, R.G.; Halloran, J.W.

"Compaction Behaviour of Spray Dried Alumina"

J. of. Am. Ceram. Soc. 1984 Vol. 67 no. 3. pp 199-203

Gambino J.P.

"The influence of microstructure, grain boundary segregation and grain boundary stiochiometry on the electrical properties of zinc oxide varistors".

Phd Thesis submitted to Massachusetts institute of technology, 1984.

Greskovich, G.

Treatise on Material Science and Technology - Vol. 9,

"Ceramic Fabrication Processes"

Ed. by F. F.Y. Wang - Publ. by Academic Press, NY, 1976.

Gupta T.K.

"Application of Zinc Oxide Varistors"

J. AM. Ceram. Soc. 73(7) 1817-1840 (1990)

Harris Semiconductor Manual "Transient Suppression Devices" (1990)

Harvey J.W. and Johnson Jr. D.W. (1980)

"Binder Systems in Ferrites" Ceramics Bulletin., 59 (6) P.637 - 645

Hoffmann B, Schwing U,

"Low voltage varistors".

Institut fur technologie der elektrotechnik, Universitat Karlsruhe.

Housner H.H. (1973)

"The Role of Interparticulate Friction in Powder Technology".

"Compaction '73' "

The Powder Advisory Centre, Ed. by A. S. Goldbertg P7 - 12.

Hausner H.H. (1981)

"Powder Characteristics and their effect on Powder Processing"

Powder Technology, 30, P3 - 8

Hoescht (Commercial Brochure)

"Manual for Mowiol, Polyvinyl Alcohol"

Hoffman E.R.

"Importance of Binders on Spray Dried Powders"

Ceramic Bulletin, 51 (3), P240 - 242. (1972)

Loubiere A, Hassanzadeh M,

"Degradation of zinc oxide varistors subjected to partial discharges in air".

Silicates Industriels 1990/1-2. p23-25.

Lukasiewics, S.L.,

"Spray Drying Ceramic Powders"

Journal American Ceramic Society, 72 (4) 617 - 24 (1989)

Lukasiewics, S.L.; Reed, J.S.,

"Character and Compaction Response of Spray Dried Agglomerates"

Ceramic Bulletin, Vol. 57, No. 9 (1978)

Martzloff F.D., Levinson L.M.,

"Surge protective devices". (Courtesy General Electric Company)

Matsuoka, M.,

"Advances in Ceramics, Vol. 1, Grain Boundaries in Electronic Ceramics"

(The American Ceramic Society, Columbus, Ohio.) (1981) pp290.308

Master, K.,

"Spray Drying Ceramic Powders"

Ceramic Bulletic, Vol. 59, No. 8 (1979)

Jerabek S.A. and Cardella S.J. (Eds.) (1986)

"Transient Voltage Suppression" 5th Edition,

General Electric Company, Syracuse, USA.

K. Kendal, W. McNalford, J.D. Birchall

"The Strength of Green Bodies"

British Ceramic Proc. 37 (October 1986).

Kao C.C.,Bow J.S.,

"Fabrication and properties of low voltage Zinc oxide varistors by the seed grain method"

Mtl.Bull.Res.DEv.,Vol 4, No2 (1990)pp(25-27)

Kim Y.S. (1976)

"Effects of Powder Characteristics" in "Ceramic Fabrication Processes"

Ed. by F.F.Y Want Treat. Mat. Sc and Techn. Vol 19.

Academic Press P51 - 67

Levinson, L.M.; Phillip, H.R.,

"The Physics of Metal Oxide Varistors"

General Electric Company Corporate Research and Development (1974)

Marshall, K.,

"Conventional Strength Testing of Ceramics"

Fracture Mechanics of Ceramics, Plenum Press.

Mizukoshi A, Ozana J,

"Influence of uniformity on energy absorption capabilities of zinc oxide elements as applied in arresters".

IEEE Transactions on power apparatus and systems, Vol.pas-102, No5, May 1983.

Nakano Y, Ichinose N,

"Effect of additives on the electrical properties and microstructure of ceramic varistors in Zno-SrO system".

J.Ceram.Soc.Jpn.Inter.Ed.Vol.97 (1229-1235) (1989)

Nishida M, Ando H, Mihara T, Kugimma k,

"Piezoelctric ceramics for high power applications-

Preparation of ultrafine particles by media agitating mill".

Central research lab., Matsushita Electrical Industrial Co. (not dated).

Nyberg, Brita, Carlstrom, Elis,

"Uniform Distribution of a Pressing Aid"

Presented at the Int. Conf. in Ceramics Powder Processing Science (1988)

Olssen E, Dunlop G.L.,

"Characterisation of individual interfaces in a ZnO varistor material"

Thesis submitted to Chalmers university of technology, Sweden, 1988.

Olssen E, Dunlop G.L.,

"Development a of a functional microstructure during sinterung of a ZnO varistor material"

J.Mater.Sci, P21-29 (1987)

Osterlund R, Dunlop G.L., Olssen E,

"The role of interfacial microstructur in ZnO varistors"

J.Mater Sci,p28-36 (1986).

Phelps J.M., (1985)

"Spray Dyring Ceramics"

Presented at Pennsylvanie Ceramic Association

40th Annual Meeting October

Pincus A. G. and Shipley L.A. (1969)

"The Role of Organic Binders in Ceramic Processing"

Ceramic Industry Magazine, 146 April P106 - 109, 146

Pentecost J.L.,

Treatise on Material Science and Technology - Vol. 9,

"Ceramic Fabrication Processes" (1976).

Reed J.S. and Bunk R.B. (1976)

"Dry Pressing" in "Ceramic Fabrication Processes"

Ed. by F.F. Y. Wang Treat. Mat. Sc. and Techn. Vol. 9, Academic Press P42.

APS Reymer, 1990

"Dry Pressing of Ceramic Powders"

Powder Technology, Vol. 9 1987, P187 - 194.

Rosen S.L. (1982)

Fundamentals and Principles of Polymeric Materials"

Wiley and Sons, New York, P84 - 87.

Rumpf, P; 1970,

"Dry Pressing in Ceramic Fabrication Process"

Mat. Sci. and Techn. Vol. 9, Academic Press p42.

Sato K, Tanaka J, Hanada H,

"Capacitance - Voltage characteristics of ZnO varistors and the role of dopants"

J.Ceram.Soc.Jpn.Inter.Ed.Vol 97 (1225- 1228) (1989)

Seitz M, Yang S.Y.,

"Thermal conductivity of ceramic varistors"

Marquette University, Milwaukee, Wis.53233.

Sheppard, Laurel M.

"Trends in Powder Processing Equipment"

American Caramic Society Bulletin, Vol. 72, No. 5, May 1993.

Sonder E, Levinson M, Katz W,

" Role of the short circuiting pathways in reduced ZnO varistors"

J.Appl.Phys.58 (11), 1 Decemeber 1985.

Smith T.A.

"Organic Binders and Other Additives for Glazes"

Research paper 486, British Ceramic Research Association.

A.L. Stuigts

"Ceramic Forming Methods"

Proc. Int. Ceram. Soc. October, 1985.

Strijbos S.

"Powder - Wall Friction; The Effects of Wall Grooves and Wall Lubricants"

Powder Technology, Vol. 8, 1977 P209 - 2214

Technical Engineers Handbook (1987)

Thompson M.S., Wisemann G.H.,

" Synthesis and microstructure of Gel - Derived varistor precursor powders"

Ceramic International 15 (1989) 281-288.

Tunno, Julian, J.

"Spray Dryer Converts Slurry to Powder in Seconds"

Ceramic Industry, May 1984.

Takahashi M. A. Suzuki S.

"Compaction Behaviour and Mechanical Characteristics of Ceramic Powders"

Handbook of Ceramics and Composites Vol. 1: Synthesis and Properties

Ed. by W. P. Cheremisinoff, Marcel Decker 1990

Union Process Company, (Commercial Brochure)

"General Information on Attritor Processing".

Jia Wang

"Effect of Pressing Method on Organic Burnout"

J. AH. Ceram. Soc. 75 (a) 2627 - 29 (1992)

## APPENDIX

### CONTENTS

**Device Ratings and Characteristics** (Notes 1, 2)

ZA Series Varistors are listed under UL File No. E135010 as a UL recognized component

| MODEL NUMBER | MODEL SIZE DISC DIA. (mm) | DEVICE MARKING | MAXIMUM RATINGS (+85°C) | | | | CHARACTERISTICS (+25°C) | | | | | |
|---|---|---|---|---|---|---|---|---|---|---|---|---|
| | | | CONTINUOUS | | TRANSIENT | | VARISTOR VOLTAGE AT 1mA DC TEST CURRENT | | | MAX CLAMPING VOLTAGE $V_C$ AT TEST CURRENT (8/20µs) | | TYPICAL CAPACITANCE |
| | | | RMS VOLTAGE | DC VOLTAGE | ENERGY (10/1000µs) | PEAK CURRENT (8/20µs) | | | | | | |
| | | | $V_{M(AC)}$ | $V_{M(DC)}$ | $W_{TM}$ | $I_{TM}$ | MIN | $V_{N(DC)}$ | MAX | $V_C$ | $I_p$ | $f$ = 1MHz |
| | | | (V) | (V) | (J) | (A) | (V) | (V) | (V) | (V) | (A) | (pF) |
| V47ZA05 | 5 | Z47 | 30 | 38 | 0.4 | 100 | 42 | 47 | 55 | 90 | 2 | 400 |
| V47ZA1 | 7 | 47Z1 | 30 | 38 | 1.8 | 250 | 42 | 47 | 52 | 92 | 5 | 800 |
| V47ZA3 | 10 | 47Z3 | 30 | 38 | 4.5 | 500 | 42 | 47 | 52 | 89 | 5 | 2000 |
| V47ZA7 | 14 | 47Z7 | 30 | 38 | 8.8 | 1000 | 42 | 47 | 52 | 89 | 10 | 4500 |
| V56ZA05 | 5 | Z56 | 35 | 45 | 0.5 | 00 | 50 | 56 | 66 | 108 | 2 | 360 |
| V56ZA2 | 7 | 56Z2 | 35 | 45 | 2.3 | 250 | 50 | 56 | 62 | 107 | 5 | 700 |
| V56ZA3 | 10 | 56Z3 | 35 | 45 | 5.5 | 500 | 50 | 56 | 62 | 103 | 5 | 1800 |
| V56ZA8 | 14 | 56Z8 | 35 | 45 | 10.0 | 1000 | 50 | 56 | 62 | 103 | 10 | 3900 |
| V68ZA05 | 5 | Z68 | 40 | 56 | 0.6 | 100 | 61 | 68 | 80 | 127 | 2 | 300 |
| V68ZA2 | 7 | 68Z2 | 40 | 56 | 3.0 | 250 | 61 | 68 | 75 | 127 | 5 | 600 |
| V68ZA3 | 10 | 68Z3 | 40 | 56 | 6.5 | 500 | 61 | 68 | 75 | 123 | 5 | 1500 |
| V68ZA10 | 14 | 68Z10 | 40 | 56 | 13.0 | 1000 | 61 | 68 | 75 | 123 | 10 | 3300 |
| V82ZA05 | 5 | Z82 | 50 | 66 | 2.0 | 400 | 73 | 82 | 97 | 135 | 5 | 240 |
| V82ZA2 | 7 | 82Z2 | 50 | 66 | 4.0 | 1200 | 73 | 82 | 91 | 135 | 10 | 500 |
| V82ZA4 | 10 | 82Z4 | 50 | 66 | 8.0 | 2500 | 73 | 82 | 91 | 135 | 25 | 1100 |
| V82ZA12 | 14 | 82Z12 | 50 | 66 | 15.0 | 4500 | 73 | 82 | 91 | 145 | 50 | 2500 |
| V100ZA05 | 5 | Z100 | 60 | 81 | 2.5 | 400 | 90 | 100 | 117 | 165 | 5 | 180 |
| V100ZA3 | 7 | 100Z | 60 | 81 | 5.0 | 1200 | 90 | 100 | 110 | 165 | 10 | 400 |
| V100ZA4 | 10 | 100Z4 | 60 | 81 | 10.0 | 2500 | 90 | 100 | 110 | 165 | 25 | 900 |
| V100ZA15 | 14 | 100Z15 | 60 | 81 | 20.0 | 4500 | 90 | 100 | 110 | 175 | 50 | 2000 |
| V120ZA05 | 5 | Z120 | 75 | 102 | 3.0 | 400 | 108 | 120 | 138 | 205 | 5 | 140 |
| V120ZA1 | 7 | 120Z | 75 | 102 | 6.0 | 1200 | 108 | 120 | 132 | 205 | 10 | 300 |
| V120ZA4 | 10 | 120Z4 | 75 | 102 | 12.0 | 2500 | 108 | 120 | 132 | 200 | 25 | 750 |
| V120ZA6 | 14 | 120Z6 | 75 | 102 | 22.0 | 4500 | 108 | 120 | 132 | 210 | 50 | 1700 |
| V150ZA05 | 5 | Z150 | 92 | 127 | 4.0 | 400 | 135 | 150 | 173 | 250 | 5 | 120 |
| V150ZA1 | 7 | Z051 | 95 | 127 | 8.0 | 1200 | 135 | 150 | 165 | 250 | 10 | 250 |
| V150ZA5 | 10 | 150Z4 | 95 | 127 | 15.0 | 2500 | 135 | 150 | 165 | 250 | 25 | 600 |
| V150ZA10 | 14 | 150Z10 | 95 | 127 | 30.0 | 4500 | 135 | 150 | 165 | 255 | 50 | 1400 |
| V180ZA05 | 5 | Z180 | 110 | 153 | 5.0 | 400 | 162 | 180 | 207 | 295 | 5 | 100 |
| V180ZA1 | 7 | 180Z | 115 | 153 | 10.0 | 1200 | 162 | 180 | 198 | 295 | 10 | 200 |
| V180ZA5 | 10 | 180Z5 | 115 | 153 | 18.0 | 2500 | 162 | 180 | 198 | 300 | 25 | 500 |
| V180ZA10 | 14 | 180Z10 | 115 | 153 | 35.0 | 4500 | 162 | 180 | 198 | 300 | 50 | 1100 |
| V220ZA05 | 5 | Z220 | 140 | 180 | 6.0 | 400 | 198 | 220 | 253 | 360 | 5 | 90 |
| V270ZA05 | 5 | Z270 | 175 | 225 | 7.5 | 400 | 243 | 270 | 311 | 440 | 5 | 70 |
| V330ZA05 | 5 | Z330 | 210 | 275 | 9.0 | 400 | 297 | 330 | 380 | 540 | 5 | 60 |
| V390ZA05 | 5 | Z390 | 250 | 330 | 10.0 | 400 | 351 | 390 | 449 | 640 | 5 | 50 |
| V430ZA05 | 5 | Z430 | 275 | 369 | 11.0 | 400 | 387 | 430 | 495 | 700 | 5 | 45 |
| V470ZA05 | 5 | Z470 | 300 | 385 | 12.0 | 400 | 420 | 470 | 517 | 775 | 5 | 35 |
| V680ZA05 | 5 | Z680 | 420 | 560 | 14.0 | 400 | 610 | 680 | 748 | 1120 | 5 | 32 |
| V750ZA05 | 5 | Z750 | 460 | 615 | 17.0 | 400 | 675 | 750 | 825 | 1240 | 5 | 30 |
| V910ZA05 | 5 | Z910 | - | - | - | - | - | 910 | - | - | 5 | 28 |

NOTES:

1. Average power dissipation of transients not to exceed 0.2W, 0.25W, 0.4W, 0.6W or 1W for model sizes 5mm, 7mm, 10mm, 14mm and 20mm, respectively.
2. Higher voltages a vailable, contact Harris Semiconductor Power Marketing

**Table A - Device ratings (Harris Semiconductor, 1994)**

## Table B

Initial electrical characterisation and powder testing data.

| Powder Type | Breakdown Voltage | | | Density g/cc | | | |
|---|---|---|---|---|---|---|---|
| | @1mA/cm2 | per unit length | % variation | Tap | Bulk | % Moisture | % Binder |
| T-S | 56.73 | 34.89 | 1.54 | 1.56 | 1.45 | 0.04 | 0.71 |
| V-S | 53.23 | 32.58 | 2.10 | 1.61 | 1.52 | 0.05 | 0.29 |
| T-T | 44.90 | 27.56 | 5.83 | 1.54 | 1.41 | 0.08 | 1.12 |
| V-A | 52.18 | 32.27 | 2.29 | 1.79 | 1.52 | 0.09 | 0.88 |
| B-S | 55.85 | 34.14 | 2.03 | 1.66 | 1.49 | 0.05 | 0.74 |
| A-A | 52.38 | 32.25 | 2.31 | 1.74 | 1.52 | 0.07 | 1.18 |
| A-S | 54.34 | 33.48 | 3.14 | 1.73 | 1.43 | 0.08 | 0.87 |
| B-B | 54.08 | 33.27 | 2.27 | 1.57 | 1.48 | 0.06 | 1.39 |

## Table C

Maximum Rated Clamp Voltage at 5Amps

| T-S | V-S | T-T | A-A | B-S | V-A | A-S | B-B |
|---|---|---|---|---|---|---|---|
| 85 | 85 | 89 | 82 | 76 | 69 | 75 | 75 |
| 89 | 83 | 89 | 84 | 77 | 71 | 74 | 74 |
| 89 | 83 | 89 | 81 | 75 | 70 | 72 | 73 |
| 86 | 86 | 88 | 84 | 77 | 72 | 71 | 75 |
| 85 | 87 | 88 | 84 | 75 | 69 | 74 | 72 |
| 88 | 84 | 89 | 82 | 76 | 69 | 71 | 72 |
| 87 | 86 | 89 | 79 | 76 | 72 | 75 | 72 |
| 87 | 87 | 88 | 84 | 76 | 71 | 72 | 74 |
| 89 | 83 | 89 | 81 | 76 | 71 | 75 | 72 |
| 88 | 83 | 88 | 81 | 75 | 73 | 72 | 72 |

## Table D1

## Voltage Shifts after Clamping at 5A (T-S) (Turbula - Shear)

COMPLETE SHIFTS PRINTOUT

MODEL NUMBER V47ZA1 Lot number Tests: 1 - 4

Date 06-01-1994 Filename 351SCPA Description 7MM

TITLE:-SHIFTS

| Shift Dev | VNOM @ 1mA 42 55 Fwd | Rev | Vx @ 100uA 1 55 Fwd | Rev | DV @ 0.000 0 0 Fwd | Rev | IL @ 23.5V 000NA 010UA Fwd | Rev | Status |
|---|---|---|---|---|---|---|---|---|---|
| 1 | -.388 | -.193 | -.308 | -.344 | 0 | 0 | -20 | -14.2 | |
| 2 | .191 | 0 | .142 | .138 | 0 | 0 | 7.40 | 4.83 | |
| 3 | .192 | .194 | .139 | .174 | 0 | 0 | 6.66 | 4.16 | |
| 4 | .196 | 0 | .162 | 8.95 | 0 | 0 | 10.5 | 7.69 | |
| 5 | .196 | 0 | .182 | .176 | 0 | 0 | 0 | 1.81 | |
| 6 | .194 | 0 | 3.74 | -8.94 | 0 | 0 | 3.70 | 1.53 | |
| 7 | 1.23 | 0 | .435 | .325 | 0 | 0 | -16.6 | -9.43 | |
| 8 | .202 | .213 | .228 | .244 | 0 | 0 | 5 | 1.78 | |
| 9 | -.213 | 0 | .140 | .106 | 0 | 0 | -4.16 | 5.45 | |
| 10 | 0 | 0 | 7.51 | .201 | 0 | 0 | -8.57 | -1.40 | |

STATISTICS

| FORWARD | VNOM | Vx | DV | IL |
|---|---|---|---|---|
| MAX VALUES | 1.2320 | 7.5139 | 0.0000 | 20.0000 |
| MIN VALUES | 0.0000 | 0.1391 | 0.0000 | 0.0000 |
| RANGE | 1.2320 | 7.3748 | 0.0000 | 20.0000 |
| AVERAGE | 0.3009 | 1.3001 | 0.0000 | 8.2709 |
| STD DEV | 0.3398 | 2.4508 | 0.0000 | 6.0861 |
| REVERSE | | | | |
| MAX VALUES | 0.2137 | 8.9505 | 0.0000 | 14.2857 |
| MIN VALUES | 0.0000 | 0.1062 | 0.0000 | 1.4085 |
| RANGE | 0.2137 | 8.8443 | 0.0000 | 12.8773 |
| AVERAGE | 0.0602 | 1.9609 | 0.0000 | 5.2423 |
| STD DEV | 0.0971 | 3.6839 | 0.0000 | 4.2007 |

## Table D2

## Voltage Shifts after Clamping at 5A (V-S) (Vibro - Shear)

COMPLETE SHIFTS PRINTOUT

MODEL NUMBER V47ZA1 Lot number Tests: 1 - 4

Date 06-01-1994 Filename 351SCPC Description 7MM

TITLE:-SHIFTS

| | VNOM @ 1mA 42 55 | | Vx @ 100uA 1 55 | | DV @ 0.000 0 0 | | IL @ 23.5V 000NA 010UA | | |
|---|---|---|---|---|---|---|---|---|---|
| Shift Dev | Fwd | Rev | Fwd | Rev | Fwd | Rev | Fwd | Rev | Status |
| 1 | 0 | 0 | 9.62 | .162 | 0 | 0 | -12.5 | -6.38 | |
| 2 | .371 | 0 | .721 | .722 | 0 | 0 | -11.7 | -2.04 | |
| 3 | .185 | .185 | .177 | .123 | 0 | 0 | -15.3 | 0 | |
| 4 | .185 | 0 | 9.52 | 5.45 | 0 | 0 | 4.76 | -100 | |
| 5 | 0 | 0 | .245 | .232 | 0 | 0 | 15.3 | -4.65 | |
| 6 | 0 | .183 | .221 | .151 | 0 | 0 | -7.69 | -2.38 | |
| 7 | 0 | .190 | .168 | .132 | 0 | 0 | 8.33 | -100 | |
| 8 | .371 | 0 | .136 | .213 | 0 | 0 | -7.69 | -100 | |
| 9 | -.186 | -.183 | .167 | .503 | 0 | 0 | -9.09 | -2.5 | |
| 10 | .193 | .583 | -.128 | .102 | 0 | 0 | 0 | -6.52 | |

STATISTICS

| FORWARD | VNOM | Vx | DV | IL |
|---|---|---|---|---|
| MAX VALUES | 0.3717 | 9.6241 | 0.0000 | 15.3846 |
| MIN VALUES | 0.0000 | 0.1280 | 0.0000 | 0.0000 |
| RANGE | 0.3717 | 9.4960 | 0.0000 | 15.3846 |
| AVERAGE | 0.1495 | 2.1115 | 0.0000 | 9.2605 |
| STD DEV | 0.1469 | 3.9369 | 0.0000 | 4.7560 |
| REVERSE | | | | |
| MAX VALUES | 0.5837 | 5.4554 | 0.0000 | 100.00 |
| MIN VALUES | 0.0000 | 0.1023 | 0.0000 | 0.0000 |
| RANGE | 0.5837 | 5.3531 | 0.0000 | 100.00 |
| AVERAGE | 0.1327 | 0.7800 | 0.0000 | 32.4478 |
| STD DEV | 0.1834 | 1.6548 | 0.0000 | 46.6576 |

## Table D3

## Voltage Shifts after Clamping at 5A (T-T) (Turbula - Turbula)

COMPLETE SHIFTS PRINTOUT

MODEL NUMBER V47ZA1 Lot number Tests: 1 - 4

Date 06-01-1994 Filename 351SCPD Description 7MM

TITLE:- SHIFTS

| | VNOM @ 1mA 42 55 | | Vx @ 100uA 1 55 | | DV @ 0.000 0 0 | | IL @ 23.5V 000NA 010UA | | |
|---|---|---|---|---|---|---|---|---|---|
| Shift Dev | Fwd | Rev | Fwd | Rev | Fwd | Rev | Fwd | Rev | Status |
| 1 | .207 | 0 | .309 | .288 | 0 | 0 | 20.8 | 12.9 | |
| 2 | 0 | .196 | 8.73 | -1.24 | 0 | 0 | 14.2 | 8.62 | |
| 3 | .202 | .200 | .608 | .538 | 0 | 0 | 15.3 | 10.6 | |
| 4 | 0 | 0 | 2.52 | -2.73 | 0 | 0 | 14.5 | 10 | |
| 5 | .213 | .427 | .686 | .590 | 0 | 0 | 18.5 | 8.95 | |
| 6 | .407 | .203 | 1.93 | .045 | 0 | 0 | 5.55 | 6 | |
| 7 | .200 | .402 | .435 | .378 | 0 | 0 | 16.6 | 5.45 | |
| 8 | .608 | 0 | .115 | .160 | 0 | 0 | 0 | 0 | |
| 9 | 0 | 0 | .259 | .235 | 0 | 0 | -100 | -100 | |
| 10 | 0 | -.194 | 6.77 | .131 | 0 | 0 | 19.0 | 0 | |

STATISTICS

| FORWARD | VNOM | Vx | DV | IL |
|---|---|---|---|---|
| MAX VALUES | 0.6085 | 8.7333 | 0.0000 | 100.00 |
| MIN VALUES | 0.0000 | 0.1154 | 0.0000 | 0.0000 |
| RANGE | 0.6085 | 8.6179 | 0.0000 | 100.00 |
| AVERAGE | 0.1840 | 2.2371 | 0.0000 | 22.4837 |
| STD DEV | 0.2021 | 3.0432 | 0.0000 | 27.9793 |
| REVERSE | | | | |
| MAX VALUES | 0.4274 | 2.7370 | 0.0000 | 100.00 |
| MIN VALUES | 0.0000 | 0.0452 | 0.0000 | 0.0000 |
| RANGE | 0.4274 | 2.6918 | 0.0000 | 100.00 |
| AVERAGE | 0.1625 | 0.6355 | 0.0000 | 16.2540 |
| STD DEV | 0.1628 | 0.8151 | 0.0000 | 29.7346 |

## Table D4

## Voltage Shifts after Clamping at 5A (B-B) (Ball - Ball)

COMPLETE SHIFTS PRINTOUT

MODEL NUMBER V472a1 Lot number Tests: 1 - 4

Date 06-02-1994 Filename 351SCPF Description 7MM

TITLE:- SHIFTS

| | VNOM @ 1mA 42 55 | | Vx @ 100uA 1 55 | | DV @ 0.000 0 0 | | IL @ 23.5V 000NA 010UA | | |
|---|---|---|---|---|---|---|---|---|---|
| Shift Dev | Fwd | Rev | Fwd | Rev | Fwd | Rev | Fwd | Rev | Status |
| 1 | .188 | 0 | -2.76 | -1.38 | 0 | 0 | -5.26 | 0 | |
| 2 | .183 | 0 | 9.44 | -.027 | 0 | 0 | 27.2 | 26.3 | |
| 3 | .943 | -.186 | .401 | .422 | 0 | 0 | 9.09 | 2.70 | |
| 4 | .186 | .186 | 4.09 | 8.41 | 0 | 0 | 0 | 0 | |
| 5 | 0 | .186 | 8.53 | 8.36 | 0 | 0 | 20 | 2.56 | |
| 6 | -.186 | 0 | .115 | 9.61 | 0 | 0 | 0 | 0 | |
| 7 | 0 | .184 | .167 | .181 | 0 | 0 | 0 | 2.38 | |
| 8 | .187 | 0 | 4.14 | 9.10 | 0 | 0 | 0 | 0 | |
| 9 | -.187 | -.185 | 5.88 | -7.87 | 0 | 0 | -8.33 | 0 | |
| 10 | 0 | 0 | 4.18 | -1.39 | 0 | 0 | 0 | -5.55 | |

STATISTICS

| FORWARD | VNOM | Vx | DV | IL |
|---|---|---|---|---|
| MAX VALUES | 0.9434 | 9.4405 | 0.0000 | 27.2727 |
| MIN VALUES | 0.0000 | 0.1156 | 0.0000 | 0.0000 |
| RANGE | 0.9434 | 9.3249 | 0.0000 | 27.2727 |
| AVERAGE | 0.2063 | 3.9739 | 0.0000 | 6.9960 |
| STD DEV | 0.2735 | 3.2998 | 0.0000 | 9.6272 |
| REVERSE | | | | |
| MAX VALUES | 0.1869 | 9.6197 | 0.0000 | 26.3157 |
| MIN VALUES | 0.0000 | 0.0270 | 0.0000 | 0.0000 |
| RANGE | 0.1869 | 9.5927 | 0.0000 | 26.3157 |
| AVERAGE | 0.0930 | 4.6794 | 0.0000 | 3.9519 |
| STD DEV | 0.0980 | 4.2605 | 0.0000 | 8.0743 |

## Table D5

## Voltage Shifts after Clamping at 5A (A-A) (Attrition - Attrition)

COMPLETE SHIFTS PRINTOUT

MODEL NUMBER V472A1 Lot number Tests: 1 - 4

Date 06-01-1994 Filename 351SCPB Description 7MM

TITLE:-SHIFTS

| | VNOM @ 1mA 42 55 | | Vx @ 100uA 1 55 | | DV @ 0.000 0 0 | | IL @ 23.5V 000NA 010UA | | |
|---|---|---|---|---|---|---|---|---|---|
| Shift Dev | Fwd | Rev | Fwd | Rev | Fwd | Rev | Fwd | Rev | Status |
| 1 | 0 | 0 | .216 | .145 | 0 | 0 | -13.3 | -6.66 | |
| 2 | 0 | .195 | .176 | .206 | 0 | 0 | 0 | -2.22 | |
| 3 | .403 | .201 | .390 | .616 | 0 | 0 | 14.2 | 2.22 | |
| 4 | .194 | 0 | 2.84 | .145 | 0 | 0 | 0 | -2.43 | |
| 5 | 0 | .191 | -.334 | -.756 | 0 | 0 | -14.2 | -4.76 | |
| 6 | .195 | 0 | .160 | .121 | 0 | 0 | 0 | -6 | |
| 7 | -.193 | .190 | .244 | .323 | 0 | 0 | -13.6 | -1.92 | |
| 8 | -.186 | -.186 | 9.61 | 4.13 | 0 | 0 | -7.69 | -2.27 | |
| 9 | 0 | .196 | -4.39 | .113 | 0 | 0 | 0 | 0 | |
| 10 | 0 | .197 | .149 | .135 | 0 | 0 | -7.14 | 2.32 | |

STATISTICS

| FORWARD | VNOM | Vx | DV | IL |
|---|---|---|---|---|
| MAX VALUES | 0.4032 | 9.6197 | 0.0000 | 14.2857 |
| MIN VALUES | 0.0000 | 0.1495 | 0.0000 | 0.0000 |
| RANGE | 0.4032 | 9.4703 | 0.0000 | 14.2857 |
| AVERAGE | 0.1172 | 1.8529 | 0.0000 | 7.0376 |
| STD DEV | 0.1387 | 3.0921 | 0.0000 | 6.5557 |
| REVERSE | | | | |
| MAX VALUES | 0.2016 | 4.1325 | 0.0000 | 6.6667 |
| MIN VALUES | 0.0000 | 0.1136 | 0.0000 | 0.0000 |
| RANGE | 0.2016 | 4.0189 | 0.0000 | 6.6667 |
| AVERAGE | 0.1361 | 0.6696 | 0.0000 | 3.0833 |
| STD DEV | 0.0940 | 1.2374 | 0.0000 | 2.0588 |

## Table D6

## Voltage Shifts after Clamping at 5A (B-S) (Ball - Shear)

COMPLETE SHIFTS PRINTOUT

MODEL NUMBER V47ZA1 Lot number Tests: 1 - 4

Date 06-01-1994 Filename 351SCPE Description 7MM

TITLE:-SHIFTS

| Shift Dev | VNOM @ 1mA 42 55 Fwd | Rev | Vx @ 100uA I 55 Fwd | Rev | DV @ 0.000 .0 0 Fwd | Rev | IL @ 23.5V 000NA 010UA Fwd | Rev | Status |
|---|---|---|---|---|---|---|---|---|---|
| 1 | .204 | .202 | .191 | .213 | 0 | 0 | 25 | 9.75 | |
| 2 | .198 | 0 | 2.90 | .177 | 0 | 0 | 0 | 8.10 | |
| 3 | 0 | .207 | 3.03 | 9.37 | 0 | 0 | 0 | 0 | |
| 4 | 0 | .193 | 1.63 | .057 | 0 | 0 | 18.1 | 5.12 | |
| 5 | 0 | 0 | 7.42 | .109 | 0 | 0 | 23.0 | 2.27 | |
| 6 | .202 | -.198 | 2.12 | .082 | 0 | 0 | 11.1 | 4.16 | |
| 7 | 0 | 0 | .492 | .492 | 0 | 0 | 0 | 2.22 | |
| 8 | .198 | 0 | 0 | -9.39 | 0 | 0 | -8.33 | 2.5 | |
| 9 | 0 | .206 | .134 | .154 | 0 | 0 | 0 | 5 | |
| 10 | .205 | 0 | 6.86 | .084 | 0 | 0 | 7.69 | 2.27 | |

STATISTICS

| FORWARD | VNOM | Vx | DV | IL |
|---|---|---|---|---|
| MAX VALUES | 0.2053 | 7.4259 | 0.0000 | 25.0000 |
| MIN VALUES | 0.0000 | 0.0000 | 0.0000 | 0.0000 |
| RANGE | 0.2053 | 7.4259 | 0.0000 | 25.0000 |
| AVERAGE | 0.1009 | 2.4804 | 0.0000 | 9.3395 |
| STD DEV | 0.1063 | 2.7046 | 0.0000 | 9.8202 |
| REVERSE | | | | |
| MAX VALUES | 0.2079 | 9.3938 | 0.0000 | 9.7561 |
| MIN VALUES | 0.0000 | 0.0574 | 0.0000 | 0.0000 |
| RANGE | 0.2079 | 9.3364 | 0.0000 | 9.7561 |
| AVERAGE | 0.1009 | 2.0136 | 0.0000 | 4.1427 |
| STD DEV | 0.1064 | 3.8855 | 0.0000 | 2.9718 |

## Table D7

## Voltage Shifts after Clamping at 5A (V-A) (Vibro - Attrition)

COMPLETE SHIFTS PRINTOUT

MODEL NUMBER V47ZA1 Lot number Tests: 1 - 4

Date 06-02-1994 Filename 351SCPH Description 7MM

TITLE:-SHIFTS

| Shift Dev | VNOM @ 1mA 42 55 Fwd | Rev | Vx @ 100uA I 55 Fwd | Rev | DV @ 0.000 0 0 Fwd | Rev | IL @ 23.5V 000NA 010UA Fwd | Rev | Status |
|---|---|---|---|---|---|---|---|---|---|
| 1 | .202 | .405 | .148 | .125 | 0 | 0 | 7.69 | 2.27 | |
| 2 | 0 | 0 | .255 | .174 | 0 | 0 | -14.2 | -2.38 | |
| 3 | .193 | .193 | 6.50 | .259 | 0 | 0 | 0 | 0 | |
| 4 | -.197 | 0 | .151 | 8.11 | 0 | 0 | -7.69 | 0 | |
| 5 | .202 | .200 | .200 | .149 | 0 | 0 | 20 | 0 | |
| 6 | .204 | 0 | .197 | .105 | 0 | 0 | 0 | 0 | |
| 7 | 0 | .198 | 7.57 | .238 | 0 | 0 | 8.33 | -2.77 | |
| 8 | 0 | .197 | .316 | .193 | 0 | 0 | -7.14 | 2.43 | |
| 9 | .392 | .195 | .292 | .340 | 0 | 0 | 8.33 | -2.32 | |
| 10 | 0 | -.189 | 4.81 | 5.02 | 0 | 0 | 21.4 | 6.52 | |

STATISTICS

| FORWARD | VNOM | Vx | DV | IL |
|---|---|---|---|---|
| MAX VALUES | 0.3929 | 7.5702 | 0.0000 | 21.4285 |
| MIN VALUES | 0.0000 | 0.1482 | 0.0000 | 0.0000 |
| RANGE | 0.3929 | 7.4220 | 0.0000 | 21.4285 |
| AVERAGE | 0.1393 | 2.0443 | 0.0000 | 9.4908 |
| STD DEV | 0.1335 | 3.0055 | 0.0000 | 7.2323 |
| REVERSE | | | | |
| MAX VALUES | 0.4057 | 8.1191 | 0.0000 | 6.5217 |
| MIN VALUES | 0.0000 | 0.1055 | 0.0000 | 0.0000 |
| RANGE | 0.4057 | 8.0135 | 0.0000 | 6.5217 |
| AVERAGE | 0.1581 | 1.4734 | 0.0000 | 1.8718 |
| STD DEV | 0.1269 | 2.7860 | 0.0000 | 2.0386 |

## Table D8

## Voltage Shifts after Clamping at 5A (A-S) (Attrition - Shear)

COMPLETE SHIFTS PRINTOUT

MODEL NUMBER V47ZA1 Lot number Tests: 1 - 4

Date 06-02-1994 Filename 351SCPG Description 7MM

TITLE:-SHIFTS

| | VNOM @ 1mA 42 55 | | Vx @ 100uA 1 55 | | DV @ 0.000 0 0 | | IL @ 23.5V 000NA 010UA | | |
|---|---|---|---|---|---|---|---|---|---|
| Shift Dev | Fwd | Rev | Fwd | Rev | Fwd | Rev | Fwd | Rev | Status |
| 1 | 0 | 0 | .145 | 8.16 | 0 | 0 | -16.6 | -8.19 | |
| 2 | 0 | .222 | .205 | .140 | 0 | 0 | -15.3 | -9.67 | |
| 3 | .452 | .228 | .439 | .291 | 0 | 0 | -8.33 | 0 | |
| 4 | 0 | .214 | -4.92 | -.241 | 0 | 0 | -14.2 | -5.66 | |
| 5 | .453 | 0 | .271 | .339 | 0 | 0 | 2.85 | -1.29 | |
| 6 | 0 | -.665 | .291 | .396 | 0 | 0 | 7.14 | 6.55 | |
| 7 | .236 | 0 | .325 | .289 | 0 | 0 | 5.26 | 2.04 | |
| 8 | 0 | 0 | .596 | -9.73 | 0 | 0 | -100 | -100 | |
| 9 | 0 | 0 | 9.67 | 5.09 | 0 | 0 | 0 | 3.63 | |
| 10 | .231 | 0 | .158 | 9.32 | 0 | 0 | 4.34 | 7.27 | |

STATISTICS

| FORWARD | VNOM | Vx | DV | IL |
|---|---|---|---|---|
| MAX VALUES | 0.4535 | 9.6777 | 0.0000 | 100.00 |
| MIN VALUES | 0.0000 | 0.1457 | 0.0000 | 0.0000 |
| RANGE | 0.4535 | 9.5321 | 0.0000 | 100.00 |
| AVERAGE | 0.1374 | 1.7038 | 0.0000 | 17.4281 |
| STD DEV | 0.1918 | 3.1588 | 0.0000 | 29.5454 |
| REVERSE | | | | |
| MAX VALUES | 0.6652 | 9.7398 | 0.0000 | 100.00 |
| MIN VALUES | 0.0000 | 0.1403 | 0.0000 | 0.0000 |
| RANGE | 0.6652 | 9.5995 | 0.0000 | 100.00 |
| AVERAGE | 0.1330 | 3.4012 | 0.0000 | 14.4340 |
| STD DEV | 0.2142 | 4.2047 | 0.0000 | 30.2295 |

## Table E

**Peak Pulse Current at Rated Values**

| T-S | V-S | T-T | A-A | B-S | V-A | A-S | B-B |
|---|---|---|---|---|---|---|---|
| 160 | 153 | 159 | 154 | 159 | 147 | 147 | 148 |
| 164 | 144 | 159 | 151 | 161 | 148 | 153 | 155 |
| 164 | 151 | 159 | 149 | 163 | 144 | 152 | 154 |
| 166 | 151 | 158 | 148 | 164 | 148 | 148 | 156 |
| 164 | 151 | 159 | 149 | 162 | 139 | 150 | 156 |
| 163 | 145 | 161 | 148 | 163 | 147 | 152 | 156 |
| 159 | 148 | 153 | 154 | 162 | 143 | 158 | 154 |
| 165 | 148 | 163 | 147 | 161 | 145 | 159 | 162 |
| 172 | 150 | 161 | 149 | 165 | 142 | 142 | 162 |
| 168 | 148 | 162 | 150 | 161 | 140 | 154 | 158 |

## Table F1

## Voltage Shifts after Clamping at 250A (T-S) (Turbula - Shear)

COMPLETE SHIFTS PRINTOUT

MODEL NUMBER V47ZA1 Lot number Tests: 1 - 4

Date 06-02-1994 Filename 351SPPH Description 7MM

TITLE:-SHIFTS

| Shift Dev | VNOM @ 1mA 42 55 Fwd | Rev | Vx @ 100uA 1 55 Fwd | Rev | DV @ 0.000 0 0 Fwd | Rev | IL @ 23.5V 000NA 010UA Fwd | Rev | Stati |
|---|---|---|---|---|---|---|---|---|---|
| 1 | -.980 | .194 | -2.83 | -2.99 | 0 | 0 | -99.3 | -99.7 | |
| 2 | -1.98 | -.198 | -4.71 | -5.00 | 0 | 0 | -99.1 | -99.6 | |
| 3 | -1.42 | -.404 | -3.44 | -3.67 | 0 | 0 | -99.0 | 0 | |
| 4 | -.784 | 0 | -2.83 | -3.05 | 0 | 0 | 683. | -99.6 | |
| 5 | -.618 | .414 | -2.16 | -2.23 | 0 | 0 | -99.4 | -99.7 | |
| 6 | -1.81 | -.790 | -3.76 | -3.99 | 0 | 0 | -99.5 | 140 | |
| 7 | -1.40 | -.402 | -4.17 | -4.27 | 0 | 0 | -99.6 | 130 | |
| 8 | -.809 | 0 | -3.04 | -3.19 | 0 | 0 | -99.0 | -99.6 | |
| 9 | -1.22 | .203 | -3.82 | -4.07 | 0 | 0 | -98.4 | -99.5 | |
| 10 | -1.04 | -.811 | -1.22 | -1.29 | 0 | 0 | -99.4 | -99.6 | |

STATISTICS

| FORWARD | VNOM | Vx | DV | IL |
|---|---|---|---|---|
| MAX VALUES | 1.9881 | 4.7152 | 0.0000 | 683.33 |
| MIN VALUES | 0.6186 | 1.2231 | 0.0000 | 98.4375 |
| RANGE | 1.3695 | 3.4922 | 0.0000 | 584.90 |
| AVERAGE | 1.2099 | 3.2034 | 0.0000 | 157.65 |
| STD DEV | 0.4500 | 1.0160 | 0.0000 | %184.7082 |
| REVERSE | | | | |
| MAX VALUES | 0.8114 | 5.0055 | 0.0000 | 140.00 |
| MIN VALUES | 0.0000 | 1.2983 | 0.0000 | 0.0000 |
| RANGE | 0.8114 | 3.7071 | 0.0000 | 140.00 |
| AVERAGE | 0.3419 | 3.3804 | 0.0000 | 96.7646 |
| STD DEV | 0.2847 | 1.0719 | 0.0000 | 37.1127 |

## Table F2

## Voltage Shifts after Clamping at 250A (V-S) (Vibro - Shear)

MODEL NUMBER V47ZA1 Lot number Tests: 1 - 4

Date 06-02-1994 Filename 351SPPG Description 7MM

TITLE:- SHIFTS

| | VNOM @ 1mA 42 55 | | Vx @ 100uA 1 55 | | DV @ 0.000 0 0 | | IL @ 23.5V 000NA 010UA | | |
|---|---|---|---|---|---|---|---|---|---|
| Shift Dev | Fwd | Rev | Fwd | Rev | Fwd | Rev | Fwd | Rev | Status |
| 1 | -1.86 | 0 | -5.09 | -5.16 | 0 | 0 | -96.8 | -99.4 | |
| 2 | -2.37 | -3.60 | -2.80 | -2.83 | 0 | 0 | -99.1 | -99.6 | |
| 3 | -1.33 | -.888 | -3.36 | -3.56 | 0 | 0 | -98.4 | -99.5 | |
| 4 | -1.51 | 0 | -4.36 | -4.46 | 0 | 0 | -97.9 | -99.5 | |
| 5 | -1.56 | -.227 | -3.06 | -3.05 | 0 | 0 | -98.3 | -99.5 | |
| 6 | -3.52 | -2.07 | -9.10 | -9.28 | 0 | 0 | -94.4 | -98.6 | |
| 7 | -1.82 | 1.12 | -4.44 | -4.60 | 0 | 0 | -97.5 | -99.4 | |
| 8 | -1.09 | -.220 | -2.65 | -2.87 | 0 | 0 | -98.5 | -99.5 | |
| 9 | -.467 | 0 | -2.34 | -2.49 | 0 | 0 | -100 | -100 | |
| 10 | -5.44 | -2.92 | -8.77 | -8.94 | 0 | 0 | -97.1 | -99.2 | |

STATISTICS

| FORWARD | VNOM | Vx | DV | IL |
|---|---|---|---|---|
| MAX VALUES | 5.4422 | 9.1094 | 0.0000 | 100.00 |
| MIN VALUES | 0.4673 | 2.3407 | 0.0000 | 94.4117 |
| RANGE | 4.9749 | 6.7687 | 0.0000 | 5.5883 |
| AVERAGE | 2.1009 | 4.6024 | 0.0000 | 97.8296 |
| STD DEV | 1.4259 | 2.4503 | 0.0000 | 1.5164 |
| REVERSE | | | | |
| MAX VALUES | 3.6017 | 9.2856 | 0.0000 | 100.00 |
| MIN VALUES | 0.0000 | 2.4956 | 0.0000 | 98.6301 |
| RANGE | 3.6017 | 6.7900 | 0.0000 | 1.3699 |
| AVERAGE | 1.1062 | 4.7279 | 0.0000 | 99.4623 |
| STD DEV | 1.3222 | 2.4710 | 0.0000 | 0.3524 |

## Table F3

## Voltage Shifts after Clamping at 250A (T-T) (Turbula - Turbula)

COMPLETE SHIFTS PRINTOUT

MODEL NUMBER V47ZA1 Lot number Tests: 1 - 4

Date 06-02-1994 Filename 351SPPF Description 7MM

TITLE:-SHIFTS

| | VNOM @ 1mA 42 55 | | Vx @ 100uA 1 55 | | DV @ 0.000 0 0 | | IL @ 23.5V 000NA 010UA | | |
|---|---|---|---|---|---|---|---|---|---|
| Shift Dev | Fwd | Rev | Fwd | Rev | Fwd | Rev | Fwd | Rev | Status |
| 1 | -3.60 | -1.31 | -10.7 | -10.4 | 0 | 0 | -94.6 | -99.0 | |
| 2 | -1.90 | .567 | -4.79 | -4.77 | 0 | 0 | -98.8 | -99.6 | |
| 3 | -.782 | .763 | -1.64 | -1.91 | 0 | 0 | -98.7 | -99.6 | |
| 4 | -1.32 | .187 | -3.15 | -3.36 | 0 | 0 | -98.5 | -99.5 | |
| 5 | -1.31 | 0 | -3.95 | -4.06 | 0 | 0 | -99 | -99.6 | |
| 6 | -1.69 | -.371 | -4.64 | -4.90 | 0 | 0 | -98.5 | -99.6 | |
| 7 | -1.49 | .369 | -4.07 | -4.30 | 0 | 0 | -98.9 | -99.6 | |
| 8 | -1.50 | 0 | -4.44 | -4.68 | 0 | 0 | -98.9 | -99.6 | |
| 9 | -1.51 | -.185 | -4.29 | -4.48 | 0 | 0 | -99 | -99.6 | |
| 10 | -1.32 | -.187 | -4.93 | -4.72 | 0 | 0 | -98.3 | -99.5 | |

STATISTICS

| FORWARD | VNOM | Vx | DV | IL |
|---|---|---|---|---|
| MAX VALUES | 3.6053 | 10.7019 | 0.0000 | 99.0000 |
| MIN VALUES | 0.7828 | 1.6441 | 0.0000 | 94.6363 |
| RANGE | 2.8225 | 9.0578 | 0.0000 | 4.3637 |
| AVERAGE | 1.6450 | 4.6654 | 0.0000 | 98.3442 |
| STD DEV | 0.7479 | 2.3330 | 0.0000 | 1.3221 |
| REVERSE | | | | |
| MAX VALUES | 1.3109 | 10.4454 | 0.0000 | 99.6500 |
| MIN VALUES | 0.0000 | 1.9139 | 0.0000 | 99.0512 |
| RANGE | 1.3109 | 8.5315 | 0.0000 | 0.5988 |
| AVERAGE | 0.3941 | 4.7685 | 0.0000 | 99.5552 |
| STD DEV | 0.4011 | 2.1898 | 0.0000 | 0.1798 |

## Table F4

## Voltage Shifts after Clamping at 250A (A-A) (Attrition - Attrition)

COMPLETE SHIFTS PRINTOUT

MODEL NUMBER V47ZA1 Lot number Tests: 1 - 4

Date 06-01-1994 Filename 351SPPE Description 7MM

TITLE:- SHIFTS

| | VNOM @ 1mA 42 55 | | Vx @ 100uA 1 55 | | DV @ 0.000 0 0 | | IL @ 23.5V 000NA 010UA | | |
|---|---|---|---|---|---|---|---|---|---|
| Shift Dev | Fwd | Rev | Fwd | Rev | Fwd | Rev | Fwd | Rev | Status |
| 1 | .393 | -.972 | -.784 | -.860 | 0 | 0 | 480 | -99.5 | |
| 2 | 1.23 | 0 | 1.26 | 1.37 | 0 | 0 | 500 | -99.5 | |
| 3 | .204 | -.808 | -1.77 | -1.67 | 0 | 0 | -99.2 | -99.3 | |
| 4 | -.790 | -1.77 | -1.98 | -1.94 | 0 | 0 | -99.4 | -99.4 | |
| 5 | -.838 | -1.24 | -2.69 | -2.69 | 0 | 0 | -99.0 | -99.2 | |
| 6 | .202 | -.803 | -1.27 | -1.34 | 0 | 0 | 429. | -99.4 | |
| 7 | -.193 | -.767 | -1.06 | -1.07 | 0 | 0 | 328. | -99.5 | |
| 8 | 0 | -1.22 | -1.32 | -1.25 | 0 | 0 | -99.4 | -100 | |
| 9 | -.198 | -.982 | -1.06 | -.992 | 0 | 0 | 335. | -99.6 | |
| 10 | .203 | -.606 | -.916 | -1.06 | 0 | 0 | 528. | -99.4 | |

STATISTICS

| FORWARD | VNOM | Vx | DV | IL |
|---|---|---|---|---|
| MAX VALUES | 1.2371 | 2.6978 | 0.0000 | 528.57 |
| MIN VALUES | 0.0000 | 0.7847 | 0.0000 | 99.0833 |
| RANGE | 1.2371 | 1.9131 | 0.0000 | 429.49 |
| AVERAGE | 0.4263 | 1.4157 | 0.0000 | 299.94 |
| STD DEV | 0.3941 | 0.5807 | 0.0000 | %183.9784 |
| REVERSE | | | | |
| MAX VALUES | 1.7751 | 2.6912 | 0.0000 | 100.00 |
| MIN VALUES | 0.0000 | 0.8602 | 0.0000 | 99.2142 |
| RANGE | 1.7751 | 1.8310 | 0.0000 | 0.7858 |
| AVERAGE | 0.9192 | 1.4272 | 0.0000 | 99.5096 |
| STD DEV | 0.4637 | 0.5516 | 0.0000 | 0.2059 |

# Table F5

## Voltage Shifts after Clamping at 250A (B-S) (Ball - Shear)

COMPLETE SHIFTS PRINTOUT

MODEL NUMBER V47ZA1 Lot number Tests: 1 - 4

Date 06-01-1994 Filename 351SPPD Description 7MM

TITLE:-SHIFTS

| | VNOM @ 1mA 42 55 | | Vx @ 100uA 1 55 | | DV @ 0.000 0 0 | | IL @ 23.5V 000NA 010UA | | |
|---|---|---|---|---|---|---|---|---|---|
| Shift Dev | Fwd | Rev | Fwd | Rev | Fwd | Rev | Fwd | Rev | Status |
| 1 | -.204 | -1.39 | -1.18 | -1.23 | 0 | 0 | -99.2 | -99.1 | |
| 2 | 0 | -1.84 | -2.83 | -2.83 | 0 | 0 | -99.1 | -99.1 | |
| 3 | -.598 | -.801 | -1.79 | -1.47 | 0 | 0 | -99.5 | -99.5 | |
| 4 | .211 | -.421 | -.601 | -.541 | 0 | 0 | -99.6 | 345. | |
| 5 | 0 | -1.37 | -1.55 | -1.53 | 0 | 0 | -99.4 | -99.3 | |
| 6 | 0 | -.599 | -.887 | -.862 | 0 | 0 | -99.5 | -99.4 | |
| 7 | -.610 | -1.42 | -1.62 | -1.63 | 0 | 0 | -99.4 | -99.3 | |
| 8 | -2.03 | -2.00 | -2.45 | -2.48 | 0 | 0 | -99.2 | -99.2 | |
| 9 | 2.55 | 1.70 | 2.41 | 2.18 | 0 | 0 | 295 | -99.4 | |
| 10 | .205 | -.813 | -1.10 | -1.03 | 0 | 0 | -99.3 | -99.3 | |

STATISTICS

| FORWARD | VNOM | Vx | DV | IL |
|---|---|---|---|---|
| MAX VALUES | 2.5586 | 2.8381 | 0.0000 | 295.00 |
| MIN VALUES | 0.0000 | 0.6011 | 0.0000 | 99.1739 |
| RANGE | 2.5586 | 2.2370 | 0.0000 | 195.83 |
| AVERAGE | 0.6426 | 1.6480 | 0.0000 | 118.96 |
| STD DEV | 0.9083 | 0.7359 | 0.0000 | 61.8552 |
| REVERSE | | | | |
| MAX VALUES | 2.0080 | 2.8319 | 0.0000 | 345.45 |
| MIN VALUES | 0.4219 | 0.5412 | 0.0000 | 99.1147 |
| RANGE | 1.5861 | 2.2907 | 0.0000 | 246.34 |
| AVERAGE | 1.2381 | 1.5817 | 0.0000 | 123.95 |
| STD DEV | 0.5473 | 0.7288 | 0.0000 | 77.8287 |

## Table F6

## Voltage Shifts after Clamping at 250A (V-A) (Vibro - Attrition)

COMPLETE SHIFTS PRINTOUT

MODEL NUMBER V47ZA1 Lot number Tests: 1 - 4

Date 06-01-1994 Filename 351SPPC Description 7MM

TITLE:-SHIFTS

| Shift Dev | VNOM @ 1mA 42 55 Fwd | Rev | Vx @ 100uA 1 55 Fwd | Rev | DV @ 0.000 0 0 Fwd | Rev | IL @ 23.5V 000NA 010UA Fwd | Rev | Status |
|---|---|---|---|---|---|---|---|---|---|
| 1 | 0 | -1.29 | -1.70 | -1.75 | 0 | 0 | -100 | -100 | |
| 2 | 0 | -1.30 | -.767 | -.791 | 0 | 0 | 253. | -99.6 | |
| 3 | .185 | -1.10 | -1.02 | -.855 | 0 | 0 | 257. | -99.6 | |
| 4 | -.364 | -1.10 | -2.42 | -2.47 | 0 | 0 | 217. | -99.6 | |
| 5 | 0 | -1.09 | -1.00 | -.857 | 0 | 0 | 300 | -99.6 | |
| 6 | 0 | -.729 | -1.01 | -.991 | 0 | 0 | 233. | -99.6 | |
| 7 | 1.19 | -.583 | -4.65 | 1.48 | 0 | 0 | 485. | -100 | |
| 8 | .732 | -2.35 | 5.56 | 6.73 | 0 | 0 | 206. | -99.6 | |
| 9 | .193 | -1.31 | -.333 | -.362 | 0 | 0 | 292. | -99.6 | |
| 10 | .559 | -.747 | -1.57 | -1.19 | 0 | 0 | 381. | -99.5 | |

STATISTICS

| FORWARD | VNOM | Vx | DV | IL |
|---|---|---|---|---|
| MAX VALUES | 1.1952 | 5.5654 | 0.0000 | 485.71 |
| MIN VALUES | 0.0000 | 0.3333 | 0.0000 | 100.00 |
| RANGE | 1.1952 | 5.2320 | 0.0000 | 385.71 |
| AVERAGE | 0.3230 | 2.0079 | 0.0000 | 272.81 |
| STD DEV | 0.3999 | 1.7456 | 0.0000 | %104.2595 |
| REVERSE | | | | |
| MAX VALUES | 2.3508 | 6.7378 | 0.0000 | 100.00 |
| MIN VALUES | 0.5837 | 0.3630 | 0.0000 | 99.5142 |
| RANGE | 1.7672 | 6.3748 | 0.0000 | 0.4858 |
| AVERAGE | 1.1629 | 1.7515 | 0.0000 | 99.7029 |
| STD DEV | 0.4923 | 1.8497 | 0.0000 | 0.1634 |

## Table F7

## Voltage Shifts after Clamping at 250A (A-S) (Attrition - Shear)

COMPLETE SHIFTS PRINTOUT

MODEL NUMBER V47ZA1 Lot number Tests: 1 - 4

Date 06-01-1994 Filename 351SPPB Description 7MM

TITLE:-SHIFTS

| | VNOM @ 1mA 42 55 | | Vx @ 100uA 1 55 | | DV @ 0.000 0 0 | | IL @ 23.5V 000NA 010UA | | |
|---|---|---|---|---|---|---|---|---|---|
| Shift Dev | Fwd | Rev | Fwd | Rev | Fwd | Rev | Fwd | Rev | Stat |
| 1 | -.192 | -1.91 | -1.50 | -1.44 | 0 | 0 | 238. | -99.6 | |
| 2 | -.202 | -.990 | -.584 | -.723 | 0 | 0 | 230. | -99.6 | |
| 3 | -.776 | -1.16 | -2.48 | -2.48 | 0 | 0 | 194. | -99.7 | |
| 4 | .579 | -1.13 | -.770 | -.693 | 0 | 0 | 300 | -99.6 | |
| 5 | -.388 | -.980 | .340 | -.555 | 0 | 0 | 250 | -99.6 | |
| 6 | .198 | -.596 | -.484 | -.427 | 0 | 0 | 256. | -99.6 | |
| 7 | -.386 | -.770 | -.932 | -.790 | 0 | 0 | 240 | -99.6 | |
| 8 | 0 | .198 | 1.51 | .323 | 0 | 0 | 5.88 | -100 | |
| 9 | .386 | -.957 | -.727 | -.701 | 0 | 0 | 453. | -99.5 | |
| 10 | .384 | -.574 | -.669 | -.742 | 0 | 0 | 235. | -99.6 | |

STATISTICS

| FORWARD | VNOM | Vx | DV | IL |
|---|---|---|---|---|
| MAX VALUES | 0.7767 | 2.4869 | 0.0000 | 453.85 |
| MIN VALUES | 0.0000 | 0.3403 | 0.0000 | 5.8824 |
| RANGE | 0.7767 | 2.1466 | 0.0000 | 447.96 |
| AVERAGE | 0.3495 | 1.0023 | 0.0000 | 240.53 |
| STD DEV | 0.2190 | 0.6542 | 0.0000 | %108.8646 |
| REVERSE | | | | |
| MAX VALUES | 1.9157 | 2.4856 | 0.0000 | 100.00 |
| MIN VALUES | 0.1988 | 0.3230 | 0.0000 | 99.5227 |
| RANGE | 1.7169 | 2.1626 | 0.0000 | 0.4773 |
| AVERAGE | 0.9286 | 0.8887 | 0.0000 | 99.6810 |
| STD DEV | 0.4563 | 0.6354 | 0.0000 | 0.1216 |

## Table F8

## Voltage Shifts after Clamping at 250A (B-B) (Ball - Ball)

COMPLETE SHIFTS PRINTOUT

MODEL NUMBER V47ZA1 Lot number Tests: 1 - 4

Date 06-01-1994 Filename 351SPPA Description 7MM

TITLE:-SHIFTS

| Shift Dev | VNOM @ 1mA 42 55 Fwd | Rev | Vx @ 100uA 1 55 Fwd | Rev | DV @ 0.000 0 0 Fwd | Rev | IL @ 23.5V 000NA 010UA Fwd | Rev | S: |
|---|---|---|---|---|---|---|---|---|---|
| 1 | -.389 | -2.31 | -3.50 | -3.50 | 0 | 0 | -98.6 | -98.4 | |
| 2 | 1.02 | -1.82 | -1.01 | -.294 | 0 | 0 | -99.4 | -99.3 | |
| 3 | .403 | -.598 | 1.07 | -4.71 | 0 | 0 | -99.4 | -99.4 | |
| 4 | -.193 | -1.33 | -1.34 | -1.43 | 0 | 0 | 357. | -99.5 | |
| 5 | .202 | -1.18 | -.859 | -.948 | 0 | 0 | -99.5 | -99.4 | |
| 6 | -2.73 | -4.88 | -5.85 | -5.83 | 0 | 0 | -99.1 | -100 | |
| 7 | .618 | -1.20 | -.761 | -.417 | 0 | 0 | -99.4 | -100 | |
| 8 | 0 | -.782 | -1.04 | -.982 | 0 | 0 | 363. | -99.4 | |
| 9 | .396 | -.787 | -.744 | -.686 | 0 | 0 | -99.3 | -99.3 | |
| 10 | .413 | -.824 | -.470 | -.493 | 0 | 0 | -99.4 | -99.2 | |

STATISTICS

| FORWARD | VNOM | Vx | DV | IL |
|---|---|---|---|---|
| MAX VALUES | 2.7335 | 5.8567 | 0.0000 | 363.16 |
| MIN VALUES | 0.0000 | 0.4710 | 0.0000 | 98.6818 |
| RANGE | 2.7335 | 5.3857 | 0.0000 | 264.48 |
| AVERAGE | 0.6378 | 1.6674 | 0.0000 | 151.56 |
| STD DEV | 0.7863 | 1.6976 | 0.0000 | %110.1431 |
| REVERSE | | | | |
| MAX VALUES | 4.8832 | 5.8336 | 0.0000 | 100.00 |
| MIN VALUES | 0.5988 | 0.2946 | 0.0000 | 98.4745 |
| RANGE | 4.2844 | 5.5390 | 0.0000 | 1.5255 |
| AVERAGE | 1.5745 | 1.9316 | 0.0000 | 99.4310 |
| STD DEV | 1.2760 | 2.0050 | 0.0000 | 0.4222 |

Table G

**ENERGY RATINGS AT PEAK CURRENT**

| Powder | Energy (J)<br>8/20$\mu$s |
|---|---|
| A-V | 57.8 |
| V-S | 52.3 |
| T-S | 56.2 |
| T-T | 49.6 |
| A-A | 52.65 |
| B-S | 56.9 |
| V-A | 52.4 |
| A-S | 53.2 |
| B-B | 53.18 |

## Table H

**Energy at 1.8 Joules**

| T-S | V-S | T-T | A-A | B-S | V-A | A-S | B-B |
|---|---|---|---|---|---|---|---|
| 79 | 77 | 81 | 76 | 79 | 71 | 76 | 76 |
| 82 | 78 | 81 | 77 | 80 | 77 | 77 | 80 |
| 76 | 78 | 82 | 74 | 80 | 78 | 80 | 79 |
| 78 | 78 | 81 | 76 | 79 | 73 | 79 | 80 |
| 79 | 77 | 81 | 78 | 79 | 74 | 78 | 78 |
| 79 | 77 | 80 | 76 | 80 | 76 | 79 | 80 |
| 80 | 77 | 81 | 76 | 80 | 74 | 79 | 78 |
| 78 | 78 | 81 | 73 | 80 | 74 | 78 | 79 |
| 76 | 75 | 80 | 74 | 81 | 75 | 77 | 78 |
| 77 | 79 | 81 | 74 | 80 | 75 | 78 | 77 |

## Table I1

## Voltage Shifts after Energy at 1.8J (T-S) (Turbula - Shear)

COMPLETE SHIFTS PRINTOUT

MODEL NUMBER V47ZA1 Lot number Tests: 1 - 4

Date 06-02-1994 Filename 351SEYH Description 7MM

TITLE:-SHIFTS

| Shift Dev | VNOM @ 1mA 42 55 Fwd | VNOM @ 1mA 42 55 Rev | Vx @ 100uA 1 55 Fwd | Vx @ 100uA 1 55 Rev | DV @ 0.000 0 0 Fwd | DV @ 0.000 0 0 Rev | IL @ 23.5V 000NA 010UA Fwd | IL @ 23.5V 000NA 010UA Rev | Status |
|---|---|---|---|---|---|---|---|---|---|
| 1 | -.400 | .199 | 0 | -1.25 | 0 | 0 | 7.69 | 10 | |
| 2 | .197 | .195 | 2.90 | .104 | 0 | 0 | 21.0 | 9.80 | |
| 3 | 0 | .383 | 5.59 | .100 | 0 | 0 | 9.09 | -2.43 | |
| 4 | .206 | .205 | .230 | .200 | 0 | 0 | 14.2 | 7.69 | |
| 5 | 0 | .404 | .229 | .345 | 0 | 0 | 14.2 | 2.22 | |
| 6 | -.195 | 0 | -.182 | -8.03 | 0 | 0 | 23.0 | 0 | |
| 7 | .200 | .603 | 1.47 | .044 | 0 | 0 | 36.3 | 17.0 | |
| 8 | .203 | 0 | .272 | .195 | 0 | 0 | 0 | 4.54 | |
| 9 | 0 | .198 | -6.07 | -2.31 | 0 | 0 | 23.0 | 2.22 | |
| 10 | 0 | .198 | .112 | .255 | 0 | 0 | 0 | 0 | |

STATISTICS

| FORWARD | VNOM | Vx | DV | IL |
|---|---|---|---|---|
| MAX VALUES | 0.4008 | 6.0783 | 0.0000 | 36.3636 |
| MIN VALUES | 0.0000 | 0.0000 | 0.0000 | 0.0000 |
| RANGE | 0.4008 | 6.0783 | 0.0000 | 36.3636 |
| AVERAGE | 0.1404 | 1.7080 | 0.0000 | 14.8925 |
| STD DEV | 0.1354 | 2.3552 | 0.0000 | 11.3663 |
| REVERSE | | | | |
| MAX VALUES | 0.6036 | 8.0388 | 0.0000 | 17.0731 |
| MIN VALUES | 0.0000 | 0.0443 | 0.0000 | 0.0000 |
| RANGE | 0.6036 | 7.9945 | 0.0000 | 17.0731 |
| AVERAGE | 0.2389 | 1.2851 | 0.0000 | 5.5998 |
| STD DEV | 0.1836 | 2.4792 | 0.0000 | 5.4740 |

# Table I2

## Voltage Shifts after Energy at 1.8J (V-S) (Vibro - Shear)

COMPLETE SHIFTS PRINTOUT

MODEL NUMBER V47ZA1 Lot number Tests: 1 - 4

Date 06-02-1994 Filename 351SEYG Description 7MM

TITLE:-SHIFTS

| Shift Dev | VNOM @ 1mA 42 55 Fwd | VNOM Rev | Vx @ 100uA I 55 Fwd | Vx Rev | DV @ 0.000 0 0 Fwd | DV Rev | IL @ 23.5V 000NA 010UA Fwd | IL Rev | Status |
|---|---|---|---|---|---|---|---|---|---|
| 1 | .233 | .705 | .455 | .340 | 0 | 0 | 10.5 | 3.84 | |
| 2 | -.863 | -1.34 | 0 | .145 | 0 | 0 | 5 | 0 | |
| 3 | .218 | 0 | .534 | .529 | 0 | 0 | -13.0 | -3.57 | |
| 4 | 0 | 0 | -6.94 | -6.94 | 0 | 0 | 4.16 | 0 | |
| 5 | .236 | 0 | 6.32 | 5.62 | 0 | 0 | -8.33 | -2.73 | |
| 6 | .446 | .689 | .514 | .654 | 0 | 0 | 0 | -1.96 | |
| 7 | 0 | -.434 | .201 | .235 | 0 | 0 | 0 | 0 | |
| 8 | -.217 | -.647 | .419 | .319 | 0 | 0 | -9.09 | 0 | |
| 9 | 0 | -.909 | -.370 | -.170 | 0 | 0 | 4.76 | 3.77 | |
| 10 | .453 | .450 | .273 | .583 | 0 | 0 | 4.54 | 0 | |

STATISTICS

| FORWARD | VNOM | Vx | DV | IL |
|---|---|---|---|---|
| MAX VALUES | 0.8639 | 6.9408 | 0.0000 | 13.0434 |
| MIN VALUES | 0.0000 | 0.0000 | 0.0000 | 0.0000 |
| RANGE | 0.8639 | 6.9408 | 0.0000 | 13.0434 |
| AVERAGE | 0.2671 | 1.6038 | 0.0000 | 5.9468 |
| STD DEV | 0.2675 | 2.6601 | 0.0000 | 4.2827 |
| REVERSE | | | | |
| MAX VALUES | 1.3423 | 6.9469 | 0.0000 | 3.8462 |
| MIN VALUES | 0.0000 | 0.1459 | 0.0000 | 0.0000 |
| RANGE | 1.3423 | 6.8010 | 0.0000 | 3.8462 |
| AVERAGE | 0.5180 | 1.5547 | 0.0000 | 1.5892 |
| STD DEV | 0.4385 | 2.5178 | 0.0000 | 1.7602 |

## Table I3

## Voltage Shifts after Energy at 1.8J (T-T) (Turbula - Turbula)

COMPLETE SHIFTS PRINTOUT

MODEL NUMBER V47ZA1 Lot number Tests: 1 - 4

Date 06-02-1994 Filename 351SEYP Description 7MM

TITLE:- SHIFTS

| | VNOM @ 1mA 42 55 | | Vx @ 100uA 1 55 | | DV @ 0.000 0 0 | | IL @ 23.5V 000NA 010UA | | |
|---|---|---|---|---|---|---|---|---|---|
| Shift Dev | Fwd | Rev | Fwd | Rev | Fwd | Rev | Fwd | Rev | Status |
| 1 | .409 | 1.03 | .441 | .521 | 0 | 0 | 0 | 0 | |
| 2 | .370 | .185 | -2.73 | -.163 | 0 | 0 | 0 | 2.77 | |
| 3 | 0 | .567 | .153 | .140 | 0 | 0 | 8.33 | 0 | |
| 4 | .190 | 0 | .117 | -6.99 | 0 | 0 | 0 | -2.85 | |
| 5 | .191 | .386 | .284 | .183 | 0 | 0 | 10 | 2.85 | |
| 6 | 0 | 0 | .168 | .175 | 0 | 0 | 0 | 0 | |
| 7 | .380 | .936 | .310 | .450 | 0 | 0 | 0 | -2.70 | |
| 8 | 0 | .559 | .166 | .112 | 0 | 0 | 6.66 | 2.22 | |
| 9 | 0 | .372 | .168 | .116 | 0 | 0 | 0 | 0 | |
| 10 | .188 | .185 | .139 | .203 | 0 | 0 | 7.69 | 0 | |

STATISTICS

| FORWARD | VNOM | Vx | DV | IL |
|---|---|---|---|---|
| MAX VALUES | 0.4098 | 2.7330 | 0.0000 | 10.0000 |
| MIN VALUES | 0.0000 | 0.1175 | 0.0000 | 0.0000 |
| RANGE | 0.4098 | 2.6155 | 0.0000 | 10.0000 |
| AVERAGE | 0.1730 | 0.4682 | 0.0000 | 3.2692 |
| STD DEV | 0.1695 | 0.8021 | 0.0000 | 4.2970 |
| REVERSE | | | | |
| MAX VALUES | 1.0309 | 6.9915 | 0.0000 | 2.8571 |
| MIN VALUES | 0.0000 | 0.1129 | 0.0000 | 0.0000 |
| RANGE | 1.0309 | 6.8786 | 0.0000 | 2.8571 |
| AVERAGE | 0.4224 | 0.9059 | 0.0000 | 1.3417 |
| STD DEV | 0.3570 | 2.1429 | 0.0000 | 1.4253 |

## Table I4

## Voltage Shifts after Energy at 1.8J (A-A) (Attrition - Attrition)

COMPLETE SHIFTS PRINTOUT

MODEL NUMBER V472A1 Lot number Tests: 1 - 4

Date 06-01-1994 Filename 351SEYE Description 7MM

TITLE:- SHIFTS

| Shift Dev | VNOM @ 1mA 42 55 Fwd | VNOM @ 1mA 42 55 Rev | Vx @ 100uA 1 55 Fwd | Vx @ 100uA 1 55 Rev | DV @ 0.000 0 0 Fwd | DV @ 0.000 0 0 Rev | IL @ 23.5V 000NA 010UA Fwd | IL @ 23.5V 000NA 010UA Rev | Status |
|---|---|---|---|---|---|---|---|---|---|
| 1 | .199 | .194 | .481 | .163 | 0 | 0 | -7.14 | 0 | |
| 2 | -.194 | -.574 | -.149 | -.223 | 0 | 0 | 30 | 2.56 | |
| 3 | -1.42 | .202 | .395 | .594 | 0 | 0 | 0 | 10 | |
| 4 | .194 | .192 | 3.66 | 4.28 | 0 | 0 | -7.69 | -100 | |
| 5 | .193 | .190 | -.220 | .216 | 0 | 0 | -7.69 | 7.89 | |
| 6 | .207 | 1.03 | -1.57 | 5.61 | 0 | 0 | 15.3 | 0 | |
| 7 | .199 | .197 | .104 | .193 | 0 | 0 | 0 | 4.54 | |
| 8 | .206 | .408 | 6.32 | .024 | 0 | 0 | -6.25 | 2.32 | |
| 9 | -.204 | .408 | 7.06 | -1.50 | 0 | 0 | 0 | 0 | |
| 10 | 0 | .200 | .173 | 7.42 | 0 | 0 | 16.6 | 0 | |

STATISTICS

| FORWARD | VNOM | Vx | DV | IL |
|---|---|---|---|---|
| MAX VALUES | 1.4257 | 7.0658 | 0.0000 | 30.0000 |
| MIN VALUES | 0.0000 | 0.1049 | 0.0000 | 0.0000 |
| RANGE | 1.4257 | 6.9609 | 0.0000 | 30.0000 |
| AVERAGE | 0.3026 | 2.0149 | 0.0000 | 9.0829 |
| STD DEV | 0.3996 | 2.7014 | 0.0000 | 9.4157 |
| REVERSE | | | | |
| MAX VALUES | 1.0373 | 7.4255 | 0.0000 | 100.00 |
| MIN VALUES | 0.1908 | 0.0240 | 0.0000 | 0.0000 |
| RANGE | 0.8465 | 7.4015 | 0.0000 | 100.00 |
| AVERAGE | 0.3607 | 2.0243 | 0.0000 | 12.7330 |
| STD DEV | 0.2729 | 2.7253 | 0.0000 | 30.8647 |

## Table I5

## Voltage Shifts after Energy at 1.8J (B-S) (Ball - Shear)

COMPLETE SHIFTS PRINTOUT

MODEL NUMBER V47ZA1 Lot number Tests: 1 - 4

Date 06-01-1994 Filename 351SEYD Description 7MM

TITLE:-SHIFTS

| Shift Dev | VNOM @ 1mA 42 55 Fwd | Rev | Vx @ 100uA 1 55 Fwd | Rev | DV @ 0.000 0 0 Fwd | Rev | IL @ 23.5V 000NA 010UA Fwd | Rev | Status |
|---|---|---|---|---|---|---|---|---|---|
| 1 | 0 | .199 | .292 | .262 | 0 | 0 | 5.26 | 3.63 | |
| 2 | .212 | .416 | .183 | .103 | 0 | 0 | 11.5 | 7.93 | |
| 3 | 0 | .616 | 7.18 | .111 | 0 | 0 | 15.3 | 3.03 | |
| 4 | 0 | .200 | -.140 | -2.94 | 0 | 0 | 11.7 | 3.92 | |
| 5 | 0 | .394 | 7.57 | .040 | 0 | 0 | 25 | -100 | |
| 6 | -.210 | .208 | 6.26 | 5.38 | 0 | 0 | -100 | -100 | |
| 7 | .200 | 0 | .142 | .157 | 0 | 0 | -100 | -100 | |
| 8 | -.200 | 0 | 4.43 | -5.07 | 0 | 0 | 5.88 | 7.84 | |
| 9 | 0 | .199 | .330 | .248 | 0 | 0 | 7.69 | 7.69 | |
| 10 | 0 | .606 | .467 | .356 | 0 | 0 | 21.4 | 2.94 | |

STATISTICS

| FORWARD | VNOM | Vx | DV | IL |
|---|---|---|---|---|
| MAX VALUES | 0.2123 | 7.5724 | 0.0000 | 100.00 |
| MIN VALUES | 0.0000 | 0.1408 | 0.0000 | 5.2632 |
| RANGE | 0.2123 | 7.4317 | 0.0000 | 94.7369 |
| AVERAGE | 0.0824 | 2.7020 | 0.0000 | 30.3954 |
| STD DEV | 0.1065 | 3.2566 | 0.0000 | 37.2306 |
| REVERSE | | | | |
| MAX VALUES | 0.6160 | 5.3823 | 0.0000 | 100.00 |
| MIN VALUES | 0.0000 | 0.0400 | 0.0000 | 2.9412 |
| RANGE | 0.6160 | 5.3422 | 0.0000 | 97.0588 |
| AVERAGE | 0.2842 | 1.4683 | 0.0000 | 33.7001 |
| STD DEV | 0.2191 | 2.1639 | 0.0000 | 45.7932 |

## Table I6

## Voltage Shifts after Energy at 1.8J (V-A) (Vibro - Attrition)

COMPLETE SHIFTS PRINTOUT

MODEL NUMBER V47ZA1 Lot number Tests: 1 - 4

Date 06-01-1994 Filename 351SEYC Description 7MM

TITLE:-SHIFTS

| Shift Dev | VNOM @ 1mA 42 55 Fwd | VNOM @ 1mA 42 55 Rev | Vx @ 100uA 1 55 Fwd | Vx @ 100uA 1 55 Rev | DV @ 0.000 0 0 Fwd | DV @ 0.000 0 0 Rev | IL @ 23.5V 000NA 010UA Fwd | IL @ 23.5V 000NA 010UA Rev | Status |
|---|---|---|---|---|---|---|---|---|---|
| 1 | .366 | .184 | .183 | .280 | 0 | 0 | -7.69 | 0 | |
| 2 | .566 | -.554 | .364 | .393 | 0 | 0 | -8.33 | 2.70 | |
| 3 | 0 | .182 | 2.70 | 5.99 | 0 | 0 | -8.33 | 0 | |
| 4 | .184 | .183 | .143 | .159 | 0 | 0 | 11.1 | -7.69 | |
| 5 | .184 | 0 | 0 | 1.34 | 0 | 0 | 0 | 0 | |
| 6 | .373 | .742 | 1.02 | 1.03 | 0 | 0 | -18.1 | -100 | |
| 7 | 0 | .185 | .190 | .143 | 0 | 0 | 0 | -3.84 | |
| 8 | .369 | .184 | -.108 | -5.62 | 0 | 0 | 27.2 | 0 | |
| 9 | -.382 | .381 | .212 | .214 | 0 | 0 | 0 | -2.56 | |
| 10 | -.184 | .183 | -.383 | 9.55 | 0 | 0 | -100 | -100 | |

STATISTICS

| FORWARD | VNOM | Vx | DV | IL |
|---|---|---|---|---|
| MAX VALUES | 0.5660 | 2.7032 | 0.0000 | 100.00 |
| MIN VALUES | 0.0000 | 0.0000 | 0.0000 | 0.0000 |
| RANGE | 0.5660 | 2.7032 | 0.0000 | 100.00 |
| AVERAGE | 0.2612 | 0.5309 | 0.0000 | 18.0925 |
| STD DEV | 0.1817 | 0.8136 | 0.0000 | 30.0417 |
| REVERSE | | | | |
| MAX VALUES | 0.7421 | 9.5548 | 0.0000 | 100.00 |
| MIN VALUES | 0.0000 | 0.1438 | 0.0000 | 0.0000 |
| RANGE | 0.7421 | 9.4110 | 0.0000 | 100.00 |
| AVERAGE | 0.2783 | 2.4752 | 0.0000 | 21.6805 |
| STD DEV | 0.2193 | 3.3482 | 0.0000 | 41.3486 |

## Table I7

## Voltage Shifts after Energy at 1.8J (A-S) (Attrition - Shear)

COMPLETE SHIFTS PRINTOUT

MODEL NUMBER V47ZA1 Lot number Tests: 1 - 4

Date 06-01-1994 Filename 351SEYB Description 7MM

TITLE:-SHIFTS

| | VNOM @ 1mA 42 55 | | Vx @ 100uA 1 55 | | DV @ 0.000 0 0 | | IL @ 23.5V 900NA 010UA | | |
|---|---|---|---|---|---|---|---|---|---|
| Shift Dev | Fwd | Rev | Fwd | Rev | Fwd | Rev | Fwd | Rev | Status |
| 1 | 0 | .384 | 9.96 | 6.32 | 0 | 0 | -5.26 | 0 | |
| 2 | .189 | .381 | .155 | 9.96 | 0 | 0 | -8.33 | -2.56 | |
| 3 | 0 | .188 | .100 | .127 | 0 | 0 | -15.3 | -2.5 | |
| 4 | 0 | .188 | 7.77 | 3.59 | 0 | 0 | 18.1 | 7.69 | |
| 5 | 0 | -.191 | 3.49 | 4.33 | 0 | 0 | 16.6 | 0 | |
| 6 | .395 | .394 | .295 | .207 | 0 | 0 | -6.66 | 0 | |
| 7 | 0 | .196 | -.308 | -.288 | 0 | 0 | 0 | 2.38 | |
| 8 | -.191 | 0 | .193 | .170 | 0 | 0 | 16.6 | 5 | |
| 9 | .202 | .199 | .439 | .395 | 0 | 0 | -7.14 | 0 | |
| 10 | .384 | .189 | -7.12 | 5.71 | 0 | 0 | 7.14 | 0 | |

STATISTICS

| FORWARD | VNOM | Vx | DV | IL |
|---|---|---|---|---|
| MAX VALUES | 0.3953 | 9.9636 | 0.0000 | 18.1813 |
| MIN VALUES | 0.0000 | 0.1007 | 0.0000 | 0.0000 |
| RANGE | 0.3953 | 9.8629 | 0.0000 | 18.1813 |
| AVERAGE | 0.1364 | 2.9856 | 0.0000 | 10.1443 |
| STD DEV | 0.1605 | 3.8591 | 0.0000 | 6.1216 |
| REVERSE | | | | |
| MAX VALUES | 0.3945 | 9.9681 | 0.0000 | 7.6923 |
| MIN VALUES | 0.0000 | 0.1272 | 0.0000 | 0.0000 |
| RANGE | 0.3945 | 9.8409 | 0.0000 | 7.6923 |
| AVERAGE | 0.2314 | 3.1131 | 0.0000 | 2.0137 |
| STD DEV | 0.1227 | 3.4513 | 0.0000 | 2.6271 |

## Table I8

## Voltage Shifts after Energy at 1.8J (B-B) (Ball - Ball)

COMPLETE SHIFTS PRINTOUT

MODEL NUMBER V47ZA1 Lot number Tests: 1 - 4

Date 06-01-1994 Filename 351SEYA Description 7MM

TITLE:-SHIFTS

| | VNOM @ ImA 42 55 | | Vx @ 100uA 1 55 | | DV @ 0.000 0 0 | | IL @ 23.5V 000NA 010UA | | |
|---|---|---|---|---|---|---|---|---|---|
| Shift Dev | % Fwd | % Rev | % Fwd | % Rev | % Fwd | % Rev | % Fwd | % Rev | Status |
| 1 | .772 | .575 | .832 | .790 | 0 | 0 | 57.1 | 25 | |
| 2 | 0 | .192 | .140 | .106 | 0 | 0 | 20 | 8.82 | |
| 3 | .201 | .591 | .198 | .146 | 0 | 0 | 16.6 | 4.10 | |
| 4 | .207 | 0 | .197 | .166 | 0 | 0 | 12.5 | 10.6 | |
| 5 | 0 | .380 | -5.43 | 2.21 | 0 | 0 | 23.8 | 7.14 | |
| 6 | .385 | .190 | .141 | 5.05 | 0 | 0 | 30 | 5.12 | |
| 7 | 0 | .189 | .042 | 5.04 | 0 | 0 | 15.3 | 4.54 | |
| 8 | .197 | .193 | .290 | .341 | 0 | 0 | 13.3 | 6.25 | |
| 9 | .210 | .821 | -.325 | -.335 | 0 | 0 | 25 | 8.51 | |
| 10 | .199 | .392 | 9.81 | .100 | 0 | 0 | 4.76 | 1.63 | |

STATISTICS

| FORWARD | VNOM | Vx | DV | IL |
|---|---|---|---|---|
| MAX VALUES | 0.7722 | 9.8121 | 0.0000 | 57.1428 |
| MIN VALUES | 0.0000 | 0.0423 | 0.0000 | 4.7619 |
| RANGE | 0.7722 | 9.7698 | 0.0000 | 52.3809 |
| AVERAGE | 0.2175 | 1.7413 | 0.0000 | 21.8599 |
| STD DEV | 0.2307 | 3.2740 | 0.0000 | 14.3365 |
| REVERSE | | | | |
| MAX VALUES | 0.8214 | 5.0526 | 0.0000 | 25.0000 |
| MIN VALUES | 0.0000 | 0.1004 | 0.0000 | 1.6393 |
| RANGE | 0.8214 | 4.9522 | 0.0000 | 23.3607 |
| AVERAGE | 0.3527 | 1.4304 | 0.0000 | 8.1788 |
| STD DEV | 0.2489 | 2.0102 | 0.0000 | 6.4649 |